Advanced Processes for Titanium Sintering

Evan Schumann

Thesis submitted for the degree of

Master of Philosophy

School of Mechanical Engineering

Faculty of Engineering, Computer and Mathematical Sciences

The University of Adelaide

THE UNIVERSITY *of* ADELAIDE

September 1, 2014

Contents

List of Tables

List of Figures

Symbols and Abbreviations

List of Abbreviations

BE Blended Elemental

BCC Body Centred Cubic

CIP Cold Isostatic Press

CHIP Cold Isostatic Press followed by Hot Isostatic Press

CP Cold Press or Commercially Pure

DSC Differential Scanning Calorimetry

EDS Energy Dispersive Spectroscopy

FCC Face Centred Cubic

FCT Face Centred Tetragonal

FWHM Full Width at Half Maximum

GA Gas Atomisation

HDH Hydride De-Hydride

HIP Hot Isostatic Press

HP Hot (Uniaxial) Press

HV Vickers Hardness Number

ICP-OES Inductively Coupled Plasma - Optical Emission Spectroscopy

LPS Liquid Phase Sintering

MA Mechanically Alloyed

PA Pre-Alloyed

PM Powder Metallurgy

REP Rotating Electrode Process

SE Secondary Electrons

SEM Scanning Electron Microscopy

XRD X-Ray Diffraction

List of Symbols

$\mathring{A}$ Angstrom (10^{-10}m)

E Young's Modulus (MPa)

ρ Density (g/cm^3)

σ_f Flexural stress (MPa)

ϵ_f Flexural strain (mm/mm)

$at\%$ Atomic percent

$wt\%$ Weight percent

$m\%$ Mass percent

$V\%$ Volume percent

$\%el$ Percent elongation

$^{\circ}C$ Degrees Celsius

Abstract

A global objective of current research is to reduce the cost of manufacturing of titanium parts by improving the efficiency of near net-shape powder metallurgy (PM) technologies. These technologies are considered to be very promising as they eliminate waste and high machining costs. However, the cost of titanium components fabricated with PM remains relatively high due to the significant rate of energy consumption needed for various stages of PM, such as powder processing and sintering. Therefore, more research is needed to reduce the cost of production further, without compromising the mechanical properties and quality of the final product.

The current research is focused on the two latest developments addressing the efficiency problems of current PM: (I) the use of hydrogen as a temporary alloying element in the production of titanium powder, and (II) the application of the Liquid Phase Sintering (LPS) method to enhance the densification of materials. The following aspects of these developments are studied in this thesis: the effect of powder characteristics obtained with the ball milling method and the influence of sintering parameters on the microstructure and mechanical properties of fabricated samples.

The experimental approach includes the following stages: (a) synthesis of TiH_2 from a commercial titanium sponge; (b) particle size reduction through ball milling; and (c) hot press sintering with and without adding a liquid aluminium

phase. The TiH_2 powders were investigated for particle size and morphology by laser granulometry and Scanning Electron Microscopy (SEM), and the dehydrogenation kinetic was studied using Differential Scanning Calorimetry, The metallic impurities introduced during ball milling were measured through Inductively Coupled Plasma Optical Emission Spectroscopy (ICP-OES). Sintered specimens were characterised by density using the Archimedes immersion method, and the microstructure and phase composition were examined using SEM Energy Dispersion Spectroscopy (EDS) and X-Ray diffraction (XRD). The hardness of pure titanium specimens was tested by microindentation and the flexural strength of selected LPS specimens was determined using the 3-point bending test. A relationship between the ball milling time and TiH_2 particle size alongside the level of contamination of the Ti powder were established. The influence of the particle size and sintering temperatures, specifically in the bottom range concerned with the energy efficiency, on the densification and dehydrogenation of TiH_2 was studied. The effect of an aluminium phase on the minimum sintering temperatures and quality of the fabricated samples was investigated by varying the concentration of liquid aluminium during hot press sintering.

The outcomes of the current research demonstrated that:

- the size of TiH_2 powder after ball milling greatly increases the density and dehydrogenation of the sintered specimens;
- the dehydrogenation is seen to be delayed by pressure assisted sintering inside a graphite mould;
- ball milling leads to the increased pickup of oxygen on the surface of fine TiH_2 due to the increased specific surface area;
- The aluminium liquid phase is shown to improve the density during pressure assisted sintering at concentrations of 5 to 10 at% aluminium;

- the use of fine particle sizes leads to a faster reaction between the liquid aluminium and titanium and promotes a solid intermetallic phase formation around the aluminium particle site;

- one interesting outcome of the completed research is that the use of a liquid aluminium phase to sinter titanium is shown to improve part density when using pressure-assisted sintering, when compared with previous studies using free sintering.

Overall, it is believed that the conducted study contributes to the understanding and further improvement of PM techniques and demonstrates a significant potential to reduce the fabrication costs of titanium components with ball milling and direct sintering TiH_2 methods. However, a further optimisation of the fabrication parameters and a more comprehensive assessment of mechanical properties are required in order to verify the quality of the fabricated components and for industry to adopt these methods.

Publications

Journal Papers

Schumann E., Silvain J.-F., Bobet J.-L., Bardet M., Lu Y., Kotousov A. and Lamirand-Majimel M. Advanced Processes for Titanium Sintering, *Materials Chemistry and Physics*, under review.

Conference Papers

Schumann E., Silvain J.-F., Bobet J.-L., Kotousov A. and Lamirand-Majimel M. Titanium Enhanced Sintering Through Liquid Phase Sintering, *International Conference on Composite Materials*, ICCM19, Montreal, Canada, July 28 - August 2, 2013. See Appendix A.

Declaration

I certify that this work contains no material which has been accepted for the award of any other degree or diploma in my name, in any university or other tertiary institution and, to the best of my knowledge and belief, contains no material previously published or written by another person, except where due reference has been made in the text. In addition, I certify that no part of this work will, in the future, be used in a submission in my name, for any other degree or diploma in any university or other tertiary institution without the prior approval of the University of Adelaide and where applicable, any partner institution responsible for the joint-award of this degree.

I give consent to this copy of my thesis, when deposited in the University Library, being made available for loan and photocopying, subject to the provisions of the Copyright Act 1968.

I also give permission for the digital version of my thesis to be made available on the web, via the Universitys digital research repository, the Library Search and also through web search engines, unless permission has been granted by the University to restrict access for a period of time.

SIGNED: . . . . . DATE: . . . . . .

Acknowledgements

I would like to express great gratitude for the teaching, guidance, motivation, joy and inspiration given by Jean-François Silvain, Mélanie Lamirand-Majimel, Jean-Louis Bobet, Matthieu Bardet and the members of groups 4 and 1 at the ICMCB, it was a pleasure.

I am also sincerely indebted to Andrei Kotousov for his dedicated support and insightful guidance.

I am grateful to Eric Lebraud, Laëtitia Etienne and Nicolas Penin for their technical assistance, to Alison-Jane Hunter for incredible speed in editing, and I would like to thank Region Aquitaine for its financial support and the DSTO and the MDE group at SES for their support.

I would also like to thank my family for their continuous and immeasurable support.

Chapter 1

Introduction

Titanium is used in high demand applications because of its high specific strength, low density, corrosion resistance, high temperature operational limit and biocompatibiltiy (Donachie, 2000; Lütjering and Williams, 2007). Its properties are attractive for engineering applications in aircraft, biomedical prostheses and chemical processing (Peters et al., 2003; Peters and Leyens, 2003; Brown and Lemons, 1996). However, the cost of titanium is 15-50 times that of conventional engineering materials such as steel or aluminium (Faller and Froes, 2001). Thus, the application of titanium is restricted to high specification applications which justify the cost of titanium (Froes, 2001).

The high cost of titanium production is linked to its high affinity for atmospheric contaminants (Gerdemann, 2001): the use of traditional fabrication techniques for titanium parts removes up to 90% of the material as waste (Barnes et al., 2009). Powder metallurgy (PM) is currently being investigated for titanium part production because it produces near net-shape parts and eliminates much of the cost of machining and waste. This thesis aims to improve the cost effectiveness of titanium powder metallurgy in order to enable the broader application of titanium. In this thesis, two powder metallurgical techniques will be studied which

have the potential to simplify the processing and improve densification at reduced sintering parameters, thereby reducing the costs.

The first of the two techniques is the direct sintering of TiH_2 powder. The use of thermo-hydrogen processing of titanium is a focus of current research efforts in order to reduce the cost of titanium. Hydrogen is useful as a temporary alloying element in titanium (Senkov and Froes, 1999). Hydrogen is absorbed by titanium to form TiH_2 in a hydrogen atmosphere and is eliminated in a vacuum at temperatures lower than those required for sintering (500°C) (Kennedy and Lopez, 2003). Increasing the concentration of hydrogen in titanium causes increased brittleness. TiH_2 is formed at the maximum concentration of hydrogen in titanium, and can be used in mechanical and forming processes where ductile titanium cannot be used. The direct use of TiH_2 in sintering has been studied previously and has been shown to improve densification when compared with conventional sintering processes and parameters (Wang et al., 2010b; Ivasishin et al., 1999, 2002; Pankevich et al., 1986). Ball milling of TiH_2 can be used to form powders of a smaller size than conventional powder production (Bobet et al., 2003; Bhosle et al., 2003), which leads to faster densification during sintering (Robertson and Schaffer, 2009).

The second of the two techniques studied in this thesis for the cost reduction of titanium is Liquid Phase Sintering (LPS) using aluminium. LPS is an advanced sintering method which uses a liquid formed during sintering to aid densification. LPS is used to consolidate materials which would be difficult to densify by normal PM methods (German, 1986). LPS of titanium has been studied with Fe, Ni and Si, and has been shown to cause part swelling and pores during sintering (Low et al., 2007; Kivalo et al., 1982; Liu et al., 2006): all studies have been performed at temperatures above 1000°C. Aluminium melts at a lower temperature (660°C) and, when studied in LPS of titanium, has been found to form pores by the diffusion between liquid aluminium and titanium particles and cause part swelling (Savitskii

and Burtsev, 1979; Liu et al., 2006). The exact diffusion mechanism which limits the use of LPS is not well understood. All swelling observed has been during free sintering, thus control of the swelling could be improved by the use of pressure-assisted sintering.

To reduce the cost of titanium PM, both of the following techniques will be studied in this thesis. The direct hot press sintering of ball milled TiH_2 powders will be studied for its ability to densify and dehydrogenate during low temperature sintering. This will help to understand the ability of ball milling of TiH_2 to reduce sintering temperatures. The sintering of titanium is also studied when coupled with a liquid aluminium phase using uniaxial hot press sintering. The effect of powder size on diffusion and phase formation will be studied. The effect of aluminium concentration and sintering temperature will be studied in order to improve densification at low temperatures.

In order to achieve the research aims, a literature review of the properties of titanium and its use in powder metallurgy is presented in Chapter 2. The properties of titanium relevant to powder metallurgy are discussed. The principles of powder metallurgy are also presented. Then, previous research into the area of sintering TiH_2 and titanium LPS is discussed and studies using these techniques are presented. Following the review of the state of the art in Chapter 2, Chapter 3 discusses the gaps in the research, and the potential for improvement of the techniques used to sinter titanium. The specific research aims are defined in order to contribute to the understanding of these techniques.

Chapter 4 presents in detail the materials and methods used for the synthesis and characterisation of ball milled TiH_2 powder. The experimental method to sinter titanium specimens are presented, as well as the methods used for their characterisation.

Chapter 5 presents the characterisation of TiH_2 powder synthesised by ball

milling. Here, TiH_2 powder of different particle sizes are synthesised through ball milling for different durations. These powders are characterised for particle size distribution, morphology, metallic impurities and dehydrogenation. The commercial titanium and aluminium powders used for comparison with ball milled TiH_2 in LPS are also characterised for particle size and morphology.

An experimental study of the effects of the characteristics of TiH_2 powders on sintering, with and without a liquid aluminium phase, are presented in Chapter 6. Direct hot press sintering of ball milled TiH_2 of different particle sizes is studied at a range of low temperatures. Ball milled TiH_2 (as is and dehydrogenated) and commercial Ti powder are sintered with varied aluminium concentrations. These specimens are characterised by density, phase composition and microstructure. The specimen quality of pure titanium specimens is determined by testing their hardness: specimens sintered with aluminium are tested through their flexural strength.

The results of the experimental study, presented in Chapter 6, are discussed in Chapter 7. The effect of the characteristics of ball milled TiH_2 powder on the densification and dehydrogenation during sintering are discussed. The densification and phase formation of specimens sintered using a liquid aluminium phase are discussed with respect to the aluminium concentration and size of the titanium powder used. The practical implications of the results in commercial titanium component production are also discussed.

Chapter 8 presents the conclusions from this study and recommended future work. The novel contributions to the understanding of these techniques, and how they can enable the cost reduction of titanium are presented. The future work which has been identified from the results of this study are presented.

This thesis will help the global effort to reduce the cost of titanium parts. The study of these techniques will contribute to the understanding of the powder metallurgy of titanium. Through better understanding of these advanced

techniques to improve sintering, the resultant reduction in the costs of titanium usage will enable its broader application.

Chapter 2

Critical Literature Review

2.1 Introduction

This Chapter provides a general overview of the material science and powder metallurgy of the production of titanium. The current approaches to titanium powder metallurgy, specifically under investigation in this thesis for their potential to reduce the cost of titanium, are described in detail.

The production of pure titanium remains expensive because of high processing and fabrication costs (Hartman et al., 1998). The processes of refinement of titanium associated with high cost are under investigation and have been improved recently (Chen et al., 2011; Doblin et al., 2013). These improvements have been directed at the production of titanium powder for use in powder metallurgy (PM) for the production of near net-shape parts, which eliminate the waste and high cost associated with the machining required for ingot metallurgy (Barnes et al., 2009). The PM methods used in the production of high quality titanium parts do not yet provide a significant reduction in cost (Fang, 2010). Consequently, advanced PM techniques are a focus of current research efforts to reduce the cost of titanium part production.

This Chapter describes two novel methods of powder metallurgy currently under development, which aim to reduce the cost of titanium part production: (1) the use of hydrogen as a temporary alloying element in the production of titanium powder and the direct sintering of TiH_2, and (2) the application of aluminium in Liquid Phase Sintering (LPS) to enhance the densification of titanium.

The use of hydrogen as a temporary alloying element in titanium facilitates processing (Senkov and Froes, 1999), enabling the production of a fine TiH_2 powder through ball milling. The direct sintering of TiH_2 has been shown to improve densification through the dehydrogenation process which takes place during sintering (Wang et al., 2010a; Pankevich et al., 1986; Ivasishin et al., 1999, 2002). These studies have used this method to improve densities through conventional sintering processes and parameters: the potential and limitations of sintering TiH_2 are not yet fully realised.

LPS is an advanced sintering technique, which uses a liquid phase to improve densification (German, 1986). Previous studies have been unsuccessful with a variety of elemental liquid phases, Fe, Ni and Si, to improve the densification of titanium (Low et al., 2007; Kivalo et al., 1982; Liu et al., 2006). The use of liquid aluminium, with its relatively low melting point, has also produced a decrease in sintered density because of the reaction between the liquid aluminium and solid titanium particles (Savitskii and Burtsev, 1979; Liu et al., 2006). These investigations have been performed under free sintering, by heating a powder compact without applied pressure, where pressure-assisted techniques are currently used for the fabrication of titanium aluminides by reaction sintering (Rawers and Wrzesinski, 1992; Paransky et al., 1996). Thus it is believed that, after further investigation, the use of pressure-assisted sintering of titanium with a liquid aluminium phase has the potential to improve densification at low temperature.

In the following Chapter, the current global understanding of these methods

Table 2.1: Comparison of basic properties of common structural materials

Material	Grade	σ_y (MPa)	ρ (g/cm^3)	σ_y/ρ (kN·m/kg)
Steel	A36	250	7.80	32
Aluminium	6061-T6	241	2.70	89
Titanium	Ti-6Al-4V	828	4.43	187

is discussed. Specific research aims are developed from the gaps identified in the understanding of these methods. Accordingly, the remaining sections of this thesis develop the experimental investigations in order to improve understanding of the sintering of TiH_2 and LPS using aluminium.

2.2 Titanium

The high specific strength (see Table 2.1), corrosion resistance, and biocompatibility of titanium make it suitable for mechanical design in many demanding applications. Titanium also is selected for its heat and temperature resistance, and creep resistance at high temperatures. For example, titanium is used in aircraft structures for its high specific strength, and in jet engines for its corrosion resistance and resistance to creep up to 550°C (Donachie, 2000). Titanium is used in prosthetic bones for its biocompatibility; the material's ability to be incorporated into the human body, without causing an immune reaction or corroding, as well as being light and strong enough to meet the loading demands of the human body (Brown and Lemons, 1996). Chemical processing also uses titanium because of its high corrosion resistance (Odwani et al., 1998). In the mechanical design of structures, the combination of low density and high strength are not offered from steel and aluminium respectively (compared in Table 2.1), and, in this regard, titanium is unique.

2.2.1 Production of Titanium

Titanium is naturally abundant in the earths crust and found in most igneous rock and soil deposits; of the different minerals found rutile (TiO_2) and ilmenite ($FeTiO_3$) are used for titanium production (Emsley, 2001).

Production of pure titanium is difficult because of its affinity for atmospheric elements. The refinement process developed has multiple steps and is not continuous (Gerdemann, 2001). The earliest used method to produce pure titanium from ore, first produces titanium tetrachloride ($TiCl_4$) by chlorination at 1000°C, then this is reduced using liquid Na or Mg. This method is still used today. The modern refined form of this method is called the Krolls process (Kroll, 1940), and uses liquid Mg in an inert gas atmosphere at temperatures between 800 and 850°C (Equation 2.1). The Krolls process produces porous globular pieces of titanium called sponge.

$$2Mg(l) + TiCl_4(g) \rightarrow 2MgCl_2(l) + Ti(sponge) \tag{2.1}$$

The refinement process represents a large cost in the processing of titanium ore into solid parts (Hartman et al., 1998), and research efforts have been aimed at reducing the cost of this process. The Krolls process is still performed in batches, while newer methods attempt to operate continuously. The Armstrong method (Crowley, 2003) is a continuous variation of the Hunter process (Hunter, 1910), which is similar to the Krolls process and uses Na reduction instead of Mg (Chen et al., 2011). During the Armstrong process, $TiCl_4$ is injected into a flow of Na and produces Ti and NaCl. NaCl is then separated and recycled. The level of oxygen concentration in this powder has been found to be too high for some applications, and the process requires further development (Gerdemann, 2001). Similarly, a newly developed continuous version of the Krolls process, call the TiRO process, is still under development (Doblin et al., 2013).

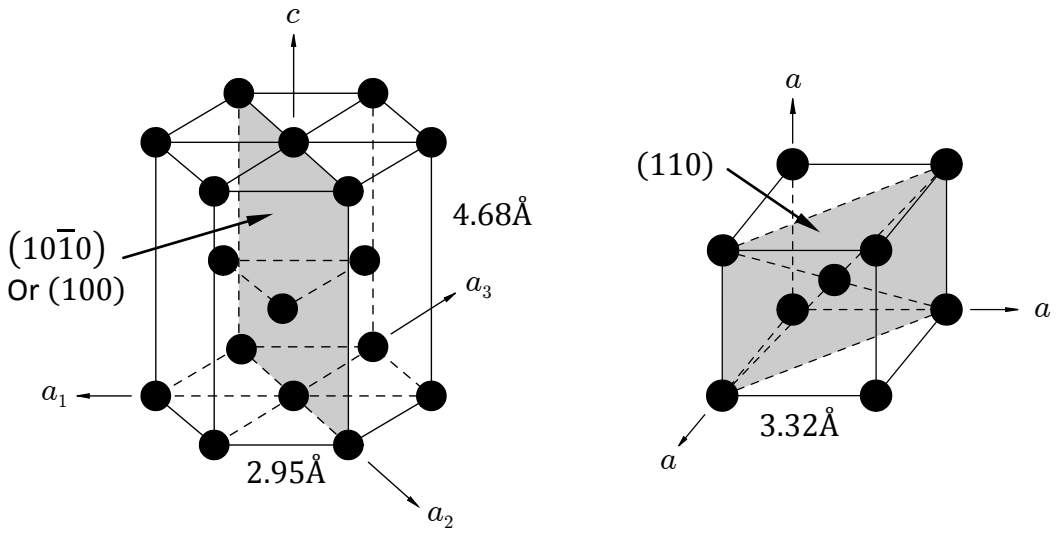

Figure 2.1: Crystal structure of α-Ti (left) and β-Ti (right)

Despite significant advances in methods of titanium production, it remains a complicated multi-step process. Even improving the reduction of $TiCl_4$ by making it continuous, still initially requires the chlorination of rutile. Therefore the cost of titanium production remains high.

2.2.2 Crystal Structure of Titanium

Pure titanium exists in two allotropic forms in solid state; titanium changes from a hexagonal close-packed (HCP) α-Ti upon heating above 882°C to a body-centred cubic lattice structure (BCC) β-Ti. Figure 2.1 shows the crystallographic structure of α and β phase titanium. The known lattice parameters, without distortion from interstitial or substitutional elements, or elastic strain, are for α phase HCP $a = b = 2.95\mathring{A}$ and $c = 4.68\mathring{A}$, and for β phase BCC at 900°C $a = b = c = 3.32\mathring{A}$ (Peters and Leyens, 2003).

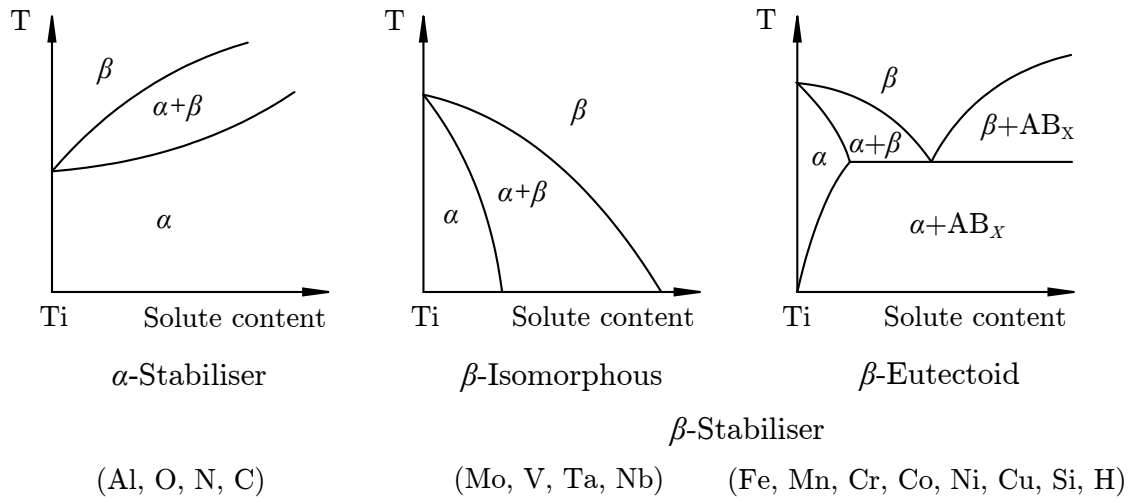

Figure 2.2: Influence of alloying elements on titanium (Peters and Leyens, 2003)

2.2.3 Titanium Alloys

A significant increase in the strength of titanium is achieved by alloying. Dislocation motion is impaired by the lattice distortions from substitutional elements (other transition metals) or by interstitial elements (such as C, H, N, and O). Ti-6Al-4V is the most widely used titanium alloy, dominating 56% of the US market (Eylon and Seagle, 2000). The interstitial elements also act to make titanium brittle. Oxygen has the most influence on strength and is used to strengthen titanium in small concentrations (Donachie, 2000).

Classification of Alloys

Alloying elements are classed as α or β stabilisers depending on their influence on the β transus temperature (Figure 2.2), either increasing or decreasing the temperature of transition between α-Ti and β-Ti.

Aluminium and interstitial elements C, N and O are α-stabilisers. Aluminium is the most widely used alloying element because of its ability to act as an α-stabiliser and its high solubility. β-isomorphous stabilisers, which simply lower the transus

temperature, have high solubility which is beneficial for strengthening. Some β-stabilisers form a eutectoid, and can lead to the formation of intermetallics (AB_X) at low concentrations. The addition of α or β stabilisers is controlled to influence the desired workability, fracture toughness and strength of the material.

2.2.4 Aluminium and Titanium

Aluminium is used widely as an alloying element in titanium, and is studied in this thesis for its interaction with titanium in prospective low temperature Liquid Phase Sintering (LPS). Figure 2.3 shows the Ti-Al phase diagram. Al has high solubility in α and β-Ti and increases the transus temperature. Several intermetallic phases are formed: α_2-Ti_3Al, γ-TiAl, $TiAl_2$ and $TiAl_3$.

The α_2-Ti_3Al phase has an HCP structure (Figure 2.4) existing with a range of Al concentrations (23-35 at% Al) at low temperatures, and is stable up to 1210°C. The γ-TiAl phase has an FCC structure (L_{10} form) existing for 48-55 at% Al at low temperature, and is stable up to 1450°C. $TiAl_2$ is a meta-stable phase of the orthorhombic form. The $TiAl_3$ phase is a line compound, existing only at exact stoichiometry, and is of the tetragonal $D0_{22}$ form.

2.2.5 Properties of Titanium Aluminides

Titanium Aluminides are of interest for their high temperature stability and high strength. However, their ductility is normally low, especially in $TiAl_2$ and $TiAl_3$, and much work has been done to improve their ductility through alloying (Lipsitt, 1986; Kim, 1998). Titanium aluminides have a high modulus of elasticity when compared with titanium, $TiAl_3$ 216 GPa (Nakamura and Kimura, 1991) and α_2-Ti_3Al and γ-TiAl at 145 GPa and 160 GPa, respectively (Westbrook and Fleischer, 2000). Titanium alumides are also stable at high temperatures: TiAl

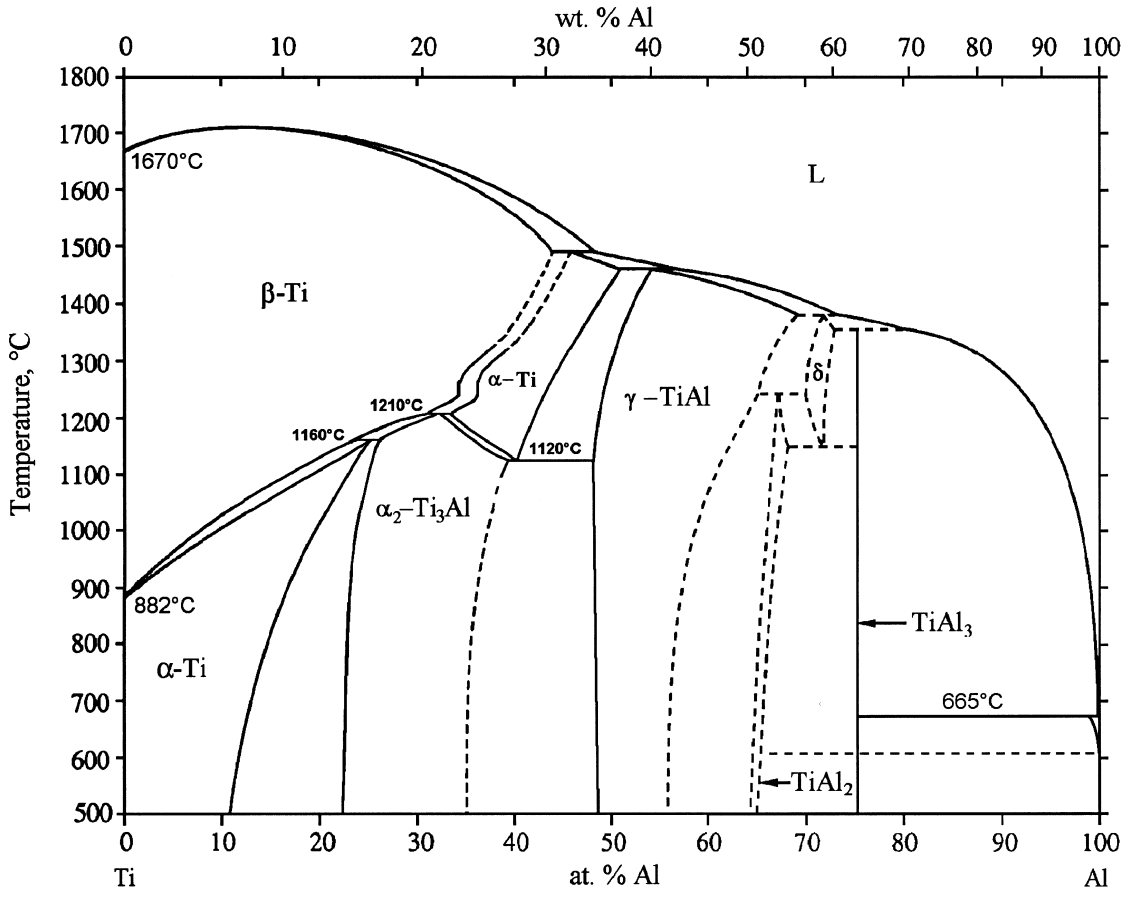

Figure 2.3: The Ti-Al phase diagram (Murray, 1987)

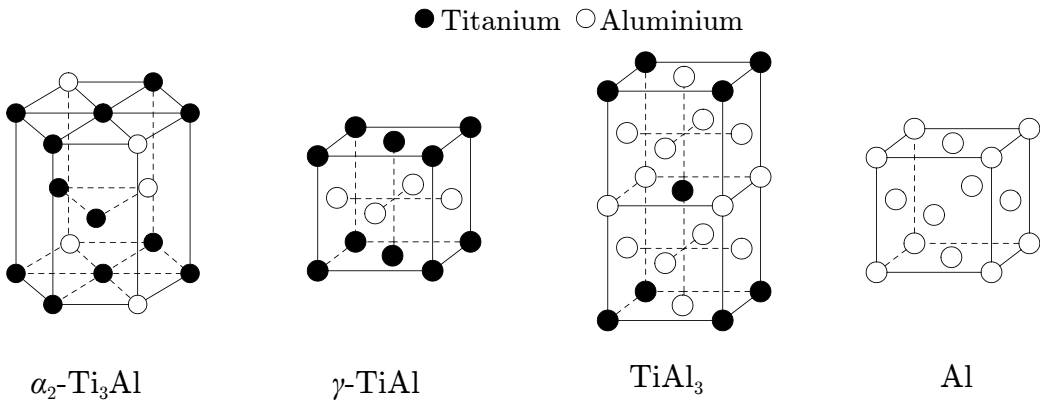

Figure 2.4: Lattice structures of titanium aluminides

Table 2.2: Properties of titanium aluminides

	α_2-Ti_3Al alloys	γ-TiAl alloys	$TiAl_3$ alloys
at% Al	23-35	48-55	75
density (g/cm^3)	4.1-4.7	3.8-4.0	3.4
Young's Modulus (GPa)	120-145	160-175	220
Ductility (%el)	2-5	1-2	-
Yield Strength (MPa)	700-990	400-650	1100
Oxidisation Limit (C)	650	900	1000
Crystal structure	HCP	FCT	FCT
Lattice parameters (nm)	a=0.5782	a=0.4000	a=0.3849
	c=0.4629	c=0.4075	c=0.8609

resists oxidation up to 900°C, and $TiAl_3$ to 1000°C (Umakoshi et al., 1989). Their strength is comparable with titanium alloys, between 400-1000 MPa. However, their ductility is low, between 1-5%el. The properties of titanium aluminides are summarised in Table 2.2. The high strength and high temperature operational limits of titanium aluminides are attractive for the aerospace and power generation industries. However, their low ductility limits their wider use in mechanical design.

2.2.6 Diffusion Between Titanium and Liquid Aluminium

A focus of this study is the densification of titanium with a liquid aluminium phase. The influence of a liquid phase on densification during sintering is determined by their interaction by diffusion. The diffusion that occurs between the titanium and aluminium is schematically shown in Figure 2.5. $TiAl_3$ forms first, and aluminium diffuses through $TiAl_3$ to the reaction front (Sujata et al., 2001). In this first stage,

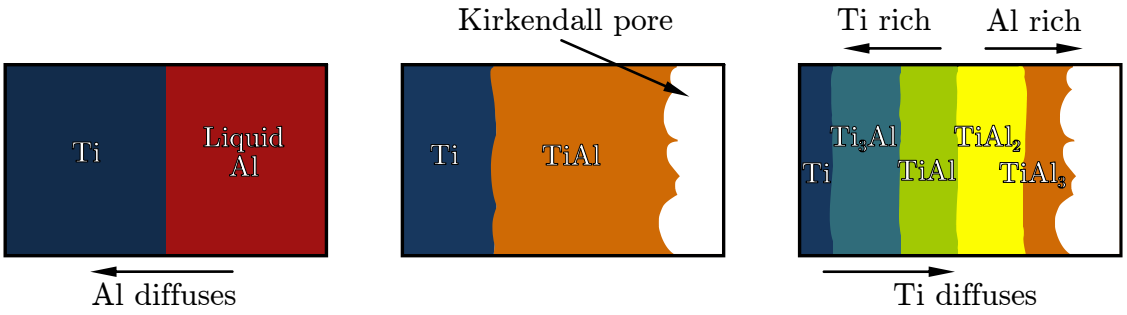

Figure 2.5: Diffusion between liquid aluminium and titanium

the motion of aluminium mass into titanium causes the formation of a special form of porosity, called Kirkendall pores. This effect is well known as the cause of porosity during the diffusion of different metals. After all the aluminium is consumed, Ti is diffused through $TiAl_3$ to form phases richer in titanium until homogenisation occurs.

2.2.7 Impurities in Titanium

The inevitable introduction of impurities occurs during titanium processing, and greatly affects the mechanical properties of titanium. Chlorine often remains as an impurity in titanium because of the chlorination process used to reduce rutile to titanium tetrachloride. During refining and processing, titanium is exposed to a range of atmospheric elements such as C, H, N and O. Furthermore, metallic elements are introduced through tooling. The inevitable introduction of these impurities has an effect on the mechanical properties of the final part.

In its purest form, titanium has a yield strength of around 100 MPa, and so, without impurities, it is not applicable for structural use. Interstitial elements cause defects in the lattice structure of titanium which impede the motion of dislocations. The deformation allowed by the motion of dislocation is restricted by these defects, causing an increase in strength and a loss in ductility. Table 2.3 shows the impurity

Table 2.3: Properties and impurity quantities of commercial grades of titanium (ASTM B 348)

				Composition (wt%)				
		σ_y (MPa)	%el	C	Fe	H	N	O
Grade 1	CP-Ti	170	24	0.08	0.20	0.015	0.03	0.18
Grade 2	CP-Ti	483	15	0.08	0.50	0.015	0.05	0.40
Grade 3	Ti-6Al-4V	828	10	0.08	0.40	0.015	0.05	0.20

levels of commercial pure grades of titanium, and the most common alloy. Excessive quantities of impurities can lead to the loss of ductility. The strength and ductility of commercially pure (CP) titanium is controlled by the level of impurities, mostly oxygen, which has the greatest influence on strength. The introduction of impurities during processing must be controlled to achieve high strength and retain ductility for the application of titanium in mechanical design.

2.3 Titanium Powder Metallurgy

Powder metallurgy is of great interest in the titanium industry because the net-shape part production eliminates much of the costly processing of current methodologies. The conventional production of titanium parts has adopted methods from other metal processing industries. To form dense titanium ingots, the sponge is arc melted in a vacuum. Then typical shaping processes, such as forging, rolling, extrusion, casting and machining, are adapted to fabricate usable products, and often remove up to 90% of the material (Barnes et al., 2009). Furthermore, machining is made difficult because of the high strength and ductility of titanium (Machado and Wallbank, 1990). Powder metallurgy processes

use titanium powder produced from sponge fines, scraps or alloyed ingots, and uses powder densification methods to create near net shape parts. This method avoids costly processing and machining, reducing the cost of titanium parts overall.

The quality of powder metallurgical parts often matches or exceeds properties produced by wrought methods because of the inherent ability to control the microstructure (Wang et al., 2010a). However, the cost of sintered titanium parts remains high. Titanium refinement and powder production are themselves costly multistage processes. To obtain high quality parts requires further elaborate sintering processes which are too expensive for commercial part production (Qian, 2010). Therefore, recent research efforts have been directed towards the simplification of sintering processes.

2.3.1 Sintering

Sintering is the process of consolidating powders in to a solid part by the application of heat or heat and pressure. The densification of a powder is driven by the reduction of surface energy of the powder particles (German, 1996). During sintering necks grow between contacting particles as a result of solid state diffusion. Then pores become rounded and are eventually eliminated. Grain growth also occurs during sintering in order to reduce the grain boundary energy. The sintering of a powder to form a solid part occurs when densification is achieved through solid state diffusion and pore closure, and the microstructure is controlled by grain growth (German and Cornwall, 1996). Solid state sintering is the most basic of sintering methods and final part density relies on the application of temperature and pressure to accelerate the diffusion of the titanium powder (Upadhyaya, 1997).

2.3.2 Titanium Powder Production

Titanium powder metallurgy uses two different methods; Blended Elemental (BE) or Pre-Alloyed (PA) powders. BE powders use a mixture of elemental powders with powders of alloying elements or a Master Alloy (MA), which are sintered to a final uniform composition. PA powders are of a uniform composition and produced from pre-alloyed feedstock. PA powders thus do not require homogenisation to occur during sintering, and form a denser and higher quality part.

The cheapest source of pure titanium powder is sponge fines, which are sifted from sponge and have an irregular shape. These powders can contain impurities from the refining process used to produce them, e.g. Mg or Cl. Pure titanium powder can also be produced using the methods used to make pre-alloyed powders, and thus better control of powder impurities and size is possible.

Pre-alloyed powders are produced from a cast or wrought feed stock metal of the same composition as the desired powder. Some common PA powder production methods are (Upadhyaya, 1997):

- Gas Atomisation (GA);
- Centrifugal atomisation Rotating Electrode Process (REP);
- Hydride-DeHydride (HDH).

Atomisation of metallic powder occurs when molten titanium is injected with an inert gas, which heats and expands before it exits through a nozzle into a collection chamber. Centrifugal atomisation of particles occurs when a titanium anode rotates at high speed and is melted by an arc or plasma arc. The molten metal spheres solidify as they fly away from the anode. GA and REP atomisation both produce spherical annealed powders. The HDH method first makes titanium, pure or alloyed, brittle through hydrogenation and then powder is produced

through crushing or grinding, and subsequently dehydrogenated by heating in a vacuum. The brittle fracture of titanium hydride forms an angular powder. Angular powders allow greater contact between particles and have a greater surface area when compared with spherical particles. Both of these factors promote sintering (Upadhyaya, 1997).

GA and REP both produce spherical powders. These methods create low impurity levels, as the atmosphere is controlled and there is little contact with processing tools. This is ideal for titanium as it is easily contaminated by atmospheric elements. Contamination can occur from the ceramic nozzle or the tungsten electrode used. HDH, by comparison, can increase the oxygen content. However, the HDH process can use a variety of stock material (including scrap or sponge) which reduces the cost.

Titanium PM uses relatively large powders because of titaniums affinity for organic elements C, H, N and O. There is a surface oxide on titanium particles which increases the oxygen content in smaller powders because of their larger surface to bulk ratio, while a smaller particle size promotes sintering (Robertson and Schaffer, 2009). Consequently, there is a limit to the improvement of densification achievable through particle size.

2.3.3 Sintering Techniques

The sintering processes used in the consolidation of titanium parts are (German and Cornwall, 1996):

- Cold (uniaxial) pressing (CP) and free sintering;
- Cold isostatic pressing (CIP) and free sintering;
- Hot (uniaxial) pressing (HP);

- Hot isostatic pressing (HIP);
- CIP then HIP.

CP and CIP consolidation use the application of pressure to create a preform (or green part) which is then sintered in a vacuum furnace. HP uses a die which presses the part during sintering. The heat is often applied by induction to the mould. The use of uniaxial pressure limits the complexity of the part because uniform compaction cannot be guaranteed to all areas of the part. Isostatic pressure can be applied inside a pressure vessel, which represents an additional cost. The increase in complexity of the processes helps to guarantee dense final parts, however they also increase the cost.

2.3.4 Liquid Phase Sintering

An enhanced sintering technique called Liquid Phase Sintering (LPS) uses a liquid phase which surrounds solid particles to encourage densification. LPS is used to densify materials which are difficult to sinter by solid state sintering. The stages of densification during LPS are often described in three stages (German, 1985; Kingery, 1959).

1. Particle rearrangement;
2. Solution precipitation;
3. Solid state bonding.

Initially solid grains are wetted in a liquid phase, which provides a capillary force, helping densification and causing the liquid to infiltrate the pores. Secondly, the mass is rearranged through the absorption and deposition of the solid through the liquid. The rearrangement of the mass causes grains to grow and their shape is driven by the capillary pressures in the liquid. During the final stages, the pores are

eliminated and grain coarsening and bonding occur until solidification upon cooling. Thus, materials which are hard to densify by solid state sintering are encouraged to bond.

LPS can use a liquid which is transient (temporary) or persistent (permanent). Figure 2.6 shows examples of phase diagrams, typical of elements used for LPS. If a composition of elements, of concentration C_P, is sintered from blended elemental or pre-alloyed powders, then upon heating to the sintering temperature, T_S, a liquid phase will precipitate and persist throughout sintering. If a composition of blended elemental powders at concentration C_T, begins to diffuse at T_S, a liquid phase may segregate when diffusion between elements takes place. The liquid phase then solidifies when further homogenisation occurs. Thirdly, intermetallic compounds can be formed by reactive sintering. Blended elements of composition C_R are sintered to form intermetallic AB_X (Figure 2.6). Element B will liquify and wet the solid particles of A, then react to form intermetallics and solidify. This can result in rapid sintering of intermetallic compounds, as the reaction between elements is often exothermic, which leads to rapid heating.

2.3.5 Titanium and Aluminium in Liquid Phase Sintering

The effect of the diffusion between titanium and liquid aluminium during LPS is discussed here. The diffusion and intermetallic compounds of the Ti-Al system have been discussed in Section 2.2.6. A liquid aluminium phase will react with solid titanium to form $TiAl_3$. The motion of aluminium mass causes Kirkendall pores to form in the aluminium phase. The remaining Ti diffuses within $TiAl_3$ to form intermetallics richer in Ti.

The use of aluminium as a liquid phase was reported to cause swelling in titanium sintered compacts by Savitskii and Burtsev (1979). The diffusion of aluminium into titanium causes growth of an intermetallic compound, $TiAl_3$, and formation of

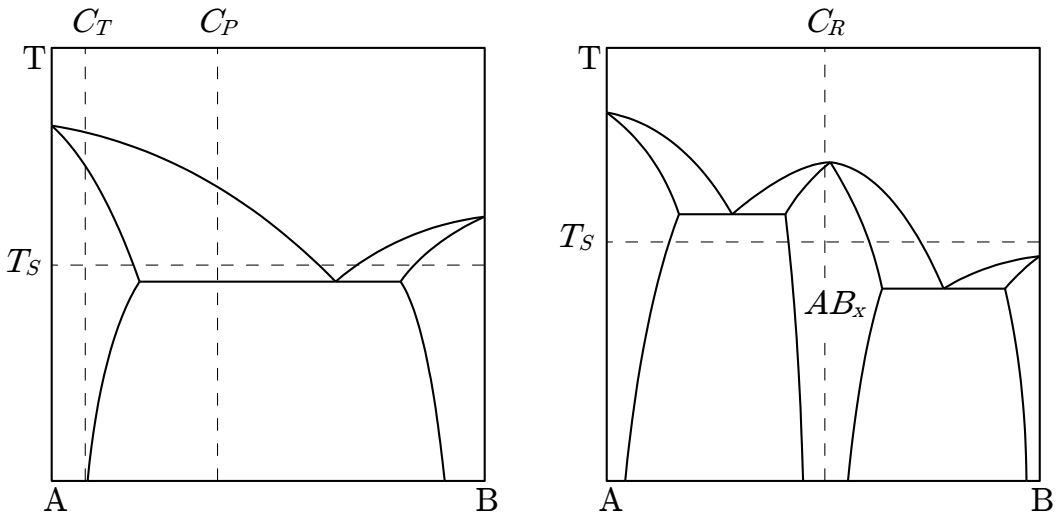

Figure 2.6: Phase diagram examples of transient and passive (left), and reactive (right) sintering, with concentrations C_T, C_P and C_R respectively, sintered at temperature T_S

pores around the titanium particles (Figure 2.7). The diffusion causing the motion of the aluminium mass is so predominant in reactive liquid phase sintering of Ti and Al, that it can be used to advantage to create a permeable open porous Ti-Al microstructure. He et al. (2007) have formed γ-TiAl by reactive sintering, and an open porous structure is left by the Kirkendall effect.

To eliminate pores caused by the Kidendall effect during the reaction sintering of titanium aluminides in a study by Rawers and Wrzesinski (1992), increased temperatures and pressures were required. Ivasishin et al. (1999) improved the densifiction of titanium aluminides using a ball milled titanium hydride powder. The reduced particle size enabled activated diffusion, which led to faster intermetallic formation and densification. To avoid a liquid phase when sintering blended aluminium and titanium (e.g. to form Ti-6Al-4V), the powder mixture can be mechanically milled beforehand. Milling blended powders before sintering begins the reaction between Ti and Al and thus avoids a liquid phase and reduces

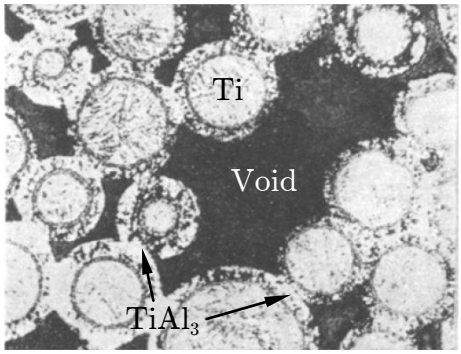

Figure 2.7: Sintered titanium with liquid aluminium causing intermetallic growth around spherical titanium powders (Savitskii and Burtsev, 1979)

the formation of pores through the Kirkendall effect (Ivasishin et al., 2002; Bolzoni et al., 2012a).

The formation of pores due to liquid aluminium in the sintering of titanium is well known to be detrimental to densification. The Kirkendall effect in the reaction to form $TiAl_3$ leaves a porous microstructure. The formation of intermetallics occurs at the surface of the Ti particles and therefore depends on the size of the particles. Savitskii and Burtsev (1981) found that above a certain titanium powder size (45 μm), the growth of the intermetallic layer on the titanium particles caused the specimen to swell. *Thus, an aim of this thesis is to study the effect of titanium powder size in conjunction with a liquid aluminium phase to improve densification during sintering.*

Past studies related to LPS of titanium with aluminium have only used pressure assisted sintering for the reaction synthesis of titanium aluminides (Rawers and Wrzesinski, 1992; Paransky et al., 1996). In these studies, pressure assistance was required to reduce pore formation from the Kirkendall effect. During the reaction of Ti and liquid Al, the liquid rearrangement could be rapid with pressure assistance. Thus, one of the aims of this thesis is to study the effect of pressure assistance during titanium LPS with aluminium.

2.3.6 Thermo-hydrogen Processing of Titanium

A method used to reduce the cost of producing titanium powder is thermo-hydrogen processing. This has already been mentioned in Section 2.3.2 in terms of the production of titanium powder. Titanium is ductile and strong, making it difficult to process into powders. Hydrogen in titanium, above a certain concentration, increases brittleness. Titanium is usually hydrogenated at approximately 500°C under gaseous hydrogen to form TiH_2 (Evard et al., 2005). In this brittle state, TiH_2 is used for PM processing. Hydrogen is then removed from titanium by heating under vacuum. The ease of adding and removing hydrogen from titanium creates a convenient method to embrittle titanium as required for processing (Senkov and Froes, 1999).

Thermo-hydrogen processing of titanium can be used in various ways in sintering. Initially, brittle TiH_2 is convenient for ball milling into fine powder, which can then be dehydrogenated before sintering. Secondly, a ball milled TiH_2 powder can be used directly in sintering and dehydrogenation occurs during the sintering process. Thirdly, a controlled hydrogen atmosphere can be used during sintering to refine the microstructure (Fang et al., 2012). Sintering with dissolved hydrogen stabilises β-Ti at lower temperatures and allows for a controlled eutectoid decomposition upon cooling. The grain size is reduced when α-Ti and γ-TiH_{1-2} phases precipitate in β-Ti. Then the hydrogen is removed from the atmosphere and additional phase transformations occur during dehydrogenation to further refine the microstructure. Titanium alloys, using pre-alloyed powders, can also be processed by these methods.

2.3.7 Properties of TiH_2

The phase diagram of the hydrogen-titanium system is shown in Figure 2.8. Hydrogen exists in titanium as an interstitial solid solution as (1) HCP α and as

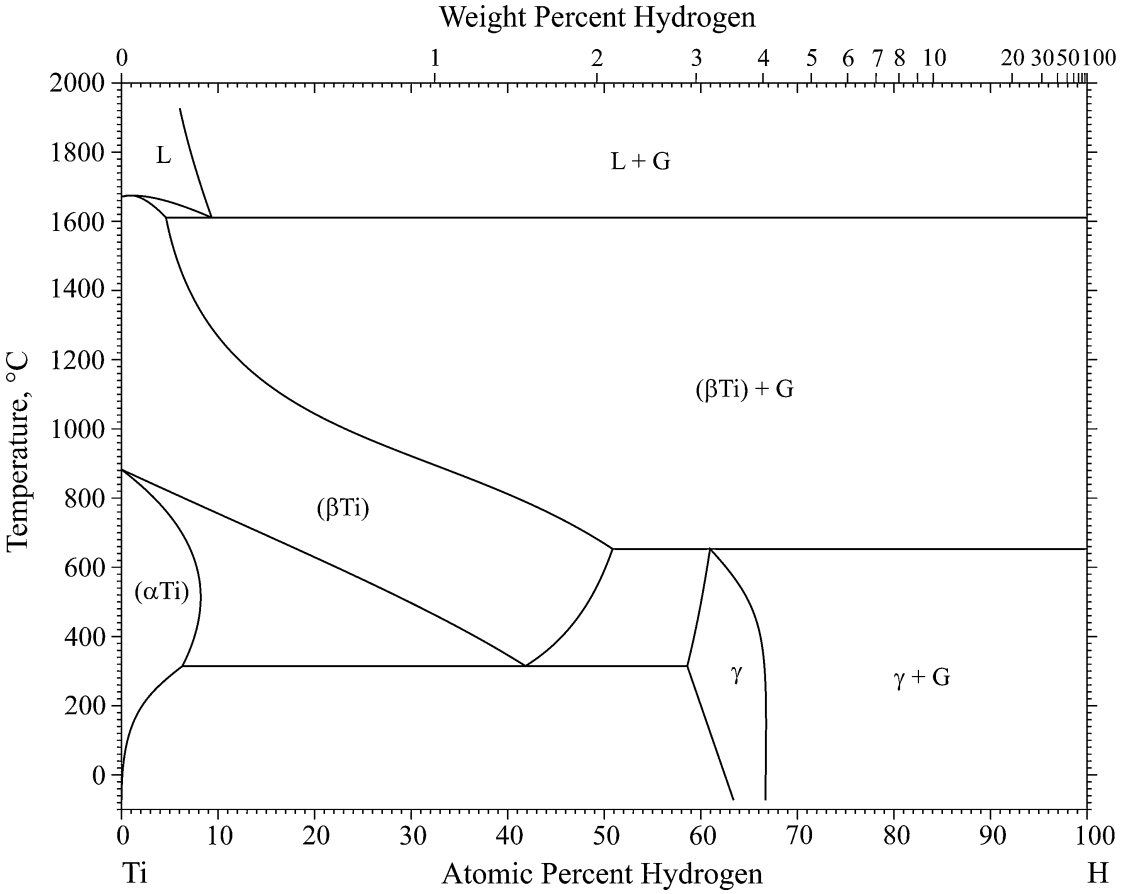

Figure 2.8: Ti-H phase diagram (Okamoto, 2011)

(2) BCC β, and at higher concentrations, (3) γ, an FCC. At room temperature α-Ti has low solubility of hydrogen, so then γ hydride precipitates as γ-TiH_2 (Numakura and Koiwa, 1984). A eutectoid ($\beta \rightleftharpoons \alpha + \gamma$) occurs at 300°C.

The structure of titanium and hydrogen are as that of α and β titanium with hydrogen in solid solution in random interstitial sites. In γ-TiH_2, titanium forms an FCC structure with a lattice parameter $a = 4.41\mathring{A}$ (Figure 2.9). Hydrogen atoms occupy tetrahedral sites, with possible vacancies when the H:Ti <2 (San-Martin and Manchester, 1987).

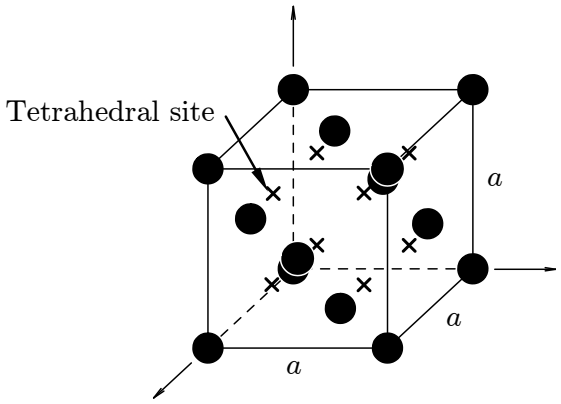

Figure 2.9: FCC crystal structure of γ-TiH_2

2.3.8 HDH Powder

Using the HDH method to produce a pure Ti powder by ball milling TiH_2, and then dehydrogenating it under a vacuum before sintering, delivers a reduced cost (McCracken et al., 2010). The cost of producing HDH powder is reduced below that of the rotating electrode process, atomisation and electrolysis because HDH powder production can occur in larger batches than the other powderisation methods, and can be produced from any raw feedstock.

2.3.9 Sintering TiH_2

The use of direct sintering of ball milled TiH_2 reduces the powder cost further and has been shown to increase densification. The already low cost of HDH is further reduced by the use of TiH_2 directly from the ball milling process, eliminating the dehydrogenation process (Saito, 2004). Dehydrogenation before sintering also involves a controlled passivation stage where the HDH powder is slowly exposed to oxygen to develop a passive oxide layer safely and avoid combustion.

Sintering from an initial TiH_2 powder can increase the sintering kinetic, increasing the density of sintered parts (Wang et al., 2010b; Ivasishin et al., 1999, 2002; Pankevich et al., 1986). The dehydrogenation of TiH_2 that occurs during

sintering aids densification by leaving a freshly dehydrogenated surface. (Wang et al., 2010b; Savvakin et al., 2012). During sintering of titanium, densification begins to accelerate at approximately 700°C due to the dissolution of the oxide layer surrounding the titanium particles (Qian, 2010), allowing faster solid/solid diffusion across particles. Sintering TiH_2 helps to lower the temperature at which the oxide layer is reduced. Dehydrogenation begins upon heating under a vacuum at approximately 400°C (Sandim et al., 2005), and initiates the reduction of the oxide layer (Pankevich et al., 1986). The TiO_2 layer on the surface of the particles is reduced when it interacts with hydrogen liberated by the dehydrogenation of TiH_2 (Ivasishin et al., 2011):

$$TiO_2 + 4H \rightarrow Ti + 2H_2O. \tag{2.2}$$

Furthermore, diffusion is enhanced in ball milled powder because of the high defect density caused by the mechanical work of brittle TiH_2 (Ivasishin et al., 1999), which also exists in HDH powder, albeit reduced by the dehydrogenation heat treatment it undergoes.

2.3.10 Dehydrogenation of TiH_2

TiH_2 begins to dehydrogenate upon heating at 400-600°C depending on its form. The evolution of hydrogen from TiH_2 is shown to be controlled by detrapping of hydrogen (Asavavisithchai et al., 2007), while further barriers for the evolution of hydrogen are the diffusion through the lattice and grain boundaries. The dehydrogenation of TiH_2 has been studied by thermal analyses (DSC, Thermogravimetric Analysis) and XRD. Study of the effects of heating on the desorption of hydrogen shows that slower heating rates lower the onset of desorption, and that the rate of desorption increases with isothermal temperature

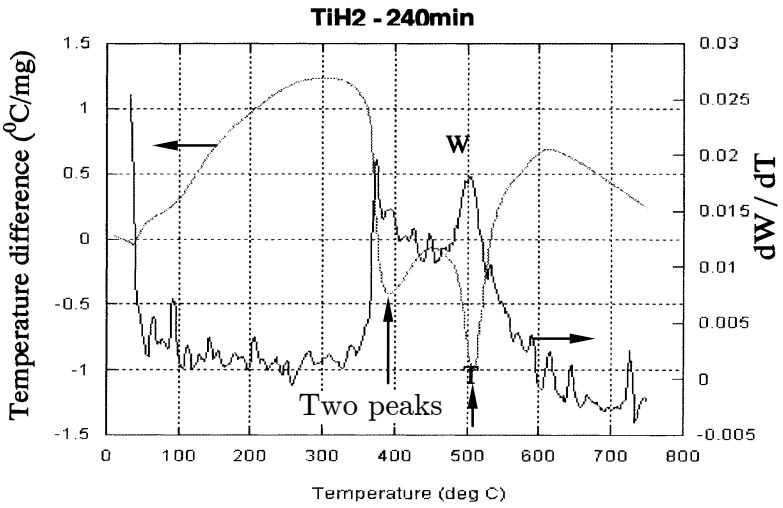

Figure 2.10: DSC and TGA of ball milled TiH_2 (Bhosle et al., 2003)

(Sandim et al., 2005). Studies of the effect of ball milling of the dehydrogenation of TiH_2 show that it increases the rate of desorption. Comparison of powder produced by mechanical milling of TiH_2 with powder produced by hydrogen absorbtion by Zhang and Kisi (1997) shows an increase in desorption kinetic in milled powders. The reduction of powder size through ball milling was shown to reduce the onset of dehydrogenation by Bhosle et al. (2003). In the study by Bhosle et al. (2003) the dehydrogenation was shown to occur in a 2 stage process. DSC and TGA analysis of ball milled powders observes two peaks (Figure 2.10). The two stage process is explained by Bhosle et al. (2003) and Wang et al. (2010b) as the phase transitions:

$$\epsilon\text{–}TiH_{1.92} \rightarrow \gamma\text{–}TiH_{(0.7-1.5)} + \beta\text{–}Ti \rightarrow \alpha\text{–}Ti \tag{2.3}$$

Analysis of the ball milled TiH_2 powders in these studies has shown the reduction of particle size and the reduction of crystallite size observed by SEM and XRD respectively. Thus, faster dehydrogenation is explained by (i) smaller particles having a greater surface area, giving a faster surface evolution from the

particle bulk, and (ii) the high defect density allows for faster diffusion paths. The separation of peaks occurs because the intermediate phase, $TiH_{(0.7-1.5)}$, is slower to react than TiH_2. As discussed in Section 2.3.9, the dehdydrogenation of TiH_2 during sintering increases densification, and the kinetic of desorption is increased by ball milling.

2.3.11 Ball Milling of TiH_2

Ball milling uses the mechanical energy of balls to grind a material. The process is used to synthesise, mix and reduce the powder size of compounds. TiH_2 can be ground to a fine powder by ball milling because of its brittle nature. Ball milling is of interest in the production of TiH_2 powders because it is better suited to a laboratory scale when compared with gas atomisation or the rotating electrode process. Ball milled TiH_2 can then be used directly or dehydrogenated before sintering.

Ball milling reduces the particle size of TiH_2 and can introduce impurities. A vial is prepared containing the material and balls, and is filled with a gas or liquid medium. In a planetary ball mill, a cylindrical vial is attached eccentrically on a rotating platform, and the vial is rotated on its axis in the opposite direction. The mechanical grinding of TiH_2 occurs by impact, shear, or friction through ball-to-ball or ball-to-vial collisions. The vial and ball material should be harder than the material to be ground. However, the impact between ball and vial unavoidably introduces contamination. Thus, the vial and ball material used will be introduced into the powder. Ball milling must be performed under an inert atmosphere to stop the pickup of atmospheric elements. The stages of hydrogenation and ball milling can be combined into one step to reduce contamination. TiH_2 can be synthesized by ball milling Ti in a hydrogen atmosphere (Bobet et al., 2003).

The effect of ball milling on brittle TiH_2 is the reduction of particle size and the increase in lattice defect density. The majority of particle size reduction occurs in

the first few minutes. Bhosle et al. (2003) reduced TiH_2 40 μm to less than 100 nm in 2 minutes of ball milling, and then to under 40 nm in the next 15 minutes. After the reduction of powder size, the ball milling energy introduces defects into the TiH_2 through the fracture and re-welding of particles. The small particle size and high defect density in ball milled TiH_2 can lead to a higher sintering kinetic, as previously discussed in Sections 2.3.10 and 2.3.9. Current research efforts show that TiH_2 improves sintering by conventional methods and temperatures, and have not investigated the potential of particle size reduction by ball milling to reduce temperatures, nor the limitations imposed by the dehydrogenation process. The characteristics of ball milled TiH_2 are studied in this thesis in order to understand their potential improvement to and limitations on sintering.

2.4 Critical Review of Current Research

Current research focuses on the general improvement of conventional sintering processes, such as CP and sinter, and the use of different starting powders. The methods of refinement and powder production are studied in order to reduce the cost. However, the process still uses multiple stages and is expensive. Significant research efforts are currently focused on improved techniques such as the use of thermo-hydrogen processing, LPS and advanced sintering techniques such as spark plasma sintering and microwave sintering. Except for thermo-hydrogen processing, which has been shown to simplify powder processing and enhance sintering (Froes, 2012), the employment of advanced techniques adds complexity and cost to titanium parts. Table 2.4 shows the properties of sintered titanium using a variety of titanium alloys fabricated by different authors (Ivasishin et al., 1999; Bolzoni et al., 2012a,b; Low et al., 2007; Liu et al., 2006; Wang et al., 2010b; Azevedo et al., 2003; Luo et al., 2013). Where high densities are achieved, it is through the

sufficient application of temperature and time. If pressure is applied during sintering, the duration can be reduced whilst still achieving high density. High strength is achieved in alloys with all methods. The ductility reported is often below that of wrought alloys because of the increased impurity levels introduced through processing. The improvement of sintered density is reported with the use of TiH_2 when compared with other powders. Thus, the current research focus is on simple powder metallurgical techniques such as CP and sinter, and the use of simple BE powders with HDH or TiH_2 powders.

2.5 Conclusion

This Chapter has reviewed titanium and the use of PM to reduce fabrication costs. The cost of titanium production remains high because of the multi-stage reduction process from ore to solid ingot. Current research towards continuous reduction methods are aimed at reducing this cost, and are focused on powder production because of the additional benefits of PM. The near net-shape part production of PM avoids ingot production and eliminates costly machining and waste. However, the consolidation of powders into high quality parts still requires expensive methods of sintering, and is another current area of research for the cost reduction of titanium.

The scope has been identified for the improvement of two specific sintering methods which will be studied in this thesis: (1) sintering ball milled TiH_2, and (2) titanium liquid phase sintering using aluminium. The thermo-hydrogen processing of titanium provides a novel method for the production of titanium powder. The sintering of TiH_2 powder is also shown to improve densification. The dehydrogenation of TiH_2 during sintering causes the reduction of the oxide layer, which decreases the temperatures at which densification commences. Furthermore, the ball milling of TiH_2 is shown to increase the dehydrogenation kinetic, which

Table 2.4: Properties of titanium sintered by various techniques

Ti Alloy	Powders	Method	Time (minutes)	Temperature (°C)	Cold compaction (MPa)	Sintering pressure (MPa)	Relative density (%)	σ_y (MPa)	%el	Reference
Ti-6Al-4V	TiH_2	CP and Sinter	Not known[a]	1350	300-1000	-	99	970	6	(Ivasishin et al., 2002)
Ti-6Al-7Nb	HDH and MA	Hot Pressing	30-60	900-1300	18	30	99	1000	2	(Bolzoni et al., 2012a)
Ti and Ti-6A-4V	TiH_2 or HDH and PA	Hot Pressing	15	1100-1300	-	50	>99	-	-	(Bolzoni et al., 2012b)
Ti-5Si and Ti-xNi	HDH and BE	CP and Sinter (Si and Ni LPS)	120	1100-1350	200-600	-	90	-	-	(Low et al., 2007)
Ti-xAl-xFe-xMo-xNd	HDH and MA	CP and Sinter	180	1200-1350	200	-	95-99	1000	6	(Liu et al., 2006)
Ti-6Al-4V	TiH_2 and MA	CP and Sinter	240	1200	100-800	-	>99	-	-	(Wang et al., 2010b)
Ti	TiH_2 and HDH	CP and Sinter	30	1300	100-200	-	>99	-	-	(Azevedo et al., 2003)
Ti	TiH_2 and HDH	Microwave Sintering	30-60	1300	200	-	93-97	400-600	13-19	(Luo et al., 2013)

[a]Unfortunately, for the sintering time used by Ivasishin et al. (2002) another publication was referenced, which was unobtainable by the author.

indicates the potential to decrease sintering temperatures. From the review of the state of the art, the application of TiH_2 for the densification of titanium at low temperatures is possible. Therefore, the consolidation and dehydrogenation of ball milled TiH_2 during sintering at low temperatures will be studied in this thesis.

The use of a liquid aluminium phase during titanium sintering has previously been shown to cause part swelling due to the formation of Kirkendall pores. The diffusion between titanium and liquid aluminium creates a stable intermetallic skeleton around Ti particles, which reduces densification. This process is not well understood under pressure assisted sintering. Thus, pressure assisted sintering of titanium using aluminium LPS will be studied in this thesis.

Consequently, it is the focus of this present research to reduce the sintering parameters by studying:

1. The process of densification using ball milled TiH_2 as a starting powder;

2. The effect of a liquid aluminium phase with a reduced powder size during pressure-assisted sintering.

Chapter 3 further elaborates the research aims, which are designed to improve the understanding of these methods. These aims are achieved through an experimental study, using methods presented in Chapter 4 and the results are presented in Chapters 5 and 6.

Chapter 3

Research Aims

Chapter 2 presented the background of titanium and the production and powder metallurgy techniques currently under research. These techniques have the potential to reduce the cost of titanium production. Research is needed to improve the understanding of these techniques to produce high quality parts and reduce costs. From these gaps in current research identified in Chapter 2, this Chapter formulates the aims of the current research and provides justification as to where there is potential to increase the efficiency of sintering.

1. The effect of ball milling on the reduction of TiH_2 particle size is known to accelerate dehydrogenation (Bhosle et al., 2003), and the direct sintering of TiH_2 can increase densification during sintering (Wang et al., 2010b; Ivasishin et al., 1999, 2002; Pankevich et al., 1986). The effect of fine ball milled powders on the improvement of densification has not yet been investigated. Therefore firstly, TiH_2 powder will be synthesised by ball milling for the study of the effect of milling duration on the reduction of particle size and dehydrogenation kinetic, as well as the introduction of metallic impurities.

2. While the benefit of directly sintering TiH_2 is known, there is not sufficient understanding of the capability of this technique to reduce the required

sintering parameters, which relates to the global objective to reduce the cost of titanium production. Furthermore, previous studies of sintering TiH_2 have found complete dehydrogenation (Bolzoni et al., 2012a; Ivasishin et al., 2002; Wang et al., 2010b; Azevedo et al., 2003): the required sintering parameters for complete dehydrogenation are not known to date. Therefore secondly, the effect of the duration of ball milling on the densification and dehydrogenation during induction hot press sintering at a low range of temperatures (700 to 900°C) is investigated. The hardness of these specimens will be tested to understand the relationship between process and part quality.

3. The use of aluminium in LPS of titanium is well known to cause Kirkendall pores (Liu et al., 2000, 2006; Savitskii and Burtsev, 1979). These studies have only used free sintering. Pressure assisted-sintering has only been used in reactive sintering of intermetallic compounds like TiAl (Lee et al., 1997; Taguchi et al., 1995; Yang et al., 1996). The application of pressure assistance for aluminium LPS of titanium has not been studied. Therefore, thirdly, the effect of aluminium concentration during LPS of titanium by induction hot press will be investigated at a range of temperatures above the melting point of aluminium (700 to 900°C).

4. The effect of LPS is largely controlled by the diffusion between the liquid and solid phases at the solid particle surface. Thus, the specific surface area is of importance during LPS. It has been reported by Savitskii and Burtsev (1981) that increased titanium particle size decreases sintered density. Therefore, finally, it is of interest to study the effect of the reduction of titanium particle size on densification during LPS. The densification and phase formation during sintering of fine ball milled TiH_2 powders will be compared with a larger commercial powder. A ball milled TiH_2 will be dehydrogenated

(an HDH powder) and used for the study of the effect of particle size without the influence of dehydrogenation during sintering.

The investigation of these aims will improve understanding of the advantages and limitations of sintering ball milled TiH_2. The study of the LPS of titanium with aluminium using pressure assistance will uncover the improvements in densification possible, as opposed to the detrimental effects seen previously, caused by the Kirkendall effect. Validating this technique will enable low temperature sintering to reduce the cost of producing titanium.

Chapter 4

Materials, Methods and Procedures

4.1 Introduction

This chapter describes the methods and equipment used for the synthesis of ball milled TiH_2, and the hot press sintering of titanium with and without the addition of aluminium. The characterisation methods are described of the TiH_2 powder particle size, morphology and dehydrogenation kinetic, as well as methods for characterisation of density, phase composition, hardness and flexural strength of the sintered titanium specimens. The results of the experimental study of the sintering of ball milled TiH_2 and titanium LPS with aluminium are presented in Chapters 5 and 6.

4.2 TiH_2 Powder Synthesis

This section describes the method used in this current study to synthesise and characterise TiH_2 powders. Ti sponge is hydrogenated and then planetary ball

Figure 4.1: Hydrogen oven

milled. TiH_2 powder is then used directly in sintering or dehydrogenated before sintering in a vacuum oven. These powders, and commercial powders, are characterised for their particle size distribution, morphology, impurities and dehydrogenation kinetic.

4.2.1 Hydrogenation of Titanium

In order to obtain TiH_2 as a starting material for ball milling, pure titanium was hydrogenated. The reaction of solid titanium and gaseous hydrogen is slow at atmospheric conditions and is greatly accelerated by temperature and pressure. Titanium sponge (Strem Chemicals, 99.8% purity) was placed inside a reaction chamber under a pressurised atmosphere of hydrogen (see Figure 4.1). The titanium sponge was subjected to 40 bar of hydrogen at 500°C for 3 hours. The hydrogen atmosphere was recharged regularly when the absorption of hydrogen into the titanium sponge had decreased the pressure of the chamber. After cooling, the TiH_2 sponge was handled under an argon atmosphere and tested by XRD.

Figure 4.2: Planetary ball mill

4.2.2 Ball milling of TiH_2

The ball milling of TiH_2 was performed at different durations in order to obtain a range of powders to study the effect of particle size and ball milling on the densification and dehydrogenation of TiH_2 during sintering. The mechanical grinding of the starting TiH_2 sponge was performed using a planetary ball mill (Fritsch Planetary Mill) shown in Figure 4.2. The ball milling method is based on extant methods used in a study by Bobet et al. (2003). The speed of rotation of the ball mill was set at 250 rpm. The duration of ball milling was varied from 5-180 minutes in order to obtain powders of various particle size. The powder was milled in a stainless steel vial with hardened steel balls of 10 mm in diameter, with a 10:1 ball to powder mass ratio. The vials were filled with 10 bar of hydrogen. After each 30 minutes of ball milling, the vials were recharged with hydrogen. The materials and vials were opened and handled inside an argon glove box to reduce atmospheric contamination.

Figure 4.3: TiH_2 sponge with stainless steel balls in a ball mill vial

4.2.3 HDH Powder

To eliminate the effect of hydrogen during sintering, a ball milled powder is dehydrogenated inside a vacuum oven. This powder, called Hydride De-Hydride (HDH) powder, keeps a fine particle size produced through ball milling, and only pure titanium remains. In this study, TiH_2, ball milled for 180 minutes, is placed inside an oven under a vacuum produced by a rotary pump of 10^{-2} torr and continuously pumped and heated to 500°C for 3 hours. The HDH powder is then tested for hydrogen content by XRD. The XRD of the HDH powder shows no detectable TiH_2 (as shown in Appendix B).

4.3 Material Characterisation

4.3.1 Granulometry

A laser granulometer (see Figure 4.4) was used to measure the particle size distribution of the ball milled powders. Inside the granulometer a fluid medium is used to suspend the powders and is pumped continuously through the path of a laser. The diffraction of the laser as it passes each particle is indicative of the

Figure 4.4: Mastersizer 2000 laser granulometer

particle size and the angle of diffraction is measured by receptors. Distilled water was used as the fluid and ultrasound (1-2 W) was used to disperse the particles and break agglomerations.

4.3.2 X-Ray Diffraction

Study of the ball milled TiH_2 powders by X-Ray Diffraction was performed in order to see the phases and crystallite size. The phase identification by XRD is used to semi-quantify the change in mass percentage of hydrogen due to ball milling. A crystallite is the volume of a solid where the atomic structure is homogeneously orientated. The crystallite size of the compound is related to the width of the XRD peaks observed. The width of a peak, β [$^{\circ}\theta$], of an XRD pattern is inversely proportional to the crystallite size, L [nm] (Scherrer, 1918):

$$\beta = \frac{K\lambda}{Lcos\theta} \tag{4.1}$$

The Scherrer constant, K, depends on how the width of the peak is measured. $K = 0.94$ if the width is measured as the full width at half maximum (FWHM). The wavelength, λ [nm], is that of the incident X-rays. The angle, θ, is the angle of

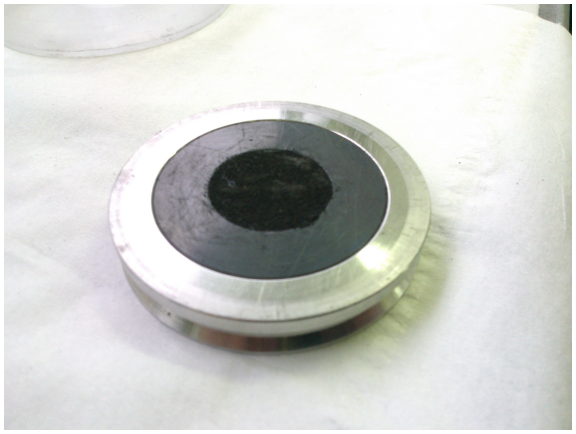

Figure 4.5: X-Ray diffraction sample holder

the peak.

Powder samples are prepared by applying the powder to a double-sided adhesive in the centre of a sample holder (Figure 4.5). Solid sintered specimens are placed in the centre of a sample holder using Plasticine. XRD was performed using a PANalytical XPert Pro (0.028°/ step from 8° to 80° and 10 s/step).

4.3.3 ICP

The contamination introduced from the ball milling equipment into the synthesised powders is measured by an Inductively Coupled Plasma Optical Emission Spectroscopy (ICP-OES). A solution of dissolved powder is passed through the flame of the ICP which ionises the atoms. The repeated ionisation gives off radiation of a wavelength characteristic to each element. The radiation produced from the solution in the plasma is separated and its intensity is measured. The intensity of radiation given by the solution is compared with a solution of a known concentration of the element under analysis and an elemental concentration is calculated.

The ball milled powders were prepared for ICP-OES by dissolving them in a solution of acid. Microwave-assisted acid dissolution was used to dissolve the TiH_2

powder completely. Previous attempts using concentrated acids at atmospheric temperatures and pressure, such as nitro-hydrochloric acid (HNO_3 + 3HCl), sulphuric acid (H_2SO_4 96% concentrated) and hydrochloric acid (HCl), were unsuccessful. Microwave dissolution heats the solution directly inside a sealed vessel, which becomes pressurised, enabling faster dissolving of materials in acid. 25-30 mg of TiH_2 powder was mixed with 30 mL of concentrated (38%) HCl for microwave digestion. A CEM MARS5 microwave was used, as shown in Figure 4.6. The solution was placed in a closed vessel with pressure and temperature control. The microwave was programmed to heat up to 160°C for 10 minutes, and then held at 160°C for 30 minutes before free cooling. The pressure was measured to reach 18-20 bars inside the vessel. After microwave digestion, the solution was diluted to 100 mL with distilled water. This solution was used to test for Fe, Mg and Cr at this concentration. The solution was diluted again by mixing 18 mL of solution in 100 mL of distilled water in order to test for Ti, because, in a more concentrated solution, the concentration of Ti will fall outside the calibration curve of the ICP-OES. The measured concentrations of the impurities are compared with the concentration of titanium, and the mass percentage of each impurity is calculated.

4.3.4 Scanning Electron Microscopy

Visual study of the powders and microstructural and phase analysis of the sintered specimens was performed using Scanning Electron Microscopy (SEM). SEM uses a focused beam of electrons which interacts with a specimen. The electrons reflected by inelastic collision with the electrons of the valence/conduction band are called Secondary Electrons (SE). SE thus gives a topographical image of the sample. Electrons which are scattered elastically by the electron field of an atom, are called Backscattered Electrons (BSE). Heavier atoms scatter more electrons and thus BSE shows the elemental composition. During SEM, bombardment from electrons

Figure 4.6: CEM MARS5 microwave

requires that the charge be carried away from the specimen, thus the sample and all connecting components must be electrically conductive. Charge build up on specimens during SEM can lead to poor image quality. To increase the surface conductivity of samples, a conductive coating was applied when necessary. The SEM was performed using a TESCAN VEGA (Figure 4.7).

4.3.5 Differential Scanning Calorimetry

The TiH_2 powders were studied by Differential Scanning Calorimetry (DSC) to anticipate how they will dehydrogenate during sintering. DSC is a technique used to measure the thermal energies required for the chemical reactions of materials. DSC measures the amount of energy required to heat a sample constantly and compares this result with the energy required to heat a reference. This difference in

Figure 4.7: TESCAN scanning electron microscope

energy measured is then the energy given or used by a material to undergo a known reaction. The dehydrogenation of TiH_2 is endothermic, which will be measured by DSC. The strain in the lattice introduced by ball milling can also be annealed and recrystallisation can occur during heating, reducing the amount of energy required to heat, which will show as an exothermic peak. Complete dehydrogenation is desired as hydrogen causes titanium to be brittle.

The DSC analysis was performed using a Setaram Sensys Evo, as shown in Figure 4.8. Approximately 23 mg of loose or previously cold compacted ball milled TiH_2 powder was used. The powder was placed in an alumina (Al_2O_3) sample holder and heated at 10 K/min up to 580°C under a flow of argon.

To study the effect of ball milling on the dehydrogenation of the TiH_2 powders, the loose powders ball milled for different durations, were placed in the alumina sample holders and examined by DSC. The effect of compaction pressure on the

Figure 4.8: Setaram Sensys Evo differential scanning calorimeter

dehydrogenation of TiH_2 was also studied. TiH_2 powder was compacted in a cylindrical die before DSC. The powder compact formed was fractured, and a piece of approximately 23 mg was placed in the alumina sample holder. Cold compacts of TiH_2, ball milled for 180 minutes, compressed under 40 MPa and 80 MPa, were compared with loose TiH_2, ball milled for 180 minutes.

4.4 Powder Preparation

The titanium powders used in the experimental study of sintering (ball milled TiH_2, HDH commercial Ti powder) are mixed with an atomic percentage of aluminium from 0 to 75. The mass of each powder required for a given atomic percentage of aluminium is calculated, shown in Appendix C. Once the powder is measured, it is mixed in a Turbula 3D-mixing machine (see Figure 4.9) for 30 minutes at 50 rpm.

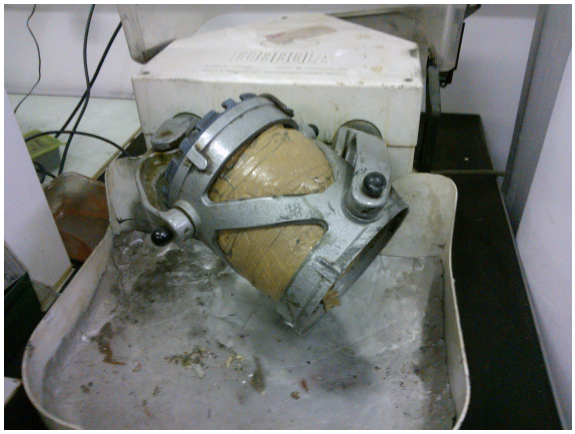

Figure 4.9: Turbula 3D mixing machine

4.5 Hot Press Sintering

The sintering of TiH_2 was performed using a hot induction press. A high frequency current induces an oscillating magnetic field around a copper coil through which it flows. A mould of electrically conductive material is placed inside the copper coil and the magnetic field induces an oscillating electric current in the mould. The local flow of electricity is met with resistance from the material and heating occurs. Induction causes heating of the outside of the mould first and the sintering part as a result. Cooling water flows through the induction coil to reduce the temperature of copper coil.

4.5.1 Induction Hot Press

The induction hot press used, shown in Figure 4.10, was fabricated by the laboratory, based around a Celes induction generator. The induction coil is inside a sealed vacuum chamber. The chamber has a manual release valve, thermocouple hole, pressure gauge and hydraulic piston. The hydraulic piston is operated by a hydraulic hand pump and the pressure is read by a manual gauge. The chamber is cooled by flowing water in copper coils on the outside of the chamber. The heating of the

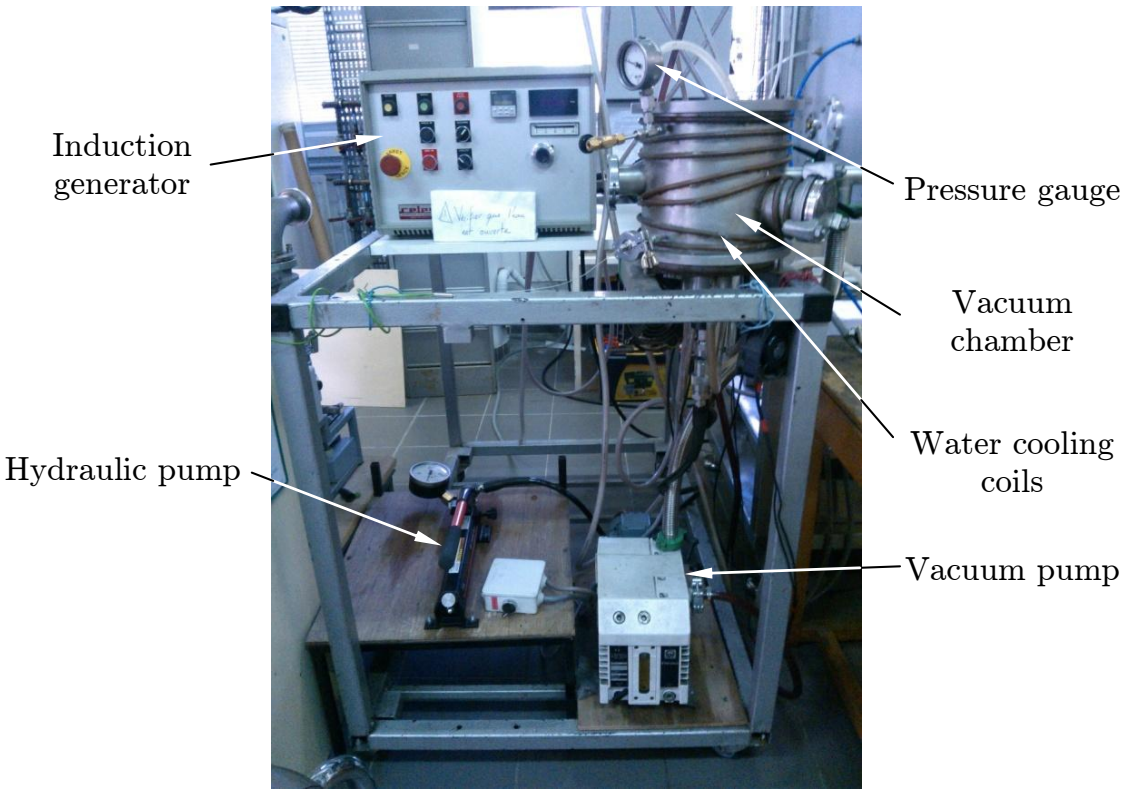

Figure 4.10: Induction Hot Press

mould by induction is controlled by adjusting the power. The heating is rapid, reaching holding temperatures in several minutes. Once the holding temperature is reached, the power is adjusted continuously to keep the temperature constant.

Inside the vacuum chamber, the mould rests on the hydraulic piston at the centre of the induction coil, as shown in Figure 4.11. The mould used is machined from graphite. As steel is ferromagnetic, its ability to be heated by induction is higher than graphite. However, graphite is stable at high temperatures, up to 3000°C, whereas a steel mould is not stable at the temperature ranges chosen for this experiment (700-900°C). Carbide moulds are also common for induction moulds, however their cost is higher compared with graphite. The mould is shown inside the chamber in Figure 4.12. The thermocouple hole reaches near to the sample to measure the temperature of the sample accurately without

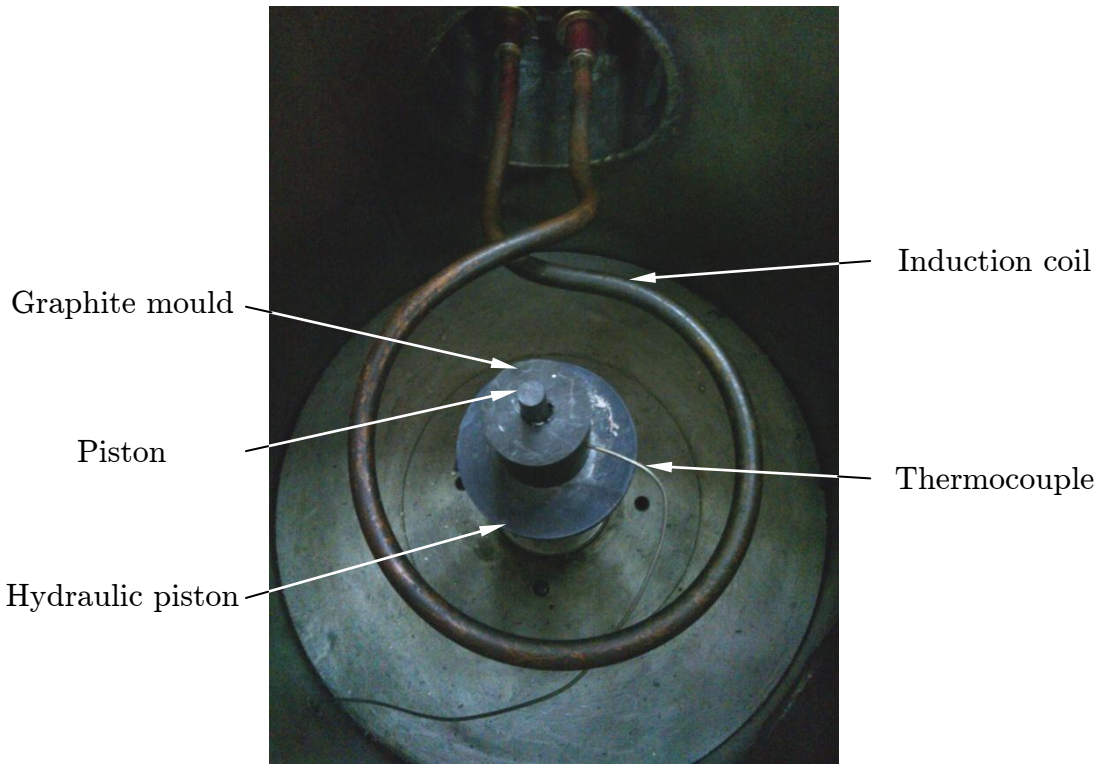

Figure 4.11: Hot induction press experimental setup inside the vacuum chamber

compromising the strength of the mould.

4.5.2 Mould Preparation

The inside of the graphite mould is lined with Papyex graphite paper to reduce sample contamination and to ensure that the sample can be removed after sintering without destroying the mould or sample. The mould is also lined at the top and bottom of the sample.

The prepared mould is placed on a balance, and the mass of the powder, as prepared in Chapter 4.4, is measured as it is added to the mould. Then the top disc of graphite paper is added and the mould is closed with the piston. The mould is then loaded into the vacuum chamber, the thermocouple is placed in the mould, and the chamber is sealed.

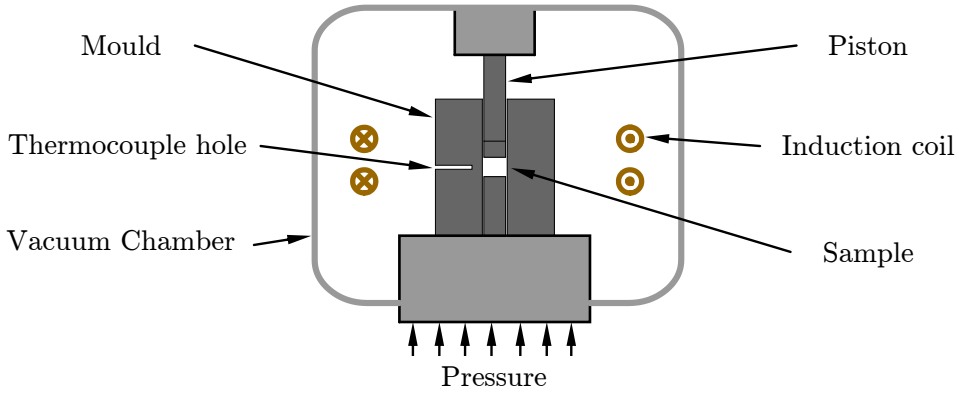

Figure 4.12: Hot induction press schematic

4.5.3 Induction Hot Press Procedure

Once the mould is ready inside the sealed chamber, the vacuum pump is started. A primary vacuum is achieved by waiting 10 minutes. The cooling water for the chamber and induction coil is turned on. The induction heating is started and the power is increased. The thermocouple temperature is monitored continuously and recorded each minute during heating. Once the holding temperature is reached, the induction power is reduced to hold the temperature stable. Uniaxial pressure is applied by the hydraulic hand pump. The applied pressure is monitored during densification and is adjusted to maintain a constant pressure. Once holding duration is reached, the induction power is stopped and the mould is allowed to cool naturally inside the vacuum chamber. Figure 4.13 shows the typical heating and cooling profiles achieved by the hot induction press. Once the mould is below 100°C, the vacuum pump is stopped and the chamber is opened. The sample is ejected from the mould using a hydraulic press.

Thermocouple verification

The verification of the thermocouple was performed by sintering aluminium at 650°C, to ensure that the temperature of the sintered material was not higher than

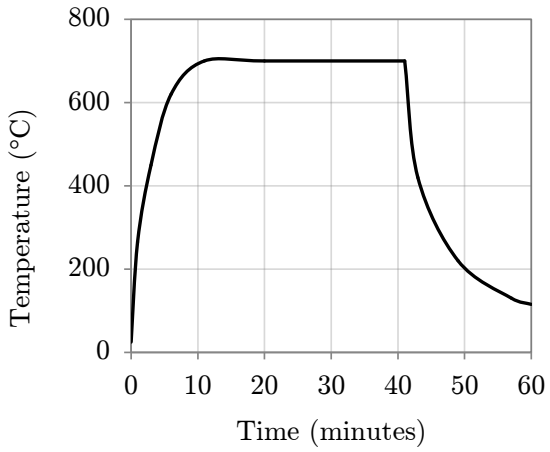

Figure 4.13: Typical temperature graph of the hot induction press

that measured by the thermocouple. The thermocouple should be sufficiently close to the sintering powder to measure its temperature accurately, without compromising the strength of the mould. During sintering at 650°C, aluminium would melt if the temperature inside the mould were greater than the melting temperature of aluminium of 660°C. If this occurs, the aluminium would be seen to have melted during sintering and have escaped the mould.

4.6 Characterisation of Sintered Specimens

Sintered specimens of ball milled TiH_2, HDH, or commercial Ti, pure or mixed with aluminium, produced by Hot Press sintering were initially cleaned by grinding with SiC paper (minimum 800 grit) to remove any papyex carbon paper or surface contamination. The density of the specimens was determined by the Archimedes method. The specimens were then analysed by XRD (described in Section 4.3.2). Then the specimens were prepared for Scanning Electron Microscopy and Energy Dispersive Spectroscopy (SEM and EDS, as described in Section 4.3.4) and Hardness measurement by being set in resin and polished.

4.6.1 Density Measurement

The density of the samples was measured using the Archimedes immersion method. This method uses the buoyancy of a body in water to calculate its density by comparing the mass of the sample measured in water, m_{wet}, with the mass of the sample in air m_s. The buoyant force, F_b, will be equivalent to the difference of measured weights in air, W_s, and water W_w, while the volume of the sample does not change whether in air, V_s, or water, V_b. The equation to calculate the density of a specimen, ρ_s [g/cm^3] is:

$$\rho_s = \frac{(\rho_w m_s)}{m_b} = \frac{(\rho_w m_s)}{m_s - m_w} \tag{4.2}$$

The density of water, ρ_w [g/cm^3], is adjusted for the temperature of the water, T [°C], using the equation:

$$\rho_w = 1.0017 - 0.0002315T \tag{4.3}$$

The mass of the sample in air is measured using a digital balance. To measure the sample's mass in water, the balance is modified to suspend the sample in a beaker of distilled water. The procedure for the measurement of density consisted of the steps:

1. Clean and dry the sample using ethanol
2. Measure the mass of sample in air using the balance
3. Suspend the sample in water using the modified balance setup and measure the mass of the sample in water
4. Dry the sample and remeasure its mass in air to determine if the sample has any open porosity

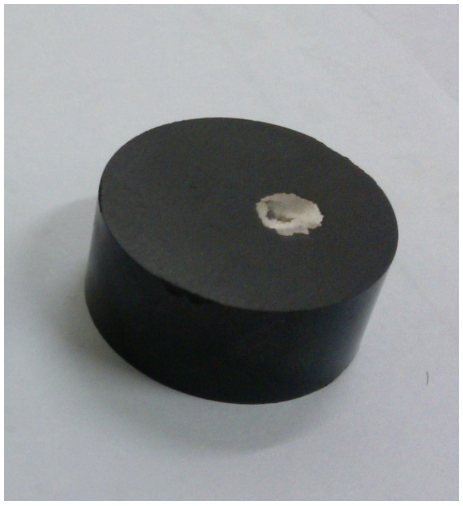

Figure 4.14: A sintered titanium sample set in phenolic resin

4.6.2 Specimen Preparation for SEM and Hardness Measurements

In addition to the operational procedure of SEM described in Section 4.3.4, sintered samples are required to be set in a conductive resin and polished. A conductive resin allows the sample to be polished and holds the sample still whilst under SEM. The resin is required to be conductive to allow the electric charge to dissipate during SEM. Figure 4.14 shows a 6 mm diameter sintered sample set in black phenolic resin. This is done using an automatic machine, where the sample is placed inside a chamber at the bottom of loose resin powder. The resin is cured by the machine at 180°C for 10 minutes under 80 MPa.

For microscopic observation, a high level of polish is required. To polish titanium samples set in resin, a Struers automatic polishing machine was used. The stages of polishing are designed to reduce the size of grit used to cut the surface until they are not visible through the microscope. The polishing stages are shown in Table 4.1.

Table 4.1: Sintered specimen polishing stages

	Stage 1	Stage 2	Stage 3
Disc	SiC Paper 360-1000 grit	MD-Largo	MD-Chem
Suspension/ lubricant	water	Diapro Largo 9 μm	OPS colloidal silica
Rotional speed (rpm)	300	200	150
Force (N)	25	30	30
Duration (minutes)	1-2 as required	8	10

4.6.3 Hardness Measurement

The hardness of sintered specimens is measured by indentation. Material hardness is an indication of strength and composition. The material hardness is based on a quantity of yielded material in an indentation zone. Thus, hardness and material yield strength are related. The measured hardness of sintered specimens can be compared with the known hardness of titanium to study their quality. Solid TiH_2 has a lower hardness than pure Ti (Setoyama et al., 2004), while small concentrations of hydrogen dissolved in a solid solution of titanium increase the material's hardness. Interstitial impurities (C, H, N and O) increase the material's strength and hardness. Therefore the measurement of hardness gives an indication of both dehydrogenation and levels of impurity.

The testing performed is based on the standard for the test method for Vickers hardness of metallic materials (ASTM E 92). A square-base diamond indenter, shown in Figure 4.15a, has two pairs of faces ground at 136° to each other. The indenter is pressed into the surface of the material by a known force for a given

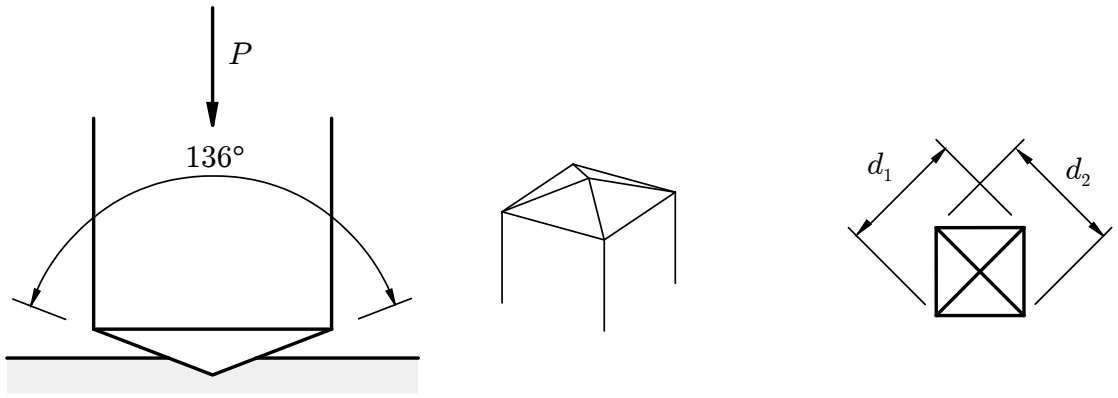

a) Indenter b) Indentation

Figure 4.15: Vickers hardness indentation test

duration. The diagonals of the indentation left, shown in Figure 4.15b, are measured.

The Vickers hardness number (HV) is defined as the load applied divided by the area of the surface of indentation. The surface area is calculated as:

$$A_{HV} = \frac{d^2}{2sin(136°/2)}, \tag{4.4}$$

and the Vickers hardness number is then:

$$HV = \frac{P}{A_{HV}} = \frac{2Psin(136°/2)}{d^2}. \tag{4.5}$$

The hardness test is performed using a Wilson Vickers hardness tester, model 452 SVD, shown in Figure 4.16. The polished samples, set in resin, are placed on the test platform. A flat polished surface is used to obtain a clear indentation, and to ensure that the indentation is not skewed. The mass force is set on the machine. A force of 5 [kgf] is used with a dwell time of 5 [s]. The indentation is made automatically and is viewed through a microscope, shown in Figure 4.17. The diagonals of the indentation are measured by the same machine through the microscope and the HV value is calculated by the machine. A mean value is taken from a minimum of 3

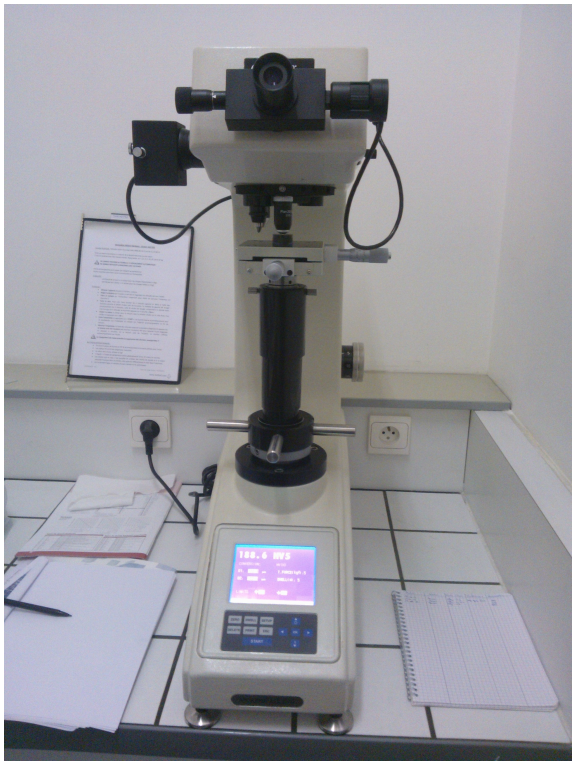

Figure 4.16: Vickers hardness testing machine

indentations per sample.

4.7 Post-treatment of Pure Ti Specimens

The post treatment of sintered parts continues the effects of sintering. Post treatment involves heating of the sample under a controlled atmosphere in order to consolidate the sample further. Upon heating, the sample can resume densification and grain growth. Furthermore, the dehydrogenation can continue until all the hydrogen is eliminated.

A high vacuum oven shown in Figure 4.18. was used for the post treatment of specimens. The specimens are heated at 10°C/min to a holding temperature of 600°C for 3 hours. The temperature is decreased at 10°C/min. The post treatment is performed under a secondary vacuum (approximately 7.6×10^{-6} mbar)and placed

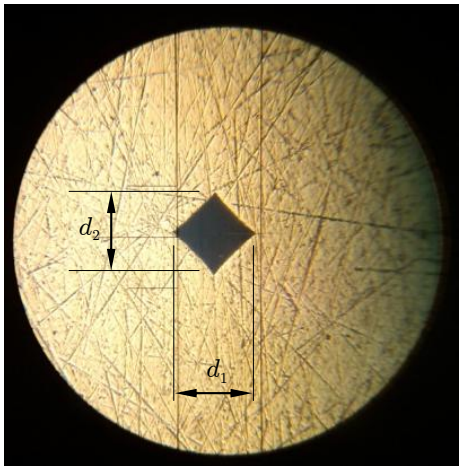

Figure 4.17: Diagonal measurement of Vickers hardness diamond indentation

in the oven on an alumina disc to avoid contamination.

4.7.1 3-Point Bending Test

The flexural strength of sintered materials is measured by the 3-point bending test. This test places a beam in pure bending until failure and measures the force applied and displacement value. A rectangular beam is supported at two points and loaded at the mid span. The specimen is loaded until failure occurs at the outer fibres. The flexural testing is performed in accordance with the Standard ASTM D 790, Flexural Properties of Unreinforced and Reinforced Plastics and Electrical Insulating Materials. This standard is used in place of standardisation for flexural testing of metals. An Instron 3369 50 kN dual column universal tensile machine (Figure 4.19) is used to perform the tests. The sintered specimen is prepared by grinding its surfaces flat on a rotating disc of SiC paper, then its width, b [mm], and depth, d [mm], are measured using Vernier callipers at different positions along its length. The machine is prepared by setting the two supports at the span length. The load applied, P [N], is measured by the head load cell of the Instron and deflection at the mid span, D [mm], is measured by an extensometer. The rate of displacement of

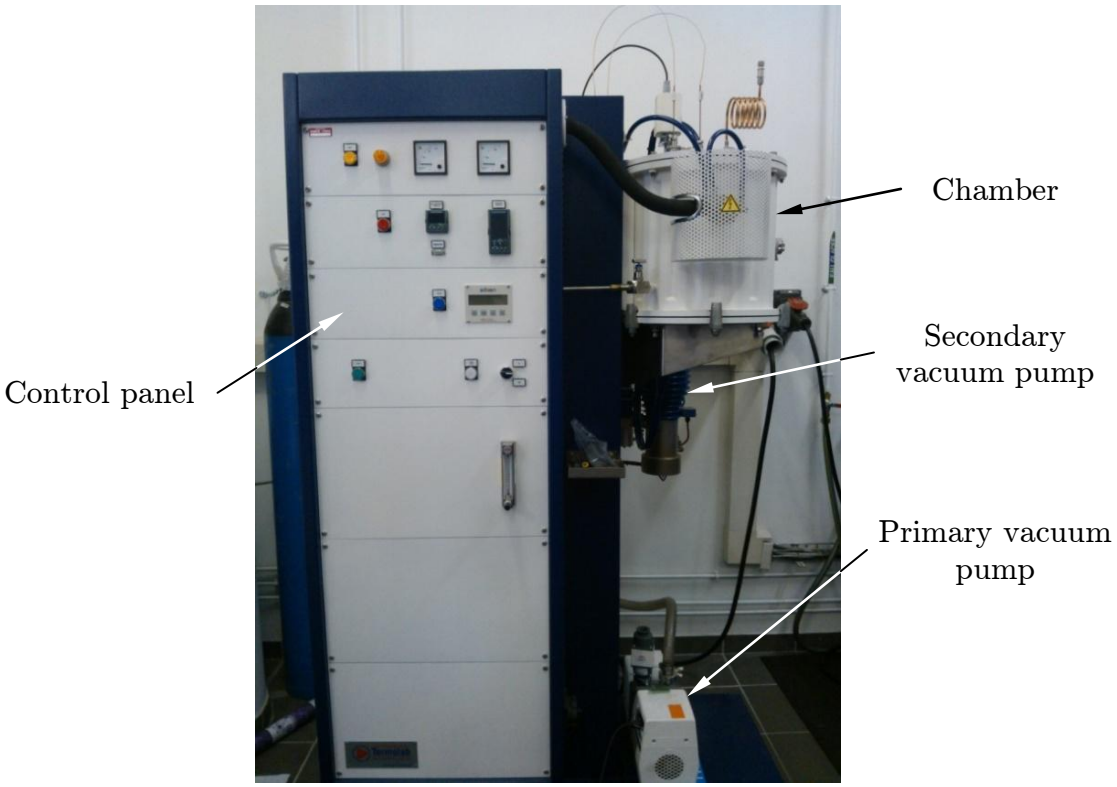

Figure 4.18: High vacuum oven

the load head is constant at 0.05 [mm/min]. The standard recommends a minimum of 5 bending tests per material for statistical analysis, however only 2 bending tests were performed per material because of the limited number of specimens.

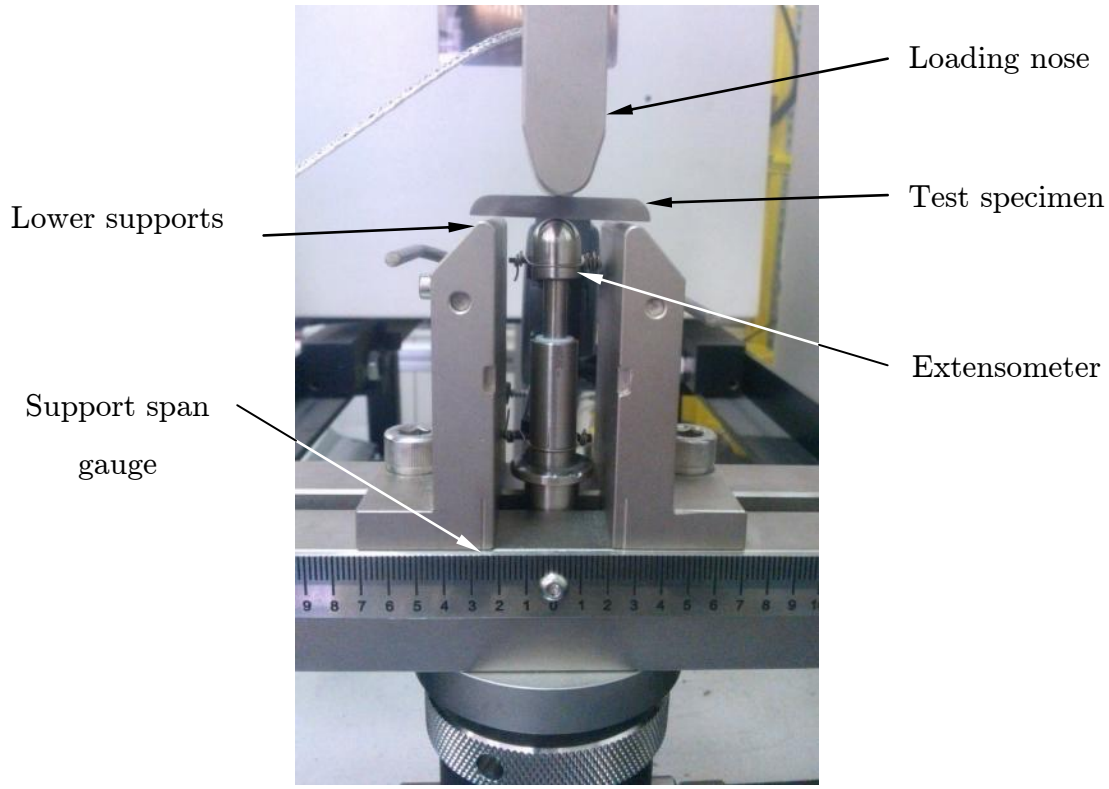

Figure 4.19: 3-point bending experimental setup

The experiment is shown schematically in Figure 4.20. The maximum bending moment is at the mid span of the beam. The stress at a point on this cross section is proportional to its distance from the neutral axis, and is greatest in tension at the bottom fibres and greatest in compression at the top fibres of the beam. Failure in the beam occurs by the initiation of fracture at the bottom of the beam, or by the propagation of plastic yield from the outer fibres of the beam to the neutral axis. The flexural stress in the outer fibres at the mid span, σ_f [MPa], and flexural strain in the outer fibres at the mid span, ϵ_f [mm/mm], are calculated by equations 4.6 and 4.7 respectively.

$$\sigma_f = 3PL/2bd^2 \tag{4.6}$$

$$\epsilon_f = 6Dd/L^2 \tag{4.7}$$

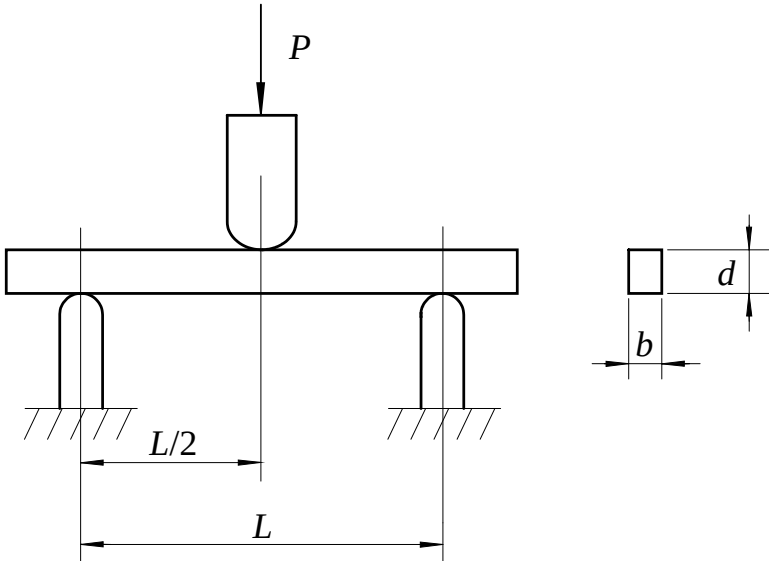

Figure 4.20: 3-point bending test diagram

A typical result of a flexural bending test is shown in Figure 4.21. The flexural stress is compared with the flexural strain. The value of flexural yield, σ_{fY}, is taken where the stress-strain curve deviates from the initial straight line. The flexural strength, σ_{fM}, is the maximum flexural stress that occurs in the specimen. The breaking strength, σ_{fB}, is the flexural stress at the break of the specimen. The flexural strain at the yield and at breaking are denoted as ϵ_{fY} and ϵ_{fB} respectively. The flexural stress measured by this test is dependent on the size of the beam used, so it is not a pure material property. The results from this test are not comparable to published material properties and will be only used to compare materials fabricated in this thesis.

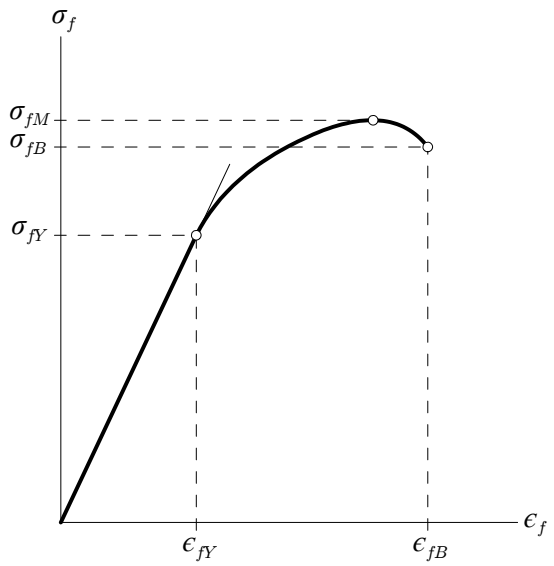

Figure 4.21: Typical bending test result of flexural stress versus flexural strain

4.8 Conclusion

This Chapter has described the methods and procedures used for the synthesis and densification of TiH_2 powder for the study of two advanced sintering techniques: (a) direct sintering of ball milled TiH_2, and (b) titanium LPS with aluminium. All the equipment described was made available for this research by the ICMCB-CNRS (Institut de Chemie de la Matière Condensée de Bordeaux - Centre Nationale de la Recherche Scientifique, France). The charactersiation methods of powder and sintered specimens described are used in the experimental investigations presented in Chapters 5 of the TiH_2 powder synthesis and Chapter 6 of the sintering of TiH_2 directly, and with liquid aluminium.

Chapter 5

Investigation of Ball Milled TiH_2 Powders

5.1 Introduction

This chapter presents the synthesis of ball milled TiH_2 and HDH powders used in the study of sintering in this thesis. TiH_2 is made by hydrogenation of titanium sponge and then ball milling, and an HDH powder is made by dehydrogenating the TiH_2, ball milled for 180 minutes, in a vacuum oven. The powders are characterised for their particle size, phase, morphology, metallic impurities and dehydrogenation by granulometry, XRD, SEM, ICP-OES and DSC respectively. The study of these powders is performed to understand the effect of particle size on densification and dehydrogenation during sintering. The properties of commercial titanium and aluminium powders used for the fabrication of specimens by aluminium LPS are also presented here.

5.2 Ball Milling of TiH_2

The ball milling of titanium hydride was performed over different times in order to obtain a range of powders to study the effect of particle size and ball milling on the densification and dehydrogenation of titanium hydride during sintering.

5.2.1 Granulometry of Ball Milled TiH_2

The particle size distribution measured by laser granulometry, as described in Section 4.3.1, of the ball milled TiH_2 powders is shown in Figure 5.1. The starting sponge is seen to reduce to 6.6 μm after 5 minutes of ball milling. After 10 minutes of ball milling, 3 populations of particle sizes are introduced: above 10 μm, 1-2 μm and 0.1 μm. An increase in ball milling duration decreases the quantity of the 0.1 μm population and increases the quantity of the 10 μm population, while the central population decreases in particle size. This is caused by the agglomeration of finer particles seen by SEM in Figure 5.2. Thus the general reduction in particle size is indicated by the central population size, which after 10 minutes of ball milling, decreases from 2 μm to 1 μm.

There are a range of particle sizes created by ball milling, from approximately 0.1 μm to 10 μm. The larger particle sizes (above 10 μm) are agglomerations made from finer particles. Ball milling reduces the overall particle size, the greatest reduction in particle size is made in the first 10 minutes of ball milling.

5.2.2 SEM of Ball Milled TiH_2

The SEM micrographs taken of the TiH_2 powders ball milled for 5-180 minutes, are shown in Figure 5.2. The micrographs show the angular shape of the powder caused by the fracture of the brittle TiH_2. The size of the particles is also seen to reduce with increased ball milling duration. A range of particle sizes is shown to be created

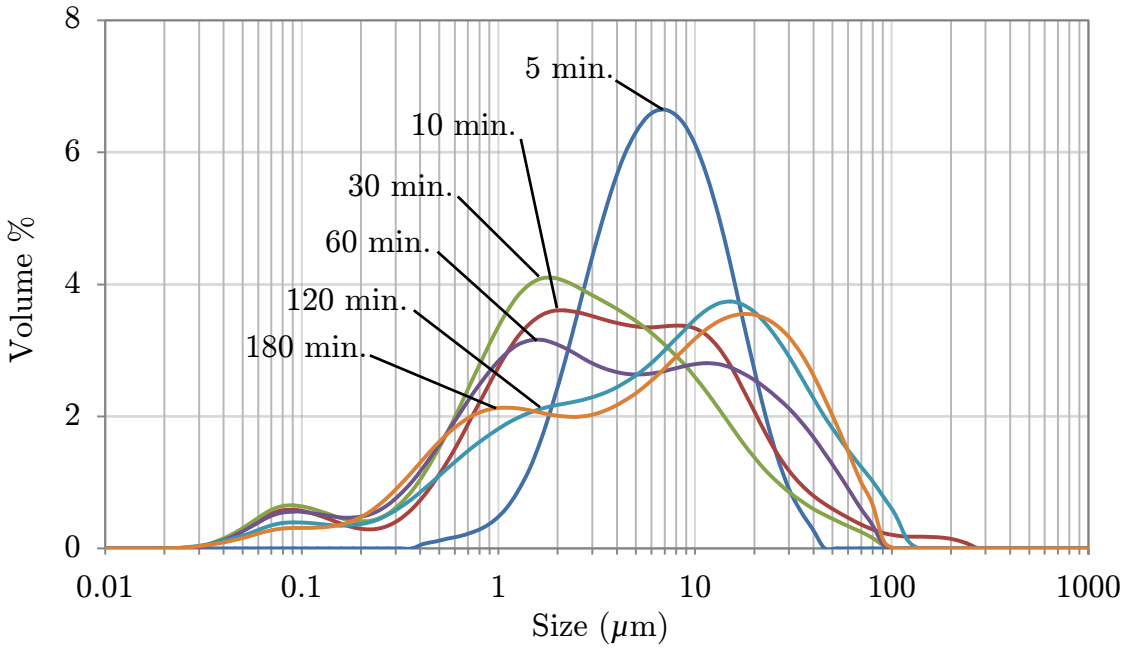

Figure 5.1: Particle size distribution of ball milled TiH_2 powders

by ball milling, not a single population of particle size, with a tendency for finer particles to agglomerate or remain on the surface of larger particles. In general, the size of particles is shown to reduce with the ball milling duration.

5.2.3 X-Ray Diffraction of Ball Milled TiH_2

Figure 5.3 shows XRD patterns of TiH_2 powder ball milled for 5 and 180 minutes. The broadening of peaks is observed for powders ball milled for longer, indicating the reduction of crystallite size.

The average crystallite size is calculated using the Scherrer formula (see Section 4.3.2), and is performed by the EVA® software. The results are shown in Figure 5.4 and are compared with the average particle size, as measured by laser granulometry. The crystallite sizes of the particles are reduced in the first 30 minutes of ball milling predominantly; for further ball milling, the crystallite size remains at approximately 100Å.

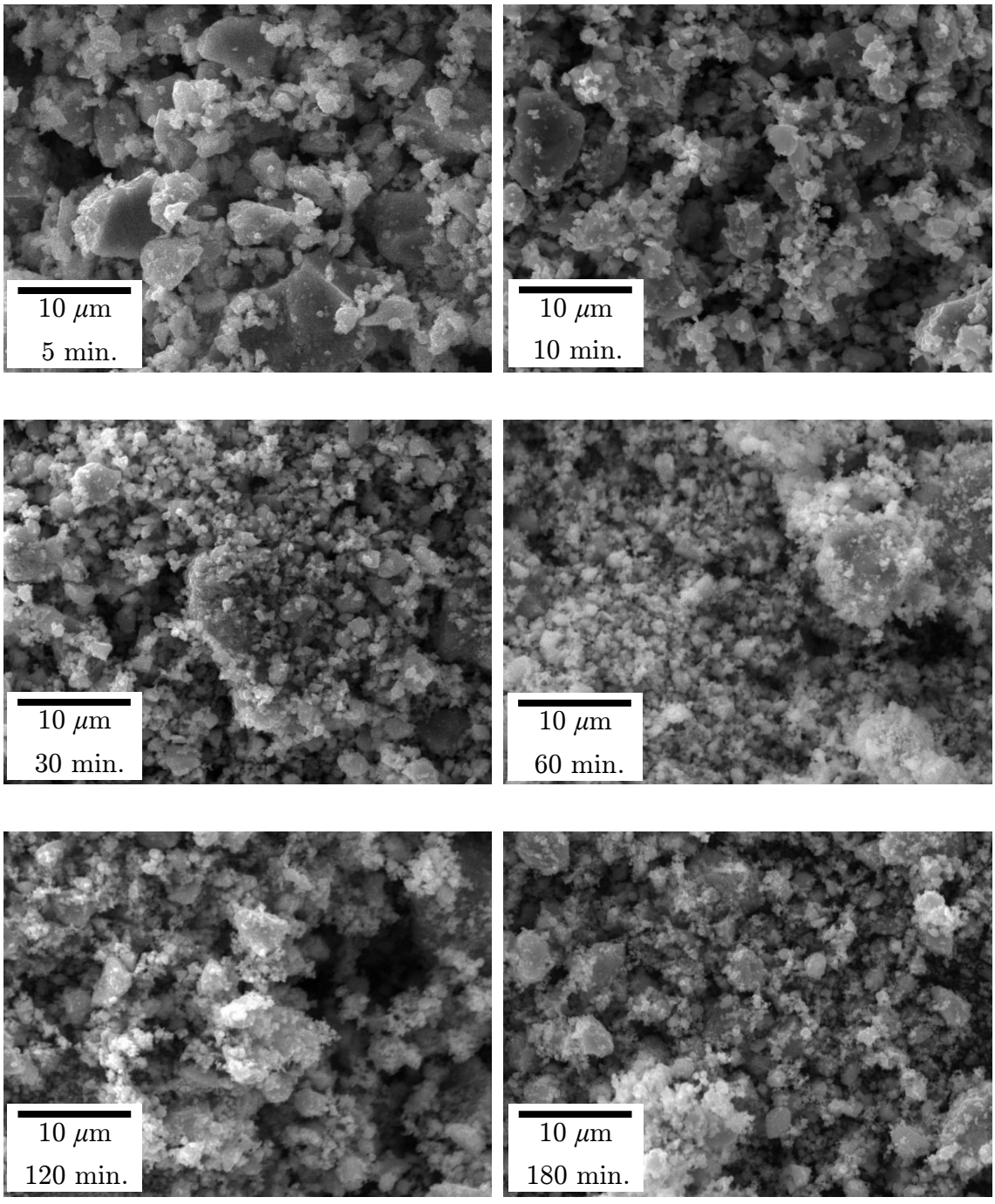

Figure 5.2: SEM micrographs of TiH_2 powder ball milled for 5-180 minutes

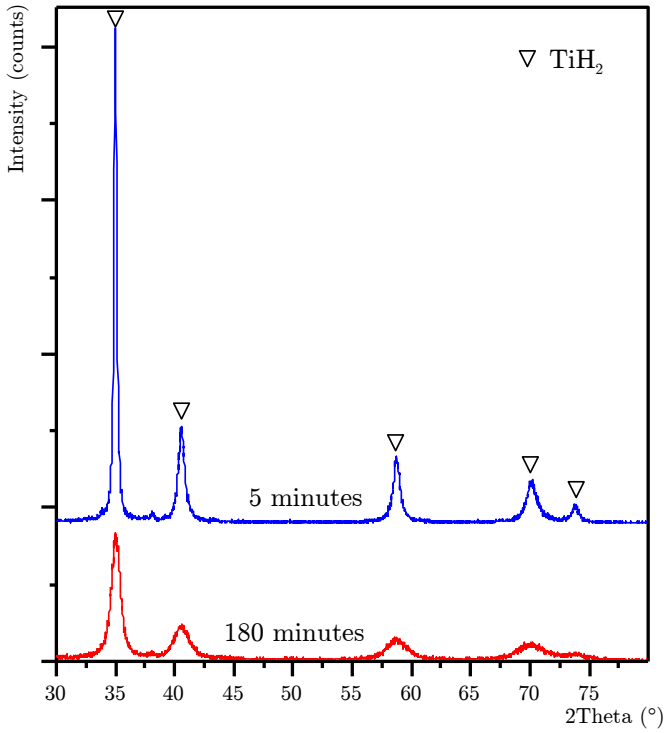

Figure 5.3: XRD patterns of TiH_2 powders ball milled for 5 and 180 minutes

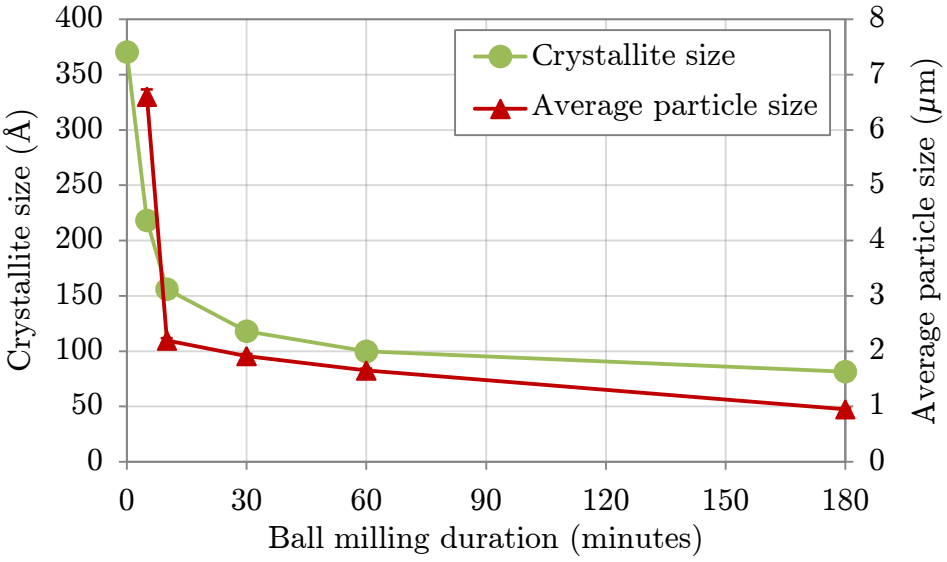

Figure 5.4: Particle size and crystallite size of ball milled TiH_2 powders

5.2.4 Metallic Impurities

During mechanical grinding of TiH_2, the introduction of impurities through collision of the vial and balls with each other is unavoidable. In this case, stainless steel balls and vials are used so Fe and Cr will be the main introduced elements. These impurities introduced into the powder will be present in the sintered part if they are not eliminated before sintering. Impurities in the lattice will cause unwanted changes to the mechanical properties of the final material. The quantity of impurities is then measured in order to estimate their impact in the final sintered part.

The Effect of Impurities on Titanium

Iron

The addition of iron strengthens titanium as discussed in Section 2.3.2. Iron causes an increase in strength and a reduction in ductility by substituting for titanium atoms in a solid solution. The atomic lattice becomes distorted, thereby creating a restriction for the motion of dislocations. The limit on the mass percentage of iron in commercially pure titanium, ASTM grade 1 to 4 (from lowest to highest strength) is 0.20 to 0.50 wt% respectively (ASTM B 348). An iron content above 0.50% causes an excessive reduction of ductility.

Chromium

Chromium was measured to confirm that the stainless steel milling equipment was the main source of iron pollution. Chromium forms a substitutional solid solution with titanium. Chromium dissolves in α-titanium only <1 wt%, and forms a eutectic with titanium. Thus it is used in titanium to control phase formation. Chromium is used as an alloying element in titanium up to 6 wt% (grades 19 and 20, ASTM B 348).

Magnesium

Magnesium has been introduced because of the processing of magnesium

hydrides in the same hydrogen equipment. Magnesium and titanium are essentially un-reactive. Thus any solid magnesium introduced will remain unreacted during sintering. The low stiffness of magnesium compared with titanium, will create discontinuities and stress concentrations detrimental to the strength of the material.

Ball milling introduces stainless steel particles of combined Fe and Cr elements. The low diffusion rates between Ti and Fe in solid form at sintering temperatures below 900°C mean that the introduced stainless steel particles will remain in the material unless sintering occurs at a high temperature.

Figure 5.5 shows the mass percentage of measured impurities of Fe, Cr, and Mg. The mass percentage of Cr remains relative at about 20% of Fe for each ball milling duration. The ratio of 20% of Cr in Fe is common for stainless steel. This indicates that the main introduction of Fe and Cr is from the milling equipment. The percentage of Fe increases with ball milling duration. Increased ball milling duration increases the number of collisions which cause the introduction of stainless steel pollution. For 180 minutes of milling, 0.5 wt% Fe is introduced which is the highest limit of any ASTM grade titanium (0.50 wt% in grade 4, ASTM B 348). Magnesium is seen to be present in the milled powder at approximately 0.1-0.2%.

5.2.5 Dehydrogenation of Ball Milled TiH_2 Powders

Effect of Ball Milling Duration

The dehydrogenation of TiH_2 of ball milled powders is captured by DSC, as is shown in Figure 5.6. The dehydrogenation process (presented in Section 2.3.10) occurs in two steps: ε-$TiH_{2(1.92)}$ transforms to δ-$TiH_{(0.7-1.5)}$ + β-Ti, then to α-Ti. Powders ball milled for 5 and 10 minutes show a single peak at 550°C and 530°C respectively. Here, the two stages of dehydrogenation are combined in a single peak.

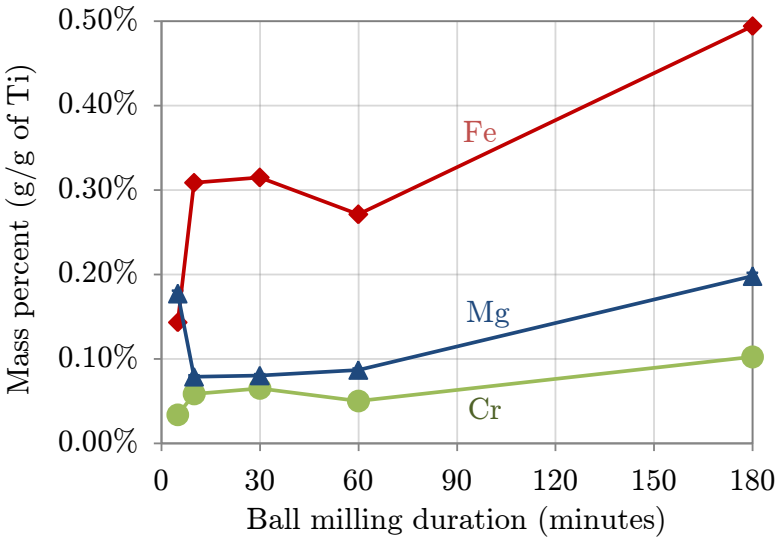

Figure 5.5: Mass percent of Fe, Mg and Cr measured in ball milled TiH_2 powders by ICP-OES

For powders milled for 60 minutes, two peaks are shown and are seen to occur at decreasing temperatures. The effect of ball milling on the dehydrogenation of TiH_2 is the movement of the peaks to lower temperatures and the increased separation of the peaks. The decrease in temperature is linked to the effects of ball milling, decreased particle size and increased defect density. The separation of the peaks is caused by the higher thermal stability of the δ-$TiH_{(0.7-1.5)}$ phase in the second stage of dehydrogenation.

Effect of Compaction Pressure

The dehydrogenation of cold compacted TiH_2 powders ball milled for 180 minutes is shown in Figure 5.7. The loose TiH_2 powder ball milled for 180 minutes shows two peaks, representing the two stage dehydrogenation process. The cold compacted powder compressed at 40 MPa shows a small second peak at an increased temperature. For compaction of 80 MPa, the second peak is not seen.

A change in specific heat starts at 400°C and 360°C for powder cold compacted

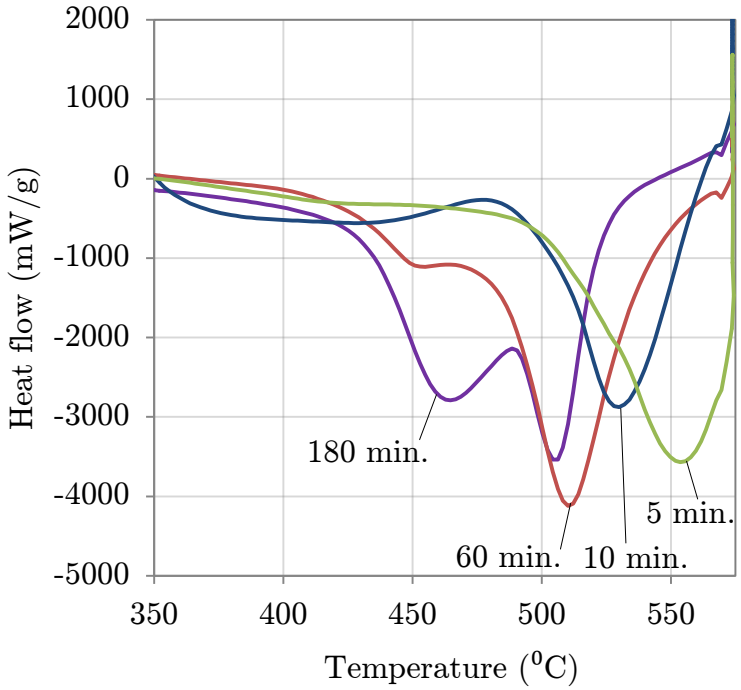

Figure 5.6: DSC of TiH_2 powder ball milled for 5, 10, 60, and 180 minutes showing the desorption of hydrogen

at 40 MPa and 80 MPa respectively. The reduced peak at 500-550°C of these curves indicates that the dehydrogenation of TiH_2 must begin during the change in specific heat at 400°C and 360°C. The easier liberation of hydrogen caused by the effects of ball milling is still effective, therefore the first stage of dehydrogenation is commenced earlier by the cold compaction of the powders.

A suggested cause for this is that it is easier to heat a cold compacted pellet evenly than a loose powder. Cold compaction increases contact between particles, enabling the direct transfer of heat, which leads to even heating and causes the overall dehydrogenation to occur, while the rate of dehydrogenation is reduced.

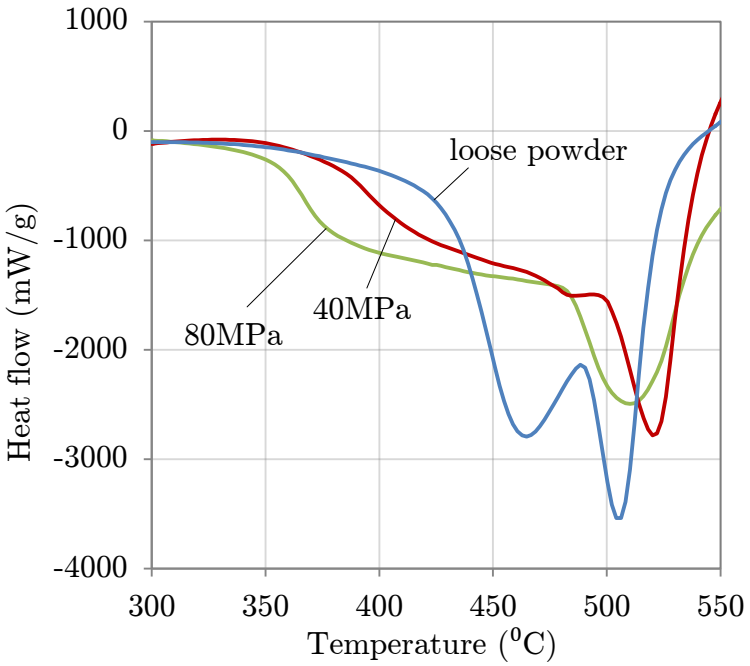

Figure 5.7: DSC of TiH_2 powder ball milled for 180 minutes, loose and cold compacted at 40 MPa and 80 MPa, showing the desorption of hydrogen

The dehydrogenation of the ball milled powders, as compared with their milling duration, was studied by DSC. The effect of ball milling to reduce particle size and to increase defect density is seen to increase the ability of the powder to dehydrogenate at lower temperatures. The two stages of the dehydrogenation process are also seen

to separate with increased ball milling. The increased ball milling of TiH_2 will decrease the minimum sintering duration needed to achieve a low hydrogen part.

DSC performed on TiH_2 powders indicates that pressure assistance in sintering will take longer for hydrogen desorption while starting at decreased temperatures. The first stage of dehydrogenation occurs earlier and slower during heating caused by the increased heat transfer through solid particle contact. The duration of the first stage is prolonged, while the completion of dehydrogenation is not greatly affected by cold compaction pressure. The dehydrogenation during sintering under compaction is seen to be relatively unaffected.

5.3 Commercial Powders

The characterisation of the commercial Ti and Al powders used in this study is presented here. Pure commercially produced titanium and aluminium powders were used for comparison with milled TiH_2 and in Ti-Al liquid phase sintering. Commercial titanium and aluminium powders were selected, based on particle size and availability. The powders' size distribution and shape were studied by XRD, granulometry and SEM.

5.3.1 Commercial Ti Powder

The commercial titanium powder used in this study is from Alfa Aesar with a purity of 99.5%. The average particle size was measured by granulometry to be 44 μm. The particle size and shape, as shown by SEM, is given in Figure 5.8. The titanium powder is seen to be angular.

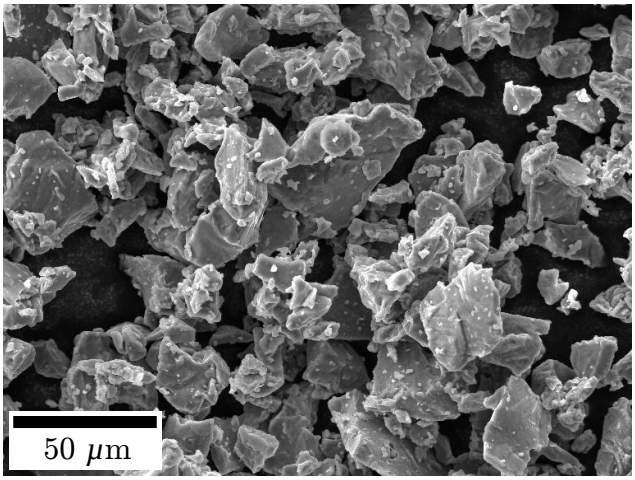

Figure 5.8: SEM micrograph of commercial titanium powder

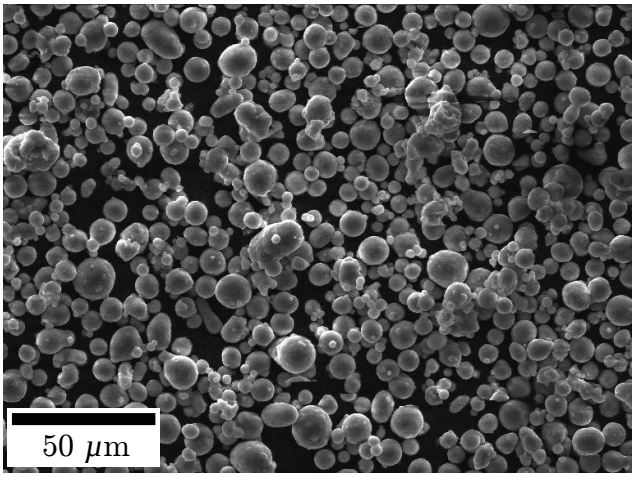

Figure 5.9: SEM micrograph of commercial aluminium powder

5.3.2 Commercial Al Powder

The aluminium powder used in the study is from Poudre Hermillon (product code F3731, purity 99.97%). The particle size distribution was measured by laser granulometry and was seen have a normal distribution with a mean particle size of 12 μm. The particle size and shape is seen by SEM in Figure 5.9.

5.4 Conclusion

In this Chapter, TiH_2 powders were synthesised by hydrogenating Ti sponge and ball milling. The ball milling of the TiH_2 was found to produce fine powder (6.6 μm) rapidly from TiH_2 sponge after 5 minutes. Further reduction of particle size from 6.6 μm to 1.0 μm was achieved with longer ball milling durations up to 180 minutes. Ball milling was also seen to reduce the crystallite size of the powders rapidly. Ball milling was also seen to introduce metallic impurities of Fe and Cr from the milling apparatus below the concentrations of ASTM standards.

The reduction of particle size, increase in lattice defect density and reduced crystallite size by ball milling TiH_2, is believed to have caused an increase in the dehydrogenation kinetic as seen by DSC. Dehydrogenation was seen to complete at temperatures below 580°C during DSC, while cold compaction pressure of these powders was also seen to reduce the dehydrogenation kinetic. As discussed in Chapter 4, the dehydrogenation of TiH_2 during sintering aids densification, and the rate of dehydrogenation is increased by ball milling, while cold compaction decreases the rate of dehydrogenation. The effect of powder characteristics on densification and dehydrogenation during hot press sintering will be investigated in Chapter 6.

The commercial titanium powder of size 44 μm will be compared with a fine ball milled TiH_2 (1.0 μm) during LPS with aluminium. Chapter 2 described that free sintering of titanium with liquid aluminium led to the formation of pores through the Kirkendall effect, and that the diffusion between liquid aluminium and titanium is affected by the size of titanium particles. In the study by Savitskii and Burtsev (1981) the increase in titanium particle size above 45 μm was seen to decrease density and cause the specimen to swell. In this present work, the reduction of titanium particle size will be studied, with the aim of reducing the formation of Kirkendall

pores using pressure-assisted sintering.

Chapter 6

Experimental Investigations of Advanced Sintering Techniques

6.1 Introduction

This chapter presents the experimental results of the two different techniques studied: (1) direct sintering of ball milled TiH_2, and (2) the use of a liquid aluminium phase during sintering of titanium powders.

The TiH_2 powders synthesised and characterised in Chapter 5 are hot press sintered and subsequently characterised for density, microstructure and hardness using the methods described in Chapter 4. The results of experimental fabrication are used to study the effect of ball milling on densification and dehydrogenation during hot press sintering, specifically at low temperatures. Assessment of the quality of the obtained microstructure will improve the understanding of the effect of this technique on reducing sintering parameters and costs to produce titanium parts.

Titanium powders are mixed with varying concentrations of aluminium to study the effects of the liquid aluminium phase during hot press sintering. Three

different titanium powders are used to study the effects of the particle sizes on phase interaction and densification during LPS. The specimens are assessed for their quality by density, microstructure and flexural strength. The obtained results are then discussed in Chapter 7 in terms of the ability of aluminium LPS to improve densification and reduce the sintering parameters.

6.2 Densification of TiH_2 to Pure Ti

6.2.1 Density of Sintered TiH_2

Figure 6.1 shows the density of samples sintered from TiH_2 powders ball milled for 5-180 minutes. These powders were characterised in Chapter 5. The density is measured by the Archimedes method and the results are compared with the density of pure titanium of 4.51 g/cm^3 (upper dashed line). The density of solid TiH_2 is 3.75 g/cm^3 (lower dashed line).

The results of density measurement shows that the sintered density increases both with ball milling duration and sintering temperature. At a sintering temperature of 700°C, the increase in ball milling duration from 5 to 180 minutes results in fully dense titanium. The increase in sintering temperature to above 850°C results in all ball milled powders being close to the density of pure Ti.

The principal effect of ball milling is to reduce particle size. This results in a higher surface energy, i.e. the unbonded atomic array at the surface of a particle has higher energy than the bonded array inside the bulk of the particle. The higher surface energy promotes the formation of a solid. Thus, a finer powder densifies more easily than a coarse powder. The increase in densification seen here is improved as a result of the reduced particle sizes from ball milling. The consequence of a broader particle size distribution on the efficiency of sintering has not yet been studied, as it is outside the scope of this thesis, and is also probably significant.

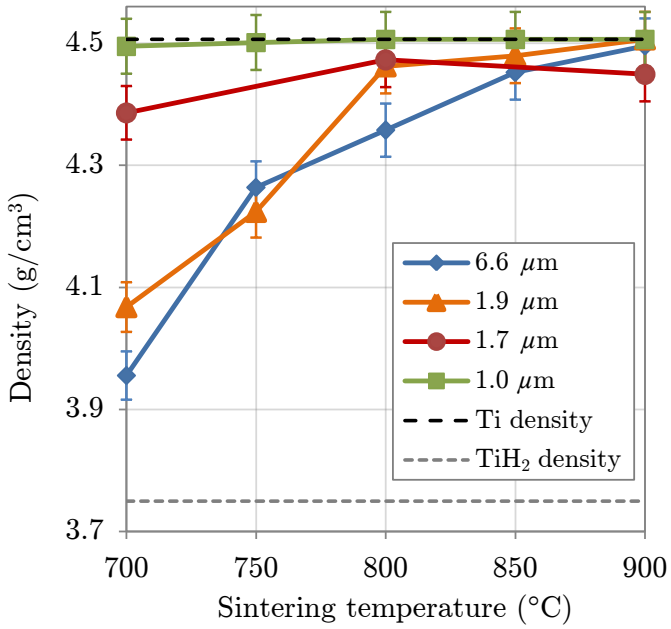

Figure 6.1: Density of sintered ball milled titanium hydride as a function of sintering temperature

6.2.2 SEM of Sintered TiH_2

The microstructure of the sintered TiH_2 can be seen on selected specimens in Figure 6.2, comparing sintering temperatures and particle sizes. The micrographs show the pore structure and grain size. The phase distribution of Ti and TiH_2 can be seen through the use of Back Scattered Electrons (BSE): micrographs which highlight different elemental compositions. The lighter phase is α-Ti and the darker phase is TiH_2. The HCP α-Ti is seen to grow in needle form in Figures 6.2 a) and b). The densities of the specimens (cf Figure 6.1) correspond to the porous microstructures seen in the micrographs. Porosity size decreases and density increases in specimens sintered from smaller TiH_2 powder sizes (seen during fabrication at T = 700°C). Also seen in the micrographs is the reduced proportion of the TiH_2 phase for both reduced particle size and increase in sintering temperature. The ball milling of TiH_2 has increased dehydrogenation during sintering, and has caused an increase in

density at reduced temperatures.

With the increase of temperature, α-Ti grain size and density also increase. The final grain size, for those specimens sintered at 900°C where TiH_2 is not present, is reduced for smaller starting powders. The reduced grain size can result in an increase in strength due to Hall-Petch strengthening.

The shape in which α-Ti grows (acicular or globular) is seen to change for different starting TiH_2 sizes. If the size of the TiH_2 starting powder is large (6.6μm), a needle like structure is seen, whereas if the particle size is smaller (1.0 and 1.7 μm), a globular structure is seen. At 900°C, grains of β-Ti begin to grow at the boundaries of α-Ti.

The dehydrogenation of TiH_2 is delayed during sintering, compared with that seen during DSC. The remaining TiH_2 in specimens, seen in the micrographs, can be compared with the dehydrogenation seen in DSC (5.6). The dehydrogenation during sintering is seen to be delayed, compared with the dehydrogenation seen during DSC. During heating, TiH_2 begins to release hydrogen below 500°C and is completely dehydrogenated below 600°C (cf Figure 5.6). This is seen in Figure 6.2 g) in which the TiH_2 phase is seen in a sample sintered at 700°C for 30 minutes, while a loose powder is completely dehydrogenated during heating much below 700°C. This indicates a delay in dehydrogenation during sintering caused by the applied pressure inside a confined graphite die. This is also confirmed by the delay in dehydrogenation seen caused by cold compaction of powders (cf Figure 5.7).

6.2.3 XRD of Sintered TiH_2

The phase composition of sintered specimens was determined using X-ray Diffraction (XRD). The phases relevant in the study of the sintering of TiH_2 powders are hydride phases and pure titanium as α or β phase. The quantity of TiH_2 remaining, when compared with pure Ti, is an indication of the amount of dehydrogenation that

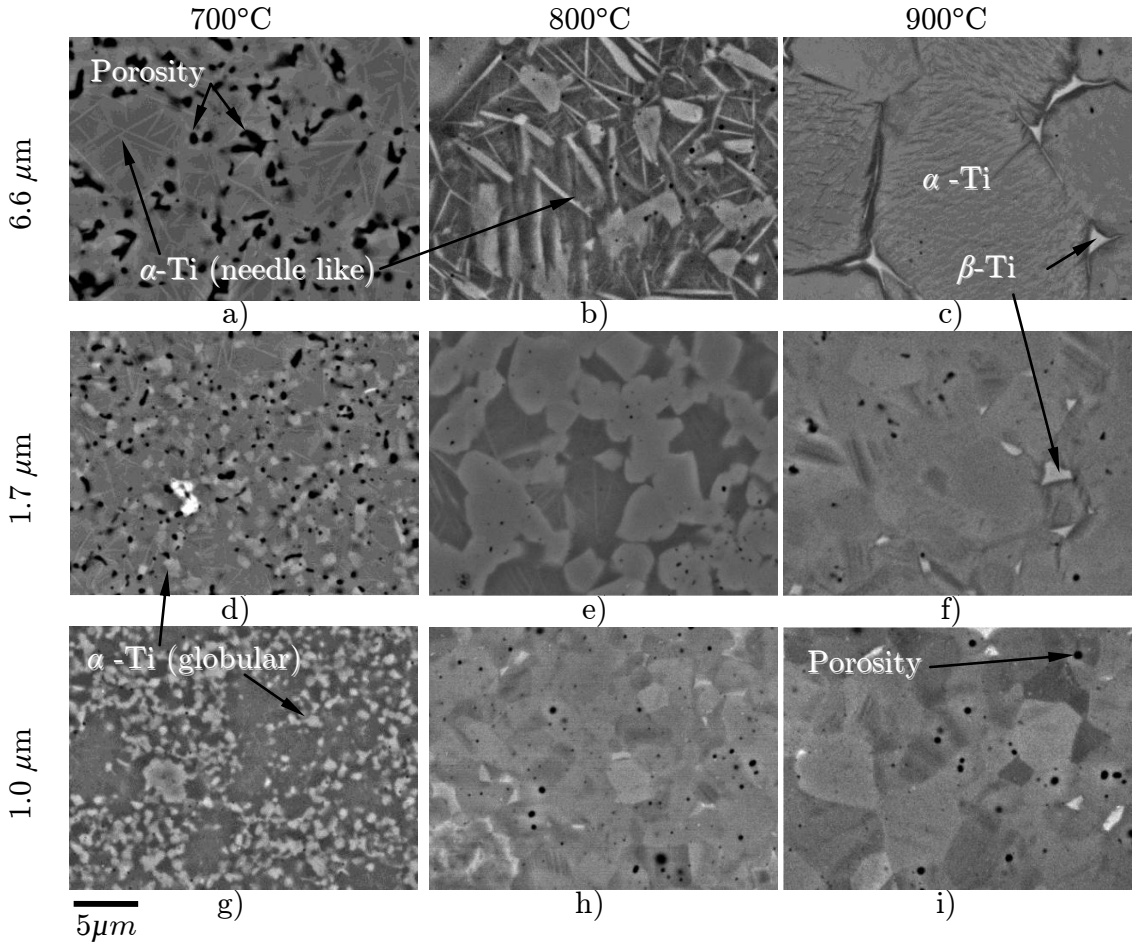

Phase	Structure	Shape	Appearance
β-Ti (>880°)	HCP	Granular	Lightest
α-Ti (<880°)	BCC	Granular/laminar	Light
TiH_2	BCT	Granular	Dark
Porosity	-	Spherical/rounded	Darkest

Figure 6.2: SEM BSE micrographs of sintered TiH_2 powders, ball milled for 5 (6.6 μm), 60 (1.7 μm) and 180 (1.0 μm) minutes, sintered at 700-900°C under 80 MPa for 30 minutes

occurs during sintering.

Figures 6.3 and 6.4 show the XRD patterns of samples hot press sintered at 700-900°C from TiH_2 ball milled powders for 5 (6.6 μm) and 180 (1.0 μm) minutes. The identified phases are α-Ti and $TiH_{1.92}$. The most distinguishable peak between the two phases when they are both present is at $2\theta = 58°$. The quantity of TiH_2 phase is seen to decrease with the increasing temperature. For powder ball milled for 5 minutes, TiH_2 is not visible by XRD when sintered at 900°C. For powder ball milled for 180 minutes, TiH_2 is not visible when sintered at 800°C. When viewed in conjunction with their SEM micrographs, the decrease in hydride phase correlates with the decrease found by XRD.

The XRD results also show the increase in grain size caused by sintering. The narrowing of XRD peaks corresponds to the increase in grain growth. Figures 6.3 and 6.4 show the narrowing of α-Ti peaks with the increase of sintering temperature. The peaks of the sintered sample from powder ball milled for 180 minutes are initially narrower than those milled for 5 minutes. Grain growth occurs during sintering because of the thermodynamic forces which act to decrease the surface energy. Grain boundaries are discontinuities in the atomic structure with a higher energy than the bulk. The grain growth seen by XRD corresponds to the grain structure seen by SEM (cf Figure 6.2).

6.2.4 Hardness of Sintered TiH_2

The hardnesses of the sintered specimens are shown in Figure 6.5. Hardness is seen to increase both when the starting powder size decreases and with sintering temperature. The increase in hardness with temperature matches the increase of the sintered density with temperature shown in Figure 6.1.

The measured hardnesses of the specimens are high when compared with pure titanium (122 HV ASTM Grade 1, Davis, 1990). The high hardness has been caused

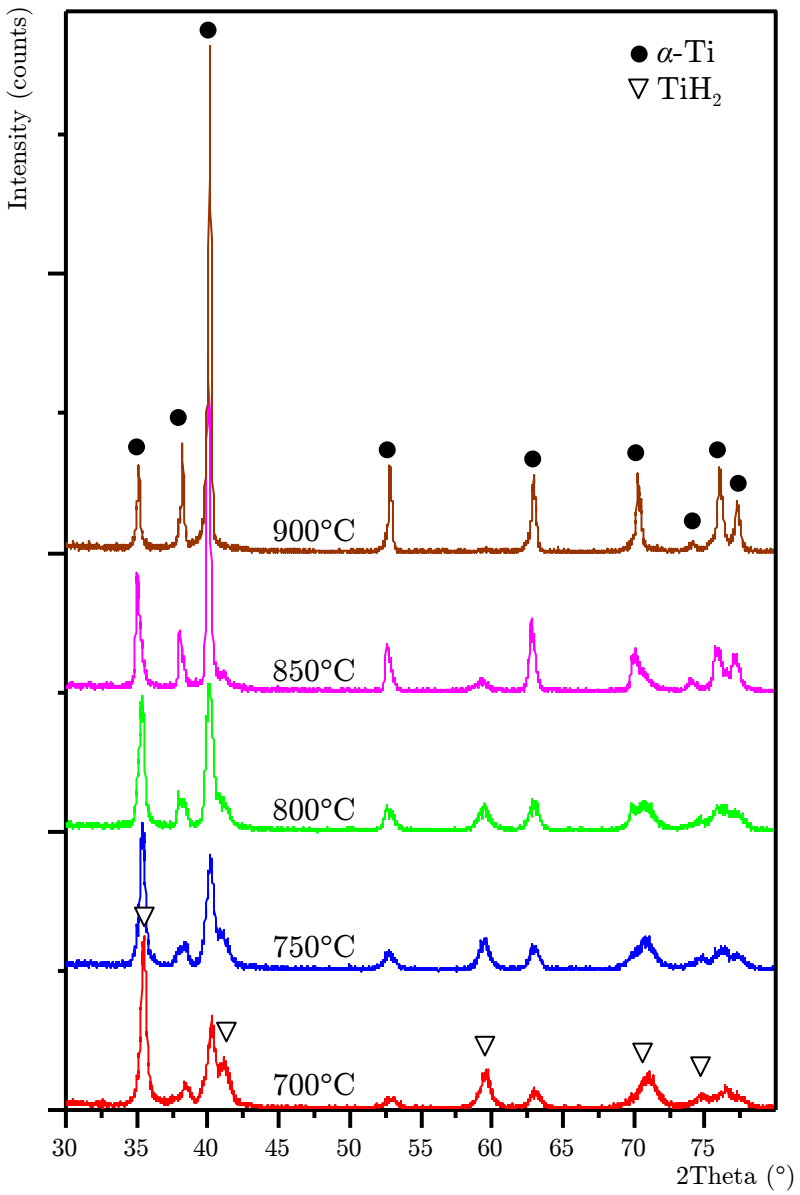

Figure 6.3: XRD patterns of TiH_2 ball milled for 5 minutes (6.6 μm) sintered at 700-900°C for 30 minutes under 80 MPa

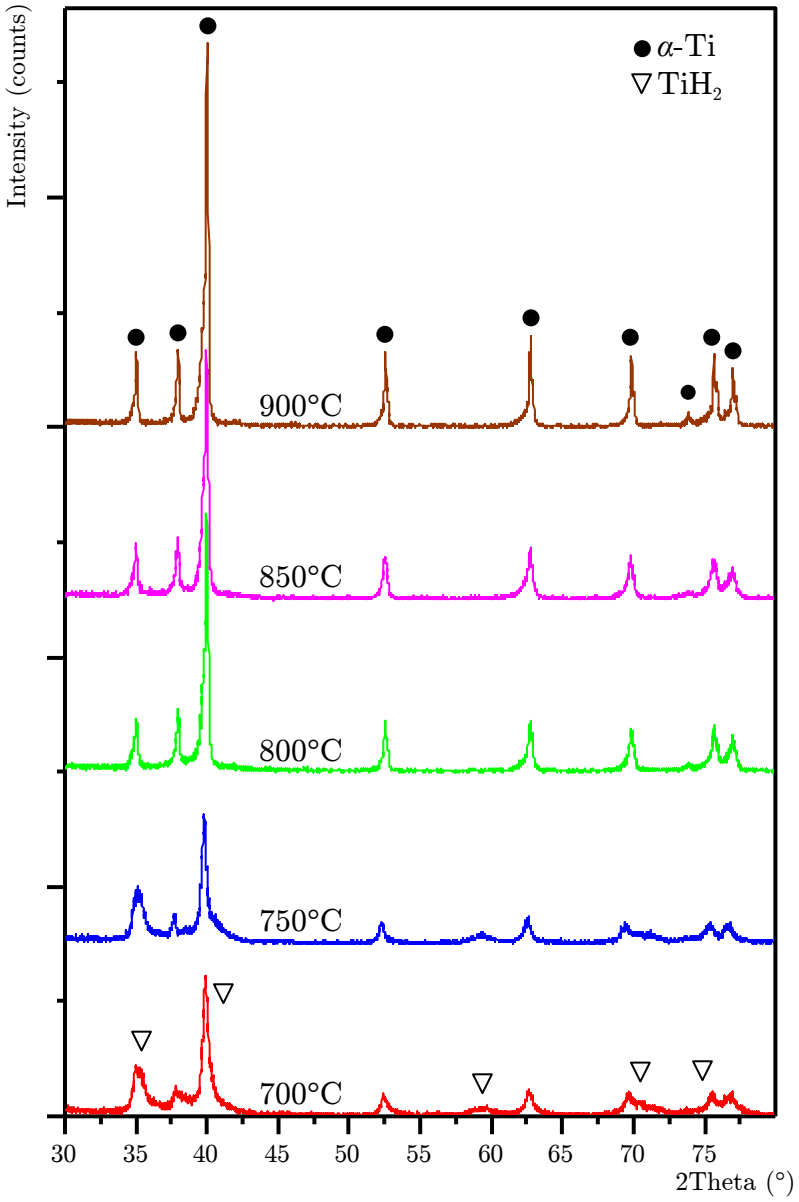

Figure 6.4: XRD patterns of TiH_2 ball milled for 180 minutes (1.0 μm) sintered at 700-900°C for 30 minutes under 80 MPa

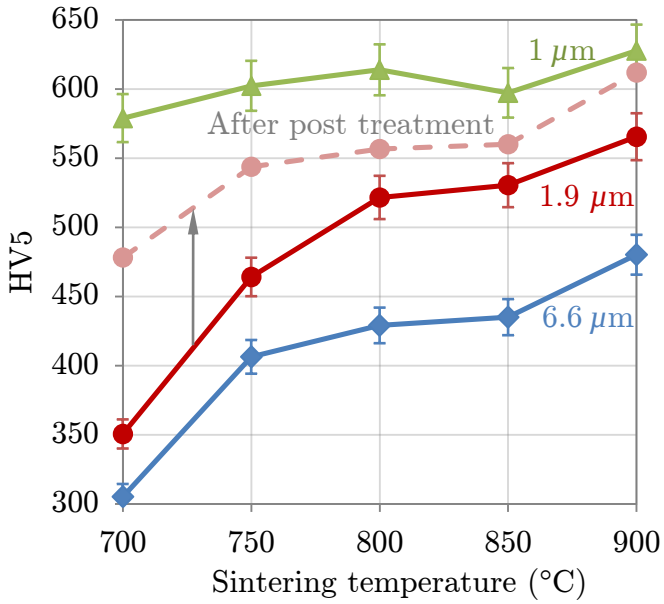

Figure 6.5: Vickers hardness of sintered TiH_2 ball milled for 5, 30 and 180 minutes, of powder size 6.6, 1.9 and 1.0 μm respectively

by the introduction of impurities during processing.

The specimens sintered from TiH_2 ball milled for 30 minutes (1.9 μm) were post treated in a secondary vacuum (approximately $7.6x10^{-6}$ mbar) oven at 500°C for 3 hours with a heating rate of 10°C/minute. The hardness after post treatment is shown in Figure 6.5. The density of these specimens before and after post treatment is shown in Figure 6.6. Post treatment was shown by XRD to eliminate the remaining TiH_2 (see Figure 6.7). The density of specimens increases after post-treatment. Specimens sintered at temperatures of 800°C and above are seen to increase to full density. The hardness of specimens is also seen to increase after post-treatment, while the hardness of specimens sintered at 800°C and above are seen to increase less than those sintered at lower temperatures.

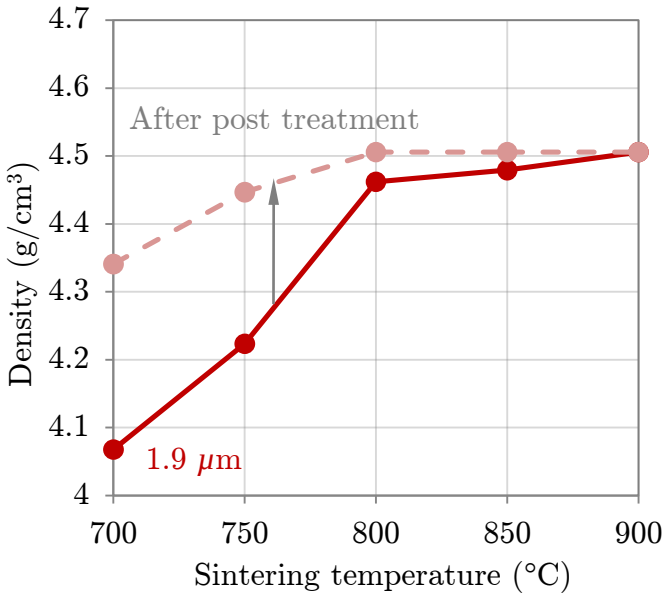

Figure 6.6: Density sintered TiH_2 ball milled for 30 minutes (1.9μm) as sintered and after post treatment

6.3 Titanium Liquid Phase Sintering with Aluminium

The second method studied in this thesis is the use of a liquid aluminium in liquid phase sintering. In this section, the use of three different powders is compared: TiH_2 powder ball milled for 180 minutes (1.0 μm), HDH powder (a dehydrogenated TiH_2 which has been ball milled for 180 minutes) and a coarser commercial titanium powder (44 μm). The densification of these differently sized powders is studied with the addition of a liquid aluminium phase. A Hydride De-Hydride (HDH) powder, dehydrogenated from TiH_2, ball milled for 180 minutes, is also used to eliminate the effects of dehydrogenation during sintering. During sintering, hydrogen can be trapped in the liquid aluminium or titanium aluminides, causing embrittlement. The diffusion and phase transformation between titanium and liquid aluminium (as discussed in Section 2.2.6) are also studied.

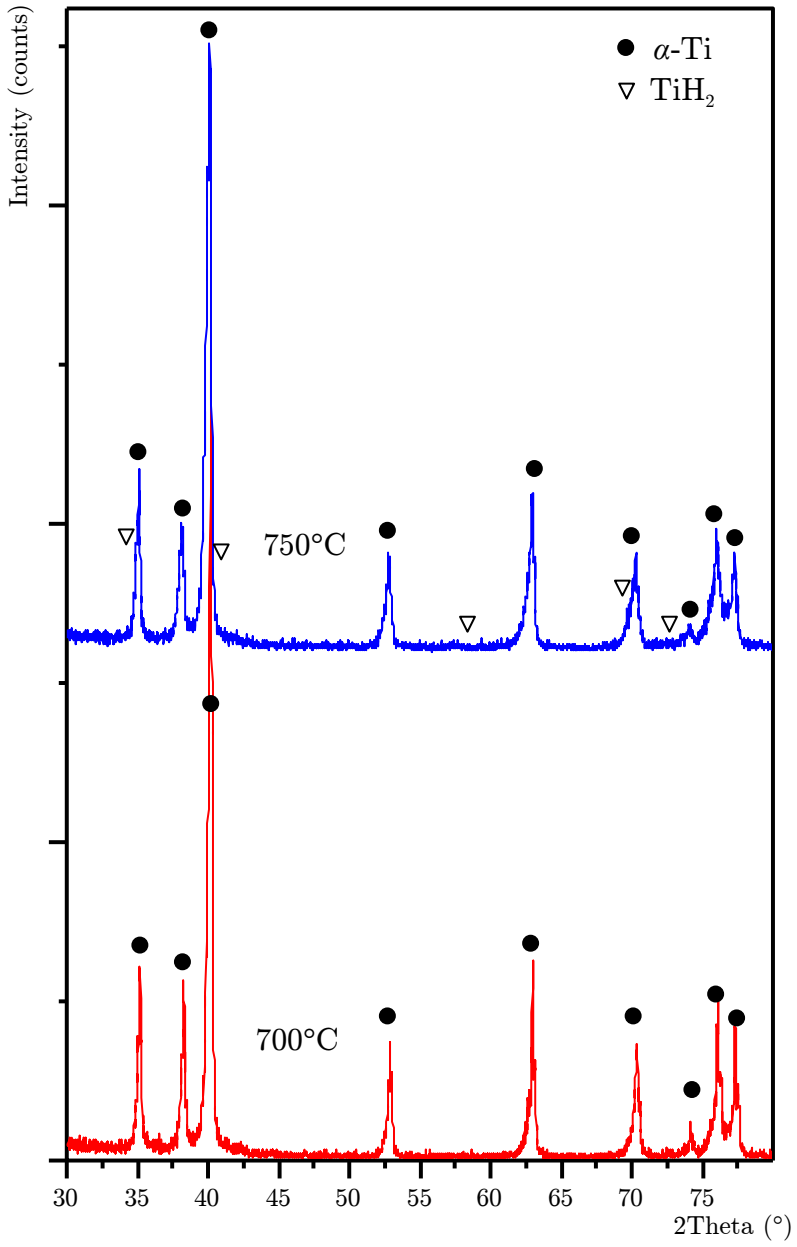

Figure 6.7: XRD patterns of TiH_2, ball milled for 30 minutes and sintered at 700 and 750°C, after post treatment

HDH, TiH_2 and commercial Ti powders were mixed with 0-75 at% aluminium powder and hot press sintered into 6 mm diameter specimens. The pressure and duration were constant at 80 MPa and 30 minutes respectively, and the temperature of sintering was varied from 700 to 900°C. The specimens were then cleaned and sanded using SiC paper to remove contamination from the mould. The cleaned specimens were then measured by the Archimedes method for density and subsequently analysed by XRD. The samples were then set in resin and polished for SEM. Selected powder blends were sintered in rectangular moulds 8 mm by 30 mm for measurement of flexural strength using the 3-point bending test.

6.3.1 HDH Titanium with Liquid Aluminium

Figure 6.8 shows the density of sintered HDH powder with blended aluminium. The theoretical density of an unreacted mixture of Ti and Al is shown as a dashed line, while the theoretical densities of intermetallic compounds, Ti_3Al, TiAL, $TiAl_2$ and $TiAl_3$, are shown joined by a dotted line. The density of sintered specimens is seen to decrease with increasing concentrations of aluminium, and is also increased at higher temperatures.

The specimens were analysed by XRD in order to understand the diffusion and phase formation that occurs during sintering. Figure 6.9 shows the XRD patterns of specimens of sintered HDH powder at 700°C with aluminium. The evolution of the titanium aluminide with the increase of added aluminium can be seen. With the addition of 10 at% Al the phase Ti_3Al is seen, as well as some TiAl, $TiAl_2$ and $TiAl_3$. With the further addition of Al, there is an increasing quantity of TiAl, $TiAl_2$ and $TiAl_3$ until 75 at%, where only $TiAl_3$ is seen.

The process of diffusion between liquid aluminium and solid titanium is described in Section 2.2.6. Ti is diffused into liquid aluminium and $TiAl_3$ forms first, then aluminium diffuses through the $TiAl_3$ layer to the reaction front, forming $TiAl_3$

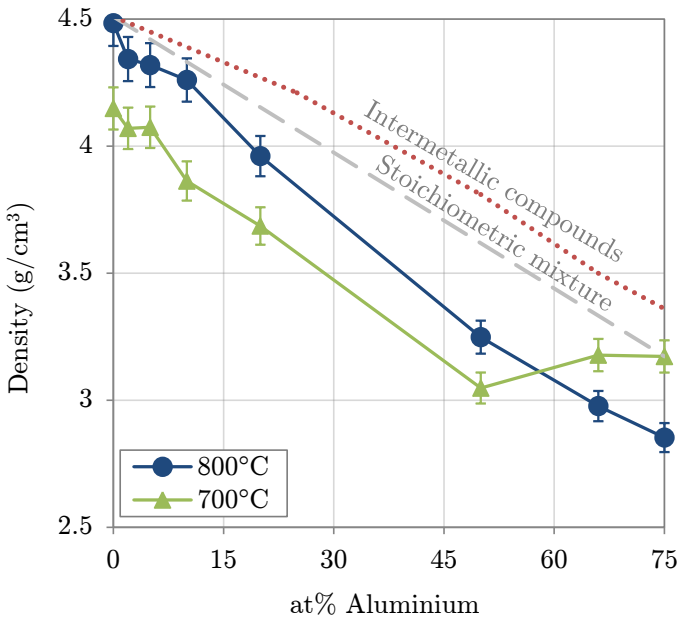

Figure 6.8: Densities of sintered HDH powder with 0-75 at% aluminium

until all the liquid aluminium is consumed. Ti and $TiAl_3$ then diffuse to form phases richer in Ti. During diffusion, the motion of aluminium into titanium causes the formation of Kirkendall pores. In the 10 at% specimen, the phase Ti_3Al has formed through almost complete diffusion between Ti and $TiAl_3$ leaving only traces of TiAl and $TiAl_2$. An increased quantity of aluminium causes incomplete diffusion, leaving increased quantities of TiAl and $TiAl_2$, and, with enough aluminium, $TiAl_3$.

Figure 6.10 shows SEM micrographs of HDH powder with liquid aluminium sintered at 700°C. This Figure shows the diffusion of the liquid aluminium with the HDH powder and its influence on the specimen densification. At low quantities of aluminium, large pores are formed, surrounded by titanium aluminide intermetallics. The aluminium has melted and reacted with the titanium, forming a solid intermetallic around the pore in place of the aluminium particle. Where the aluminium has not been distributed during the time that it was liquid, there remains pure titanium. This effect causes pore densification and continues until higher quantities of aluminum (66 and 75 at%) are introduced. Here the increased

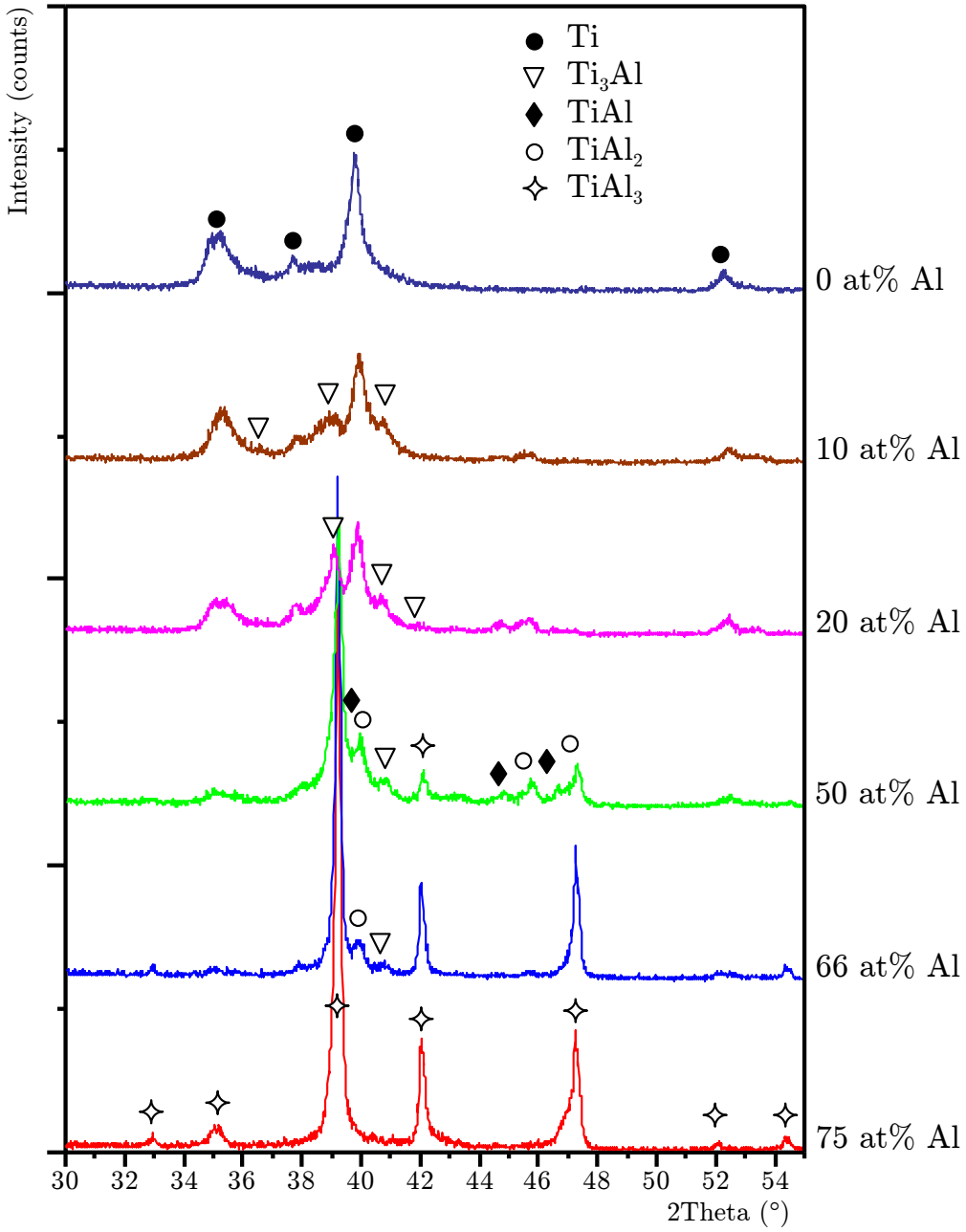

Figure 6.9: XRD patterns of HDH powder sintered with 0-75 at% aluminium and sintered at 700°C under 80 MPa for 30 minutes

quantity of liquid aluminium has improved densification through rearrangement before the reaction to form $TiAl_3$ has been completed.

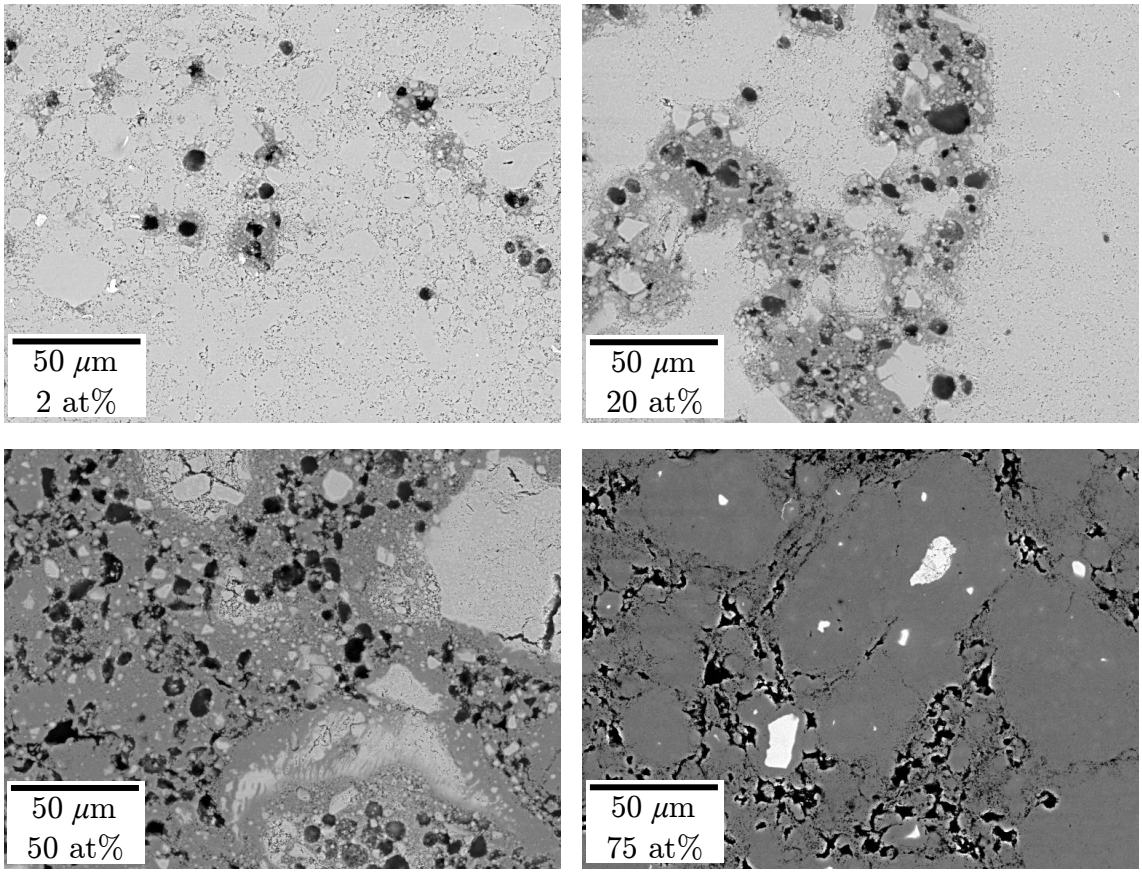

Figure 6.10: SEM micrographs of HDH powder sintered with 2-75 at% aluminium and sintered at 700°C under 80 MPa for 30 minutes

HDH with Liquid Aluminium at 800°C

Figure 6.11 shows the XRD patterns of sintered HDH power with aluminium and 800°C. Here the increased rate of diffusion at higher sintering temperature is seen. At concentrations of 20 and 50 at% Al, greater quantities of phases higher in Ti are seen when compared with sintering at 700°C. After the liquid aluminium is consumed and $TiAl_3$ is formed, the higher sintering temperature increases the rate of diffusion between Ti and $TiAl_3$. As a result, intermetallics higher in Ti, such as

$TiAl_2$ and TiAl, are seen by XRD.

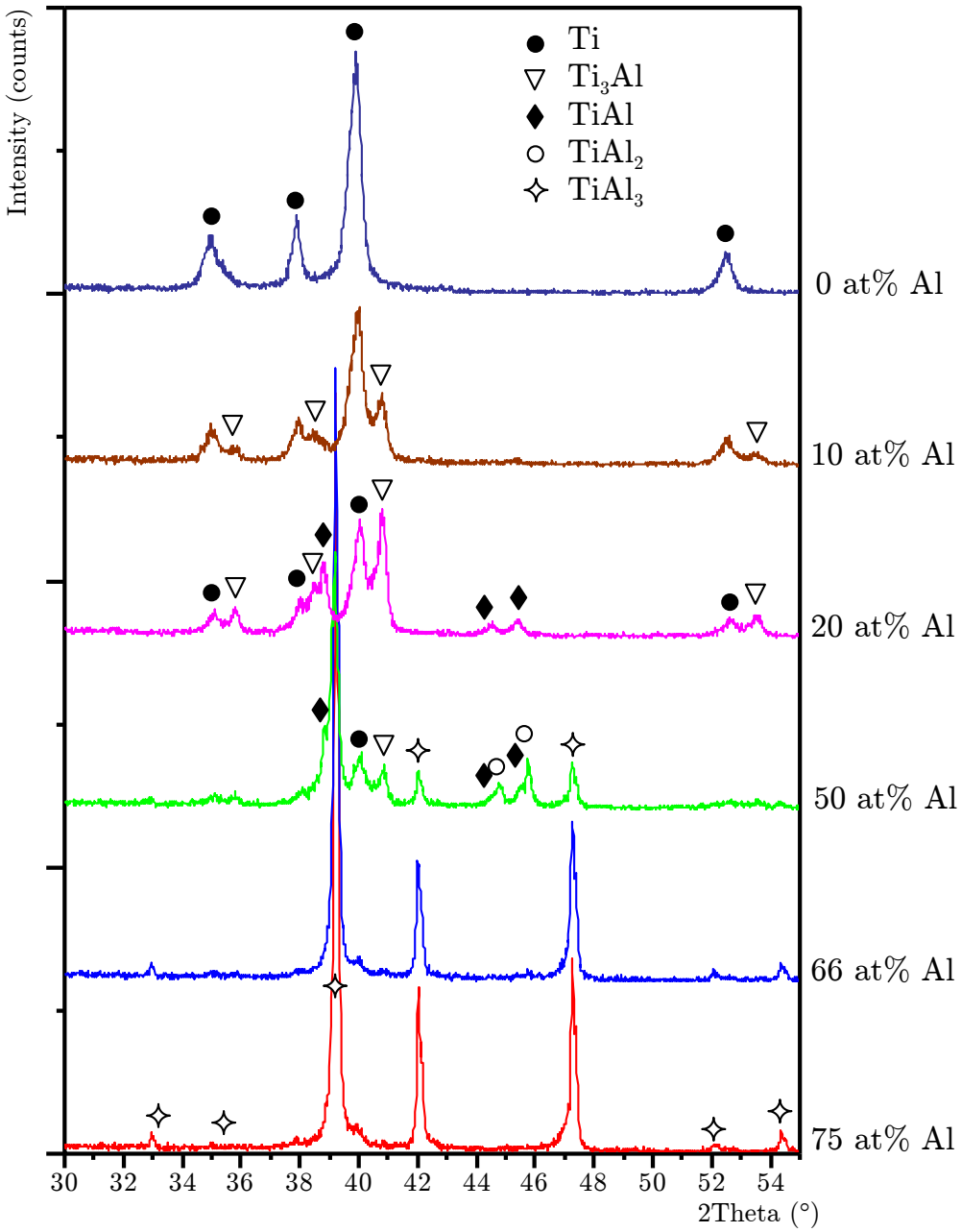

Figure 6.11: XRD patterns of HDH powder sintered with 0-75 at% aluminium and sintered at 800°C under 80 MPa for 30 minutes

Figure 6.12 shows the microstructure of HDH powder sintered with liquid aluminium at 800°C. The solidification of titanium aluminides around a pore is

seen. The densification behaviour is improved, compared with sintering at 700°C. The density of the surrounding titanium is seen to improve. However the pore formation behaviour is the same.

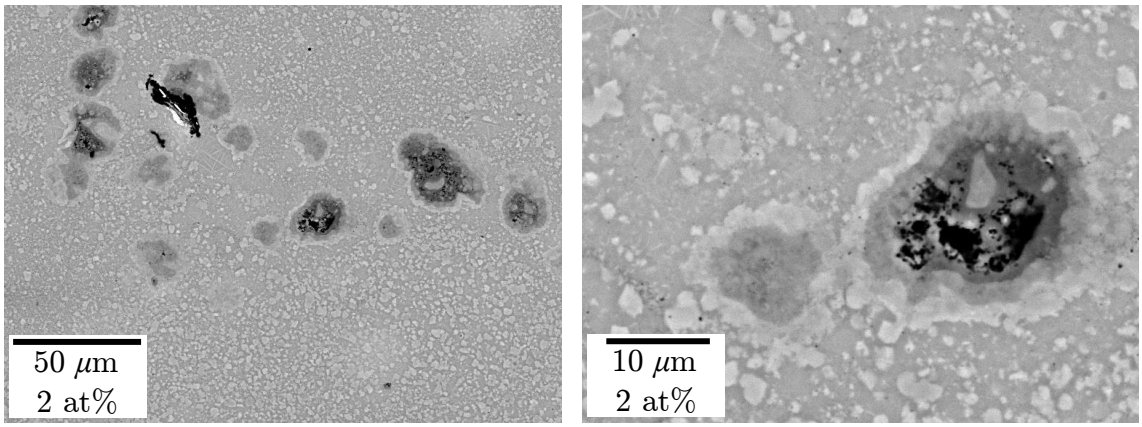

Figure 6.12: SEM micrographs of HDH powder sintered at 800°C with 2 at% Al shown at 1k and 4k times magnification

6.3.2 Ball Milled TiH_2 with Liquid Aluminium

A limited series of samples of ball milled TiH_2 was sintered with liquid aluminium for comparison with HDH powder. The densities of sintered TiH_2 with liquid aluminium are shown in Figure 6.13. Similar to the results seen with HDH powder (cf Figure 6.8), the density is seen to decrease with the increase in aluminium concentration, and is increased further with the higher sintering temperature.

Figure 6.14 shows the XRD patterns of TiH_2 sintered at 700°C with 0-75 at% Al. The formation of intermetallic phases is similar to the results observed for the HDH powder (cf Figure 6.10).

6.3.3 Commercial Ti with Liquid Aluminium

Commercial titanium with a larger size (44 μm) than ball milled titanium is used to compare the effect of titanium particle sizes on the densification due to a liquid

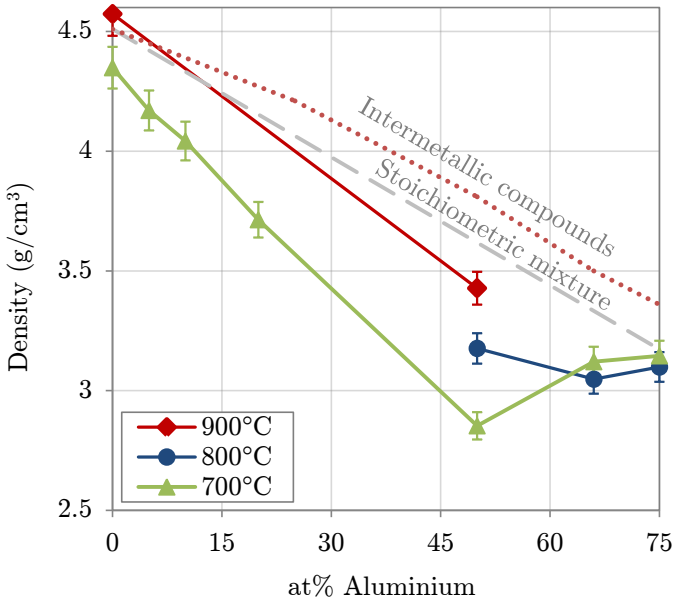

Figure 6.13: Densities of sintered TiH_2 powder with 0-75 at% aluminium

aluminium phase. Figure 6.15 shows the density of sintered commercial Ti powder with 0-50 at% Al hot press sintered from 700-800°C. Again, the densities are compared with the density of an unreacted mixture of Ti and Al is shown as a dashed line, while the densities of intermetallic compounds, Ti_3Al, TiAL, $TiAl_2$ and $TiAl_3$ are shown joined by a dotted line. At 700°C, the addition of 5 at% Al shows an improvement in densification, and at 800 and 900°C, there is an improvement in density at 10 at% Al. With the increase of aluminium concentration from 10 to 20 at%, the density is decreased at all sintering temperatures. At a low concentration of aluminium (0-20 at%), the density is increased alongside the temperature. Conversely, at 50 at% Al, the densification is decreased with increasing sintering temperature.

The phase formation of commercial titanium powder with liquid aluminium during sintering at 700°C is seen in Figure 6.16. With 10 at% Al, the phase Ti_3Al is detected by XRD. This phase forms after the initial formation of $TiAl_3$ and then the diffusion of Ti and $TiAl_3$ to form $TiAl_2$ and then TiAl and finally Ti_3Al. Thus

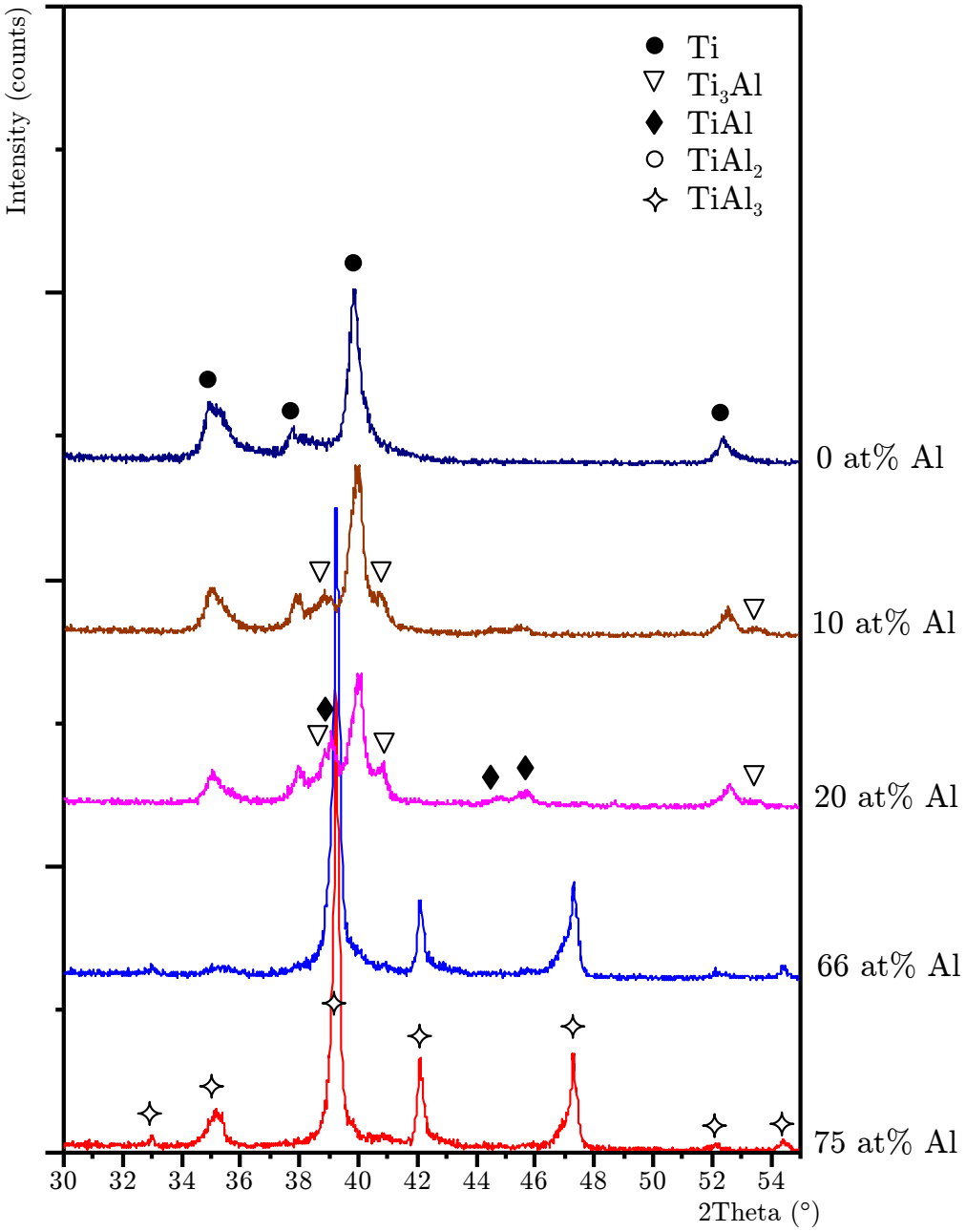

Figure 6.14: XRD patterns of TiH_2 ball milled for 180 minutes, blended with 0-75 at% Al powder and sintered at 700°C under 80 MPa for 30 minutes

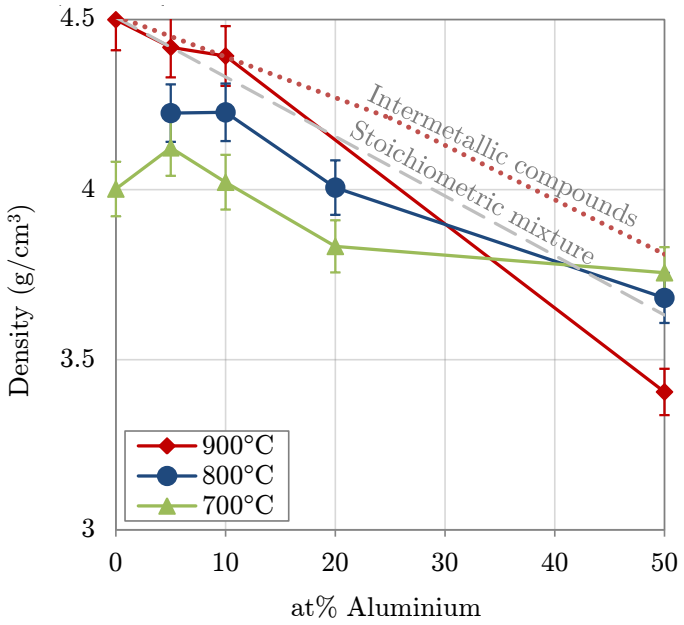

Figure 6.15: Density of commercial Ti powder sintered with 0, 5, 10, 20 and 50 at% Al at 700-900°C under 80 MPa for 30 minutes

the conditions are sufficient for this process of diffusion. At 50 at% Al, a range of titanium aluminides is detected by XRD, from pure Ti to $TiAl_3$. In this case, the additional aluminium has led to the increased quantity of intermetallics, and has meant that the diffusion process was not able to progress as far during sintering. A more complete diffusion process would show increased quantities of the intermetallic, which closely matches the stoichiometric ratio of the mixed powders. For example, at 25 at% Al, Ti_3Al would be the only intermetallic phase remaining, and at 50 at% Al, TiAl would be the only phase remaining.

Figure 6.17 shows XRD patterns of commercial Ti with liquid Al sintered at 900°C. Here the increased sintering temperature from 700 to 900°C is seen to advance the diffusion of Ti and Al. At 10 at% Al, the phase Ti_3Al is detected. At 50 at% Al, the diffusion to form the titanium aluminides TiAl, $TiAl_2$, and Ti_3Al from $TiAl_3$ has advanced as they are seen to be in higher quantities than when sintered at 700°C. A more advanced stage of diffusion has been caused by the increase in

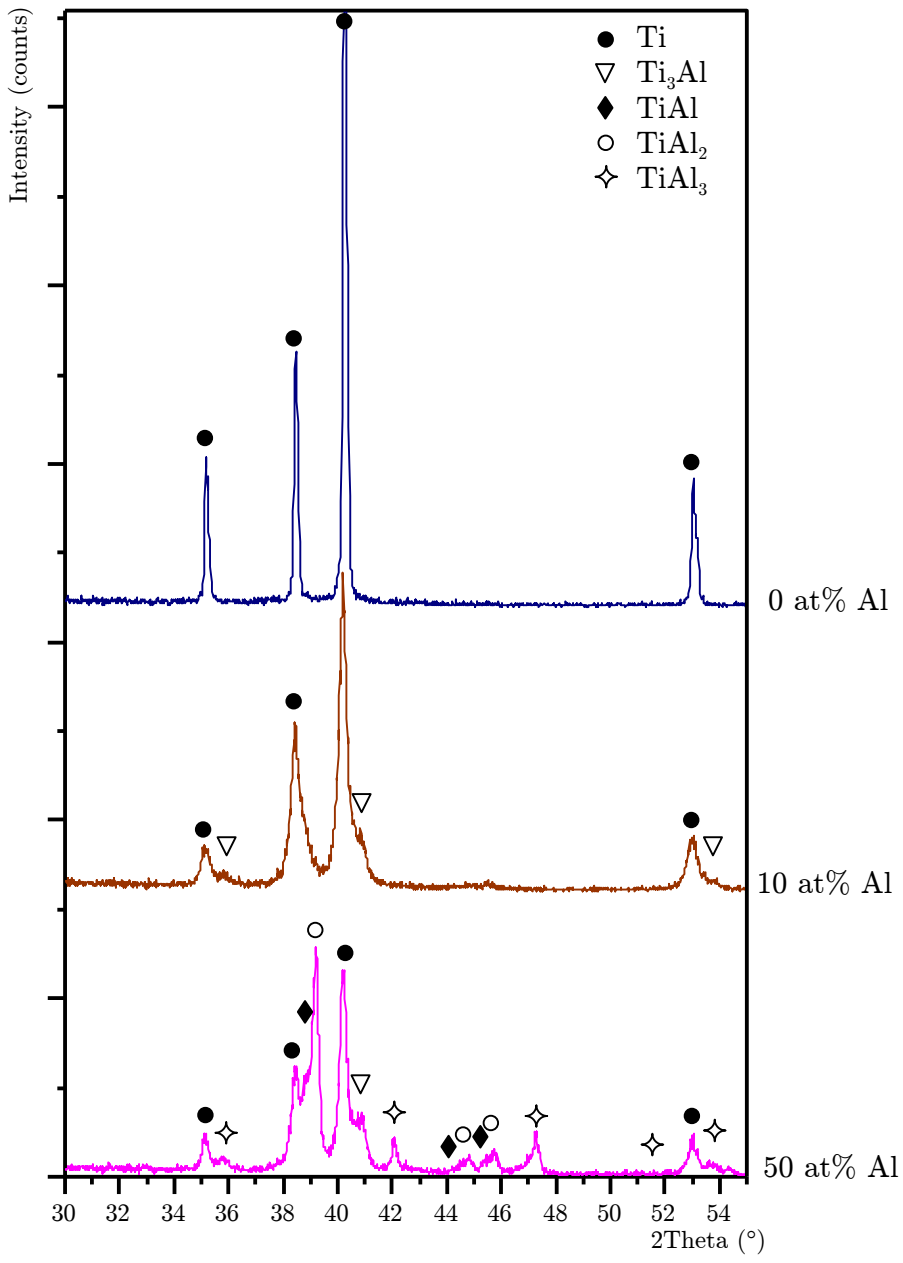

Figure 6.16: XRD patterns of commercial Ti sintered with 0, 10 and 50 at% Al, at 700°C under 80 MPa for 30 minutes

sintering temperature. There has been an increase in intermetallics which matches the stoichiometry of the powder mixture.

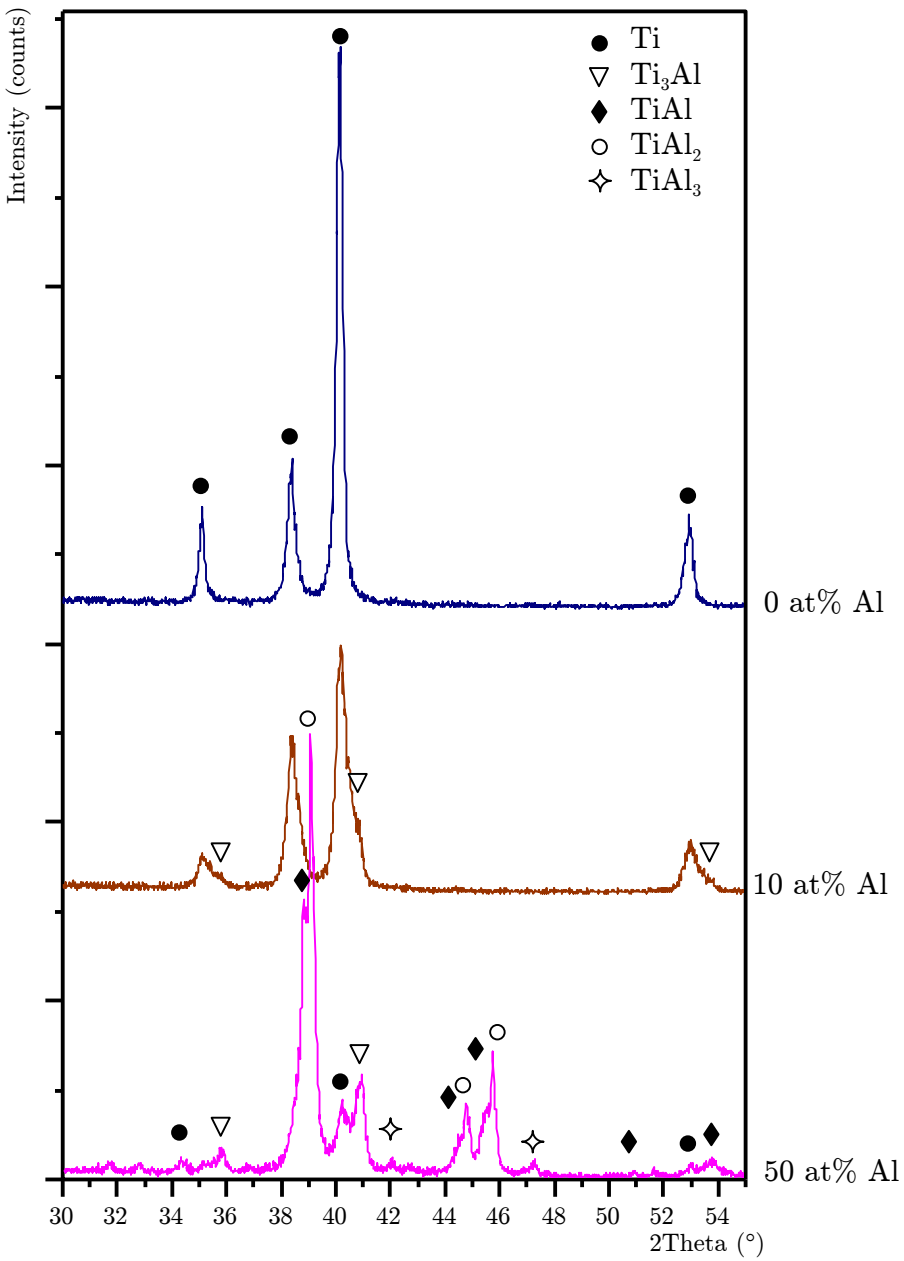

Figure 6.17: XRD patterns of commercial Ti sintered with 0, 10 and 50 at% Al, at 900°C under 80 MPa for 30 minutes

The microstructure of commercial Ti with liquid Al is shown in Figure 6.18. The SEM micrographs show the pure titanium (lightest phase) and the intermetallic

phases (from light, which have greater quantities of Ti, to dark, which have greater quantities of Al) and the pores (black). The intermetallic phases have formed around the titanium particles. The aluminium has become liquid and wet the titanium particles, triggering diffusion.

At 5 at% Al, the liquid aluminium is seen not to have a uniform distribution. In some areas, titanium is not surrounded by a darker intermetallic phase. Where the aluminium has not reached the titanium particles, the titanium has densified through solid state sintering, and some pores remain. At 10 at% Al, the distribution of aluminium is sufficient to surround all the titanium particles. At 50 at% Al, the titanium particles have an increased intermetallic layer on the outside.

The increase in sintering temperature decreases the quantity of pores for 5 and 10 at% Al, and has better densification. At 50 at% Al, the quantity of pores is increased. These micrographs correspond well with the density measurements made (cf Figure 6.15). The decrease in densification observed when the temperature is increased with 50 at% Al is caused by the increased rate of diffusion at a higher temperature. The intermetallics layered on the outside of the commercial titanium particles have further diffused with the titanium, as seen by XRD (cf Figure 6.16 and 6.17). Further diffusion continues the mass displacement of aluminium towards the centre of the particle, continuing the pore formation (known as the Kirkendall effect).

The formation of intermetallics surrounding the titanium particles is seen by SEM in Figure 6.19 and the phases are identified by EDS in Figure 6.20. The solid titanium particles are surrounded by a range of titanium aluminides. The initial reaction between liquid aluminium and titanium to form $TiAl_3$ has occurred. This reaction gives rise to Kikendall pores around the particles, and $TiAl_3$ forms a rigid skeleton. The further diffusion between Ti and $TiAl_3$ has formed layers of intermetallics surrounding the titanium particles.

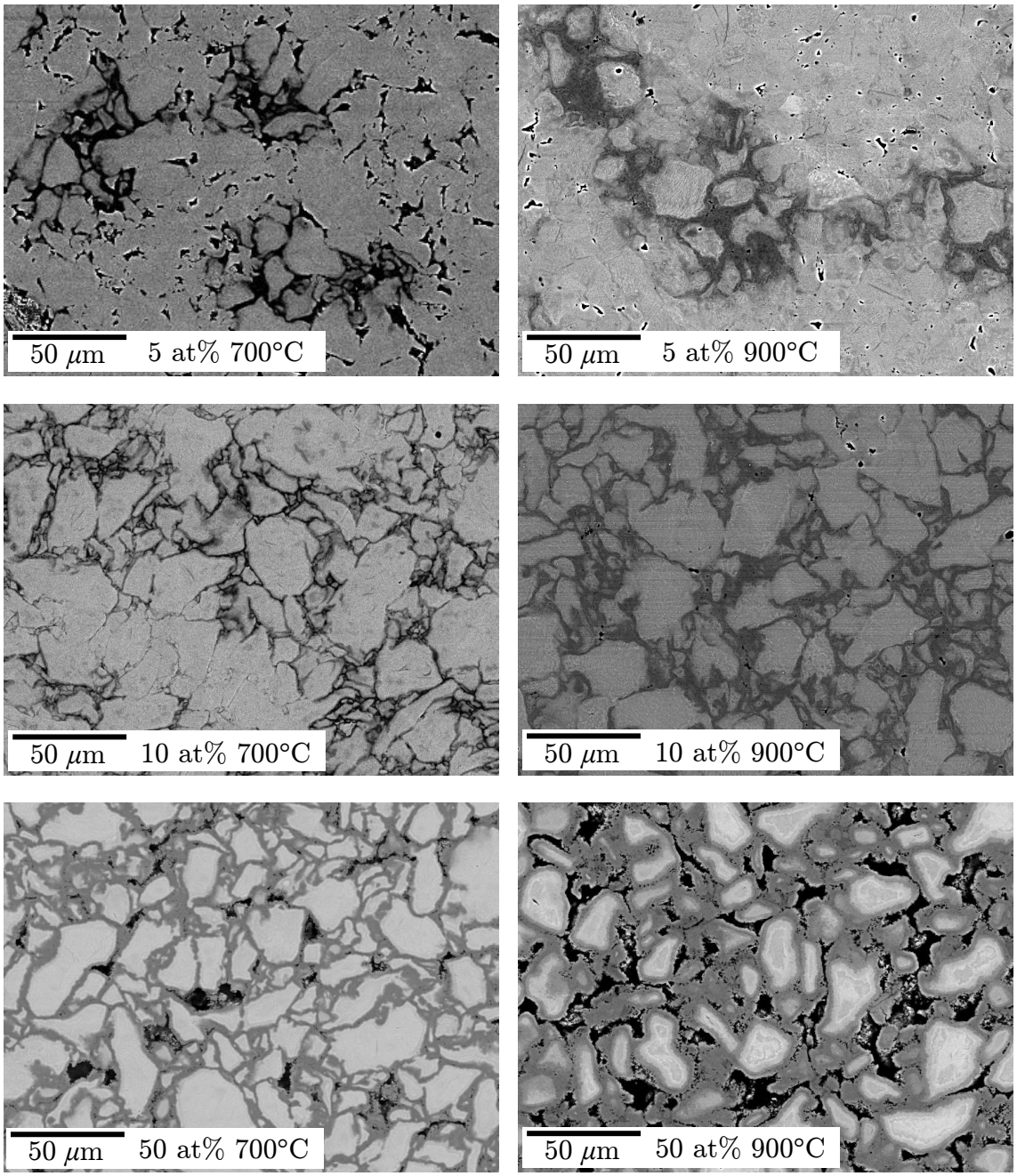

Figure 6.18: SEM micrographs of commercial Ti sintered with 5, 10 and 50 at% Al, at 700 and 900°C

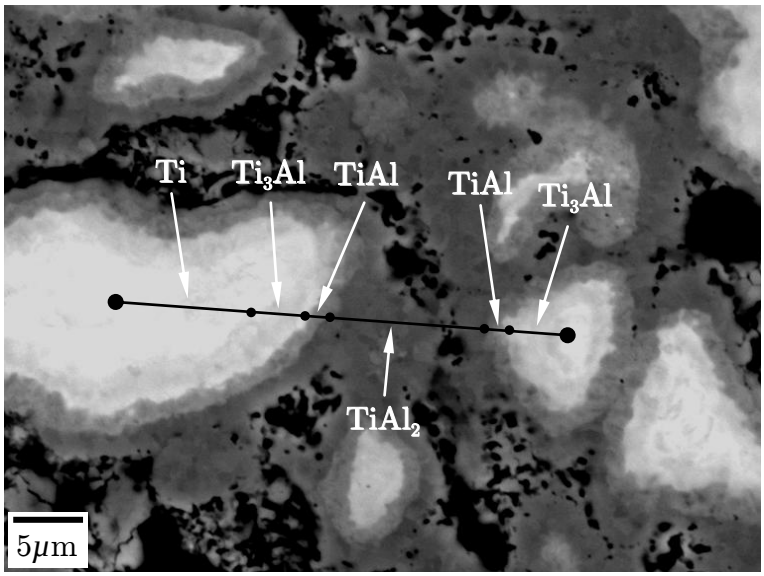

Figure 6.19: SEM micrograph of commercial Ti sintered with 50 at% Al, at 900°C under 80 MPa for 30 minutes

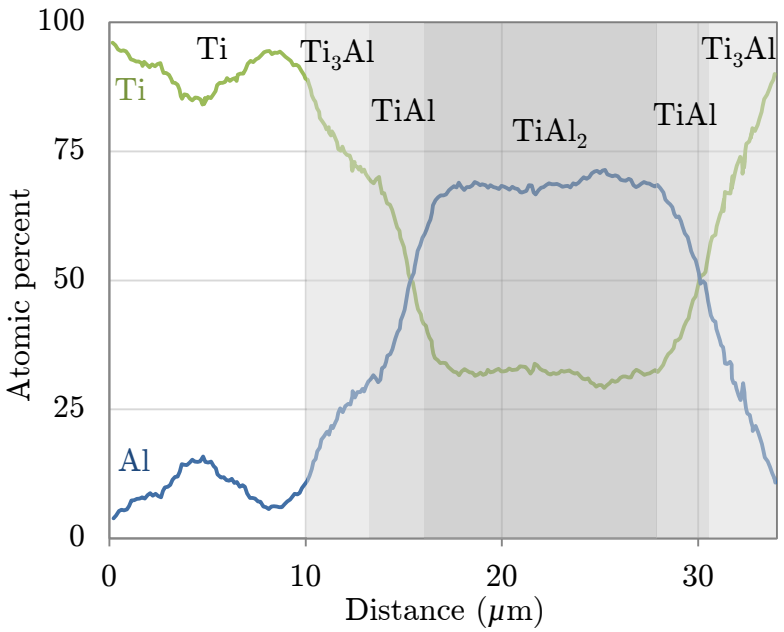

Figure 6.20: EDS elemental line profile of commercial Ti sintered with 50 at% Al at 900°C under 80 MPa for 30 minutes

Finally, the specimens of commercial Ti powder sintered with liquid aluminium are compared using a flexural bending test. Figure 6.21 shows the results of flexural testing of commercial Ti with 0, 10 and 50 at% Al, sintered at 900°C. The addition of 10 at% Al creates an increased flexural strength, and a complete loss of ductility is seen. If the ductility of pure titanium of 15%el (ASTM grade 4, see Table 2.3) is compared with the ductility of titanium aluminides of 1-5%el (see Table 2.2), we see that the loss of ductility in the specimen is due to the brittle titanium aluminide phase surrounding the ductile titanium particles. At 50 at% Al, the strength is decreased further. The porous microstructure seen in SEM micrographs (see Figure 6.18) of this specimen is the cause of the low strength.

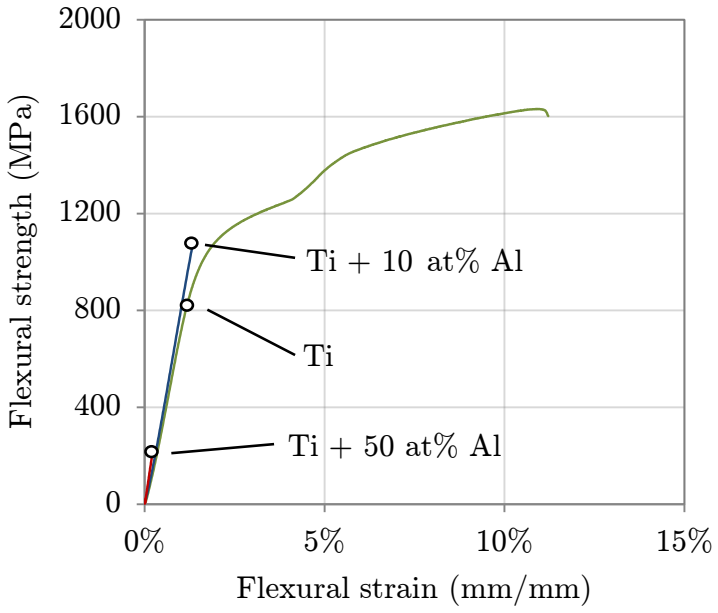

Figure 6.21: Flexural bending test of commercial Ti sintered with 0, 10 and 50 at% Al, at 900°C under 80 MPa for 30 minutes

6.4 Conclusion

TiH_2 powders produced by ball milling were hot press sintered and characterised for density, microstructure and hardness. The density of sintered specimens measured by the Archimedes immersion test, was seen to increase significantly with further ball milling duration (leading to particle size reduction). Dehydrogenation during sintering was seen by XRD and SEM to improve with ball milling duration. Dehydrogenation during hot press sintering was impaired when compared with the dehydrogenation of loose powders studied by DSC in Chapter 5. The grain size of the sintered specimens was seen by SEM to reduce by using smaller starting powders. Finally, specimen hardness, tested by microindentation, was seen to increase with sintering temperature, and significantly with ball milling duration. These results indicate the potential for improving titanium sintering using ball milled TiH_2, by reducing the temperature required.

Powders of different sizes were mixed with varying concentrations of aluminium and hot press sintered. The density of the HDH and TiH_2 ball milled powders decreased with increasing concentrations of aluminium. SEM of these specimens showed that aluminium diffuses rapidly around the immediate titanium and leaves a pore surrounded by intermetallic phases. The use of a liquid aluminium phase with commercial titanium powders, of a larger size than the HDH and TiH_2 powders, was seen to improve density at concentrations of 5 to 10 at% Al, indicating the potential for LPS with aluminium to improve titanium sintering at low temperatures.

The results of the experimental study of sintering ball milled TiH_2 and aluminium LPS are discussed in Chapter 7.

Chapter 7

Analysis of Results and Discussion

7.1 Introduction

This chapter discusses the experimental results of the study of sintering ball milled TiH_2 and titanium LPS using aluminium. The practical implications of the experimental results are also discussed. The study of these techniques is aimed at improving titanium sintering at reduced parameters in order to reduce the cost of production. The potential for direct sintering of ball milled TiH_2 powder to improve sintering at low temperatures is discussed. The effect of the powder characteristics presented in Chapter 5 are related to the density, microstructure and hardness obtained by hot press sintering presented in Chapter 6.

The addition of aluminium to fine ball milled powders and coarser commercial powders was studied at low temperatures to improve densification. The effects of powder size and aluminium concentration on the density, microstructure and flexural strength of the specimens examined in Chapter 6 are discussed.

7.2 Dehydrogenation Behaviour of ball milled TiH_2 powders

TiH_2 powder synthesis was performed by hydrogenating titanium sponge and then ball milling at different durations to study the effects of particle size reduction on dehydrogenation. A rapid decrease in particle size from ball milling TiH_2 sponge was seen in the first 10 minutes of ball milling to under 2 μm. Subsequent milling from 10 minutes to 180 minutes reduces the size further only from 2 μm to 1 μm. This result is in concordance with the studies by Bobet et al. (2003) and Bhosle et al. (2003). The study of ball milled TiH_2 also shows the rapid decrease in crystallite size of the powder particles caused by mechanical work. It was observed by granulometry and SEM that a broad range of particle sizes was created by ball milling and the agglometration of fine powder formed.

The dehydrogenation of the TiH_2 powders was studied by DSC at a heating rate of 10K/min to 580°C. The dehydrogenation was seen to occur in two stages with the phase changes $TiH_2 \rightarrow \delta\text{-}TiH_{(0.7-1.5)} + \beta\text{-}Ti \rightarrow \alpha\text{-}Ti$ as observed by Bhosle et al. (2003); Asavavisithchai et al. (2007); Kennedy (2002); Wang et al. (2010b); Liu et al. (2009). The dehydrogenation started at 500°C for TiH_2, ball milled for 5 minutes, and reduced to below 450°C for TiH_2, ball milled for 180 minutes. The reduction of the temperature at which dehydrogenation occurs is expected to improve dehydrogenation and densification during sintering.

Different pressures of cold compaction change the rate of dehydrogenation. The results of DSC show that pre-compaction of the powder causes the particles to dehydrogenate slowly (Figure 5.7). While the pre-compaction does not directly relate to the hot press sintering process, it is indicative that dehydrogenation will be delayed by pressure assistance during sintering.

7.3 Densification Behaviour of Ball Milled TiH_2 powders

The ball milled TiH_2 powders, synthesised and characterised for their dehydrogenation behaviour, were densified by induction hot press sintering. Sintering was performed at 80 MPa for 30 minutes at 700-900°C. The densification of specimens was analysed by density measurement and SEM. The density was observed to increase with ball milling duration. Powders ball milled for 180 minutes were fully dense when sintered at 700°C, whilst powder ball milled for 5 minutes did not achieve full density until 900°C was achieved.

The level of dehydrogenation of these specimens was determined by XRD and SEM. XRD analysis showed the phases of α-Ti and remaining TiH_2. The TiH_2 phase was shown to decrease with sintering temperature, and was eliminated at lower temperatures for powders ball milled for longer times. TiH_2 was not observed by XRD for powder ball milled for 180 minutes and sintered at 800°C, while for powder ball milled for 5 minutes TiH_2 was first not observed at 900°C.

The results observed in this study indicate the restriction on sintering imposed by the dehydrogenation process. In previous studies by Wang et al. (2010b), Azevedo et al. (2003) and Bolzoni et al. (2012a), complete dehydrogenation has been achieved during sintering of TiH_2, and the minimum required parameters to reduce the hydrogen concentration below general limits have not been investigated. The incomplete dehydrogenation during sintering seen in this study indicates that the sintering temperature must be sufficient to ensure complete dehydrogenation, and that ball milling duration decreases the required sintering temperature.

The difference in the level of dehydrogenation of TiH_2 powders from the DSC experiment and sintering indicates that pressure-assisted sintering in a graphite mould restricts the dehydrogenation. In this present study, dehydrogenation of

TiH_2 powder was completed when tested by DSC below 580°C in under 15 minutes. The dehydrogenation of TiH_2 from pressure assisted sintering was incomplete at higher temperatures and longer durations. This indicates that dehydrogenation is delayed by the mould or pressure. Thus, this is a limitation on sintering TiH_2 at low temperatures using pressure assisted sintering. These results have not been reported before because previous studies of sintering TiH_2 have always resulted in complete dehydrogenation.

A study by Bolzoni et al. (2012b) has used similar sintering parameters to those used in this study, where TiH_2 was hot press sintered at 1100-1300°C at 50 MPa for 15 minutes. At 1100°C density of 98% was achieved, and at 1300°C 100% density was achieved. This present study uses hot pressing sintering of TiH_2 ball milled for 180 minutes at 700-900°C at 80 MPa for 30 minutes. Theoretical densities of 100% are achieved by an increase in ball milling duration and temperature. The sintering parameters vary between the study by Bolzoni et al. (2012b) and this thesis. However, this thesis contributes the unique insight that ball milling greatly increases the densification of TiH_2 powders.

7.3.1 Hardness and Microstructure of Sintered TiH_2

The Hardness Vickers values of the specimens sintered from ball milled TiH_2 were determined by the indentation method (Figure 6.5). The hardness of the sintered specimens is shown to increase with sintering temperature. The increase in the specimens' hardness mimics the increase in the specimen density with temperature (Figure 6.1). Additionally, hardness increases with ball milling duration for sintering at all temperatures.

The values of hardness of dense sintered pure titanium are between 500-600 HV and are high compared with pure titanium of 122-280 HV (ASTM Grade 1 and Grade 4, Davis, 1990). This high level of hardness could be the effect of:

- Remaining hydrogen from incomplete dehydrogenation;
- The level of density;
- Grain refinement;
- Remaining interstitial impurities (C, N, O).

The following discussion will show that it is likely that increased oxygen pickup caused by the increased specific surface area of fine ball milled powders is the likely cause of high hardness. The increase in hardness with sintering temperature is shown to be caused by increased density.

The hardness of titanium sintered from TiH_2 can be increased by incomplete dehydrogenation. The remaining hydrogen, dissolved in a solid solution with titanium, will cause hardening. Post-treatment of sintered specimens was performed and was seen by XRD to eliminate hydrogen (Appendix B) and increase the density of the specimens (Figure 6.6). After post-treatment, the hardness of the specimens was seen to increase (Figure 6.5) contrary to the hardening effect of hydrogen. The increase in hardness was then caused by the increased density caused by post-treatment.

Density of a sintered part directly relates to its strength (Wang et al., 2010b). Porosity reduces the amount of solid material available to resist deformation, so a denser part will have higher strength and hardness. The increase in hardness of specimens matches the increase in density observed. The hardness of the post-treated specimens also matches the increase in density. The increase in density with increased sintering temperatures has caused an increase in hardness.

A fine microstructure as a result of a fine starting powder also contributes to the increase in hardness. Microstructure grain refinement is known to increase materials' strength (Fang et al., 2012), which is related to hardness (Zhang et al., 2011). A fine microstructure causes hardening because the motion of dislocation is restricted

by the increase in grain boundaries. In this study, a finer microstructure is observed by SEM through the use of finer powders (Figure 6.2), which leads to a higher measured hardness. However, it is currently impossible to evaluate the level of hardness increased by grain size hardening because of the unknown influence of other hardening factors.

Other atmospheric impurities, C, N, and O, are known to increase the hardness of titanium, as discussed in Section 2.2.7. Interstitial elements create distortions inside the crystal lattice which impede the motion of dislocations, leading to strengthening and hardening. The processing of titanium leads to the pickup of impurities. The surface of TiH_2 particles is coated with an oxide layer (Tsuchiya et al., 2005). The reduction of particle size increases the specific surface area, and therefore the quantity of oxygen in a powder material.

The high hardness of the titanium specimens has been caused by the introduction of increased levels of oxygen through the reduction of particle size by ball milling. The increased oxygen concentration from mechanical milling has been reported previously to cause increased hardness (Ivasishin et al., 2002; Bolzoni et al., 2012a). Oxygen is transferred into a specimen through the oxide layer of the TiH_2 powders used and the high specific surface area of fine ball milled powder increases the level of oxygen introduced.

7.4 Densification of Ti LPS using Al

The second sintering method studied in this thesis for the enhanced densification of titanium is the use of aluminium in LPS. Titanium was mixed with 0 to 75 at% elemental aluminium powder and hot press sintered. Aluminium was used in the investigation of LPS because of its low melting point, which enables densification at low temperatures. The study was performed at temperatures between 700 to 900°C,

at 80MPa, for 30 minutes. The specimens were characterised for density, phase and microstructure. Selected specimens were tested for flexural strength using the 3-point bending test. The results of three different powders were compared: TiH_2 ball milled for 180 minutes (1.0 μm), TiH_2 ball milled for 180 minutes which has been dehydrogenated (HDH), and commercial titanium powder (44 μm).

The densities of the three different powders sintered at 700°C at 80MPa for 30 minutes are shown in Figure 7.1. The densities are compared with an unreacted mixture of titanium and aluminium (lower dashed line) and the density of a fully reacted intermetallic compound (upper dotted line). The intermetallic compound has a higher atomic packing and density than the unreacted mixture (Froes, 1992). The commercial Ti powder with 5 at% Al has increased density, while for the TiH_2 and HDH powders, density is reduced by the addition of aluminium.

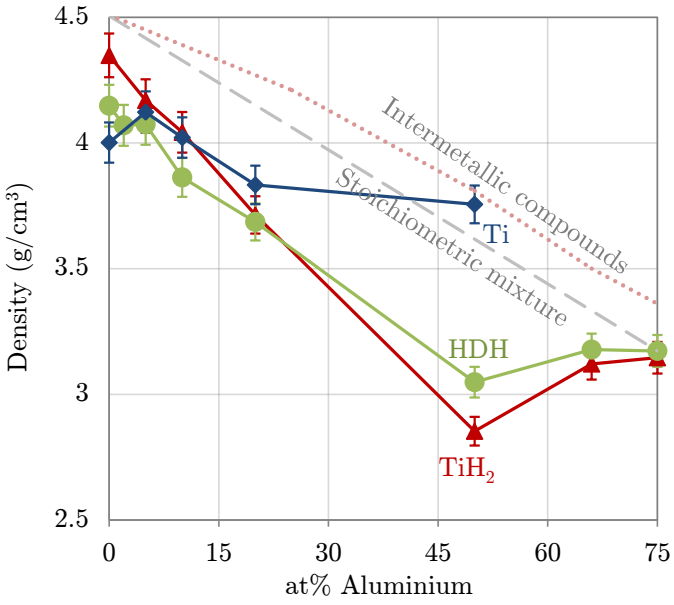

Figure 7.1: Densities of commercial Ti, ball milled TiH_2 and HDH powders, sintered with 0-75 at% Al at 700°C under 80 MPa for 30 minutes

The densities of TiH_2 and HDH follow the same trend of densification with the addition of aluminium. The density of these powders decreases with increased

aluminium concentrations. The density of sintered HDH powder is generally lower when compared with TiH_2. The difference between these powders is that the HDH has no hydrogen (or the level is undetectable by XRD) and that the dehydrogenation performed on the HDH powder before sintering has begun to crystalise the particles. The HDH particles have re-crystalised and annealed prior to sintering and the energy of the grain boundaries has decreased, essentially decreasing the driving force for densification during sintering. Furthermore, the enhancements caused by dehydrogenation during sintering are eliminated.

While there are similar results between HDH and TiH_2 powder, the commercial Ti powder of larger size (44 μm compared to 1.0 μm) shows a different trend. The commercial Ti powder shows an increase in density when sintered with 5 to 10 at% Al. Figure 7.2 compares the microstructure of an HDH powder sintered with 5 at% Al, with the microstructure of a commercial Ti powder sintered with 10 at% Al. The commercial Ti powder has Ti-Al intermetallics (mainly Ti_3Al) surrounding the titanium particles, while the HDH powder has intermetallics surrounding pores at the aluminium particle sites.

The causes for the differences of densification between the ball milled powders (TiH_2 and HDH) and the commercial powders lie in their different size and morphology. Diffusion between solid Ti and liquid Al starts at the surface of the Ti particle. The increased specific surface area of the finer ball milled powders increases the surface area at which the diffusion can take place, thus diffusion occurs faster. The reaction between liquid Al and solid commercial Ti powder is slowed by the increased size of the particles, and the liquid Al is able to surround the commercial Ti particles to encourage rearrangement and densification. The HDH powder reacts faster with liquid aluminium, a pore is created and is surrounded by intermetallics at the site where the aluminium particle lies.

A study by Savitskii and Burtsev (1981) showed that the increase in Ti particle

size above 45 μm caused additional swelling because of the stress in the solid intermetallic layer that grows around the Ti particles. This present study uses a finer Ti powder (1.0 μm) and it is seen that a decreased particles size acts to decrease density. The increased reaction rate between fine Ti particles and liquid Al decreases densification.

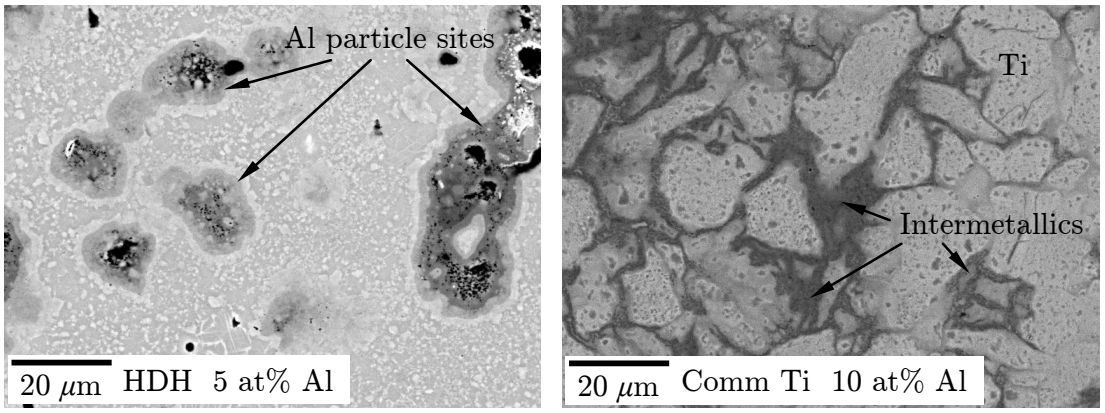

Figure 7.2: SEM mircrographs of HDH and commercial Ti powder sintered with 5 and 10 at% Al respectively, at 800°C under 80 MPa for 30 minutes

Importantly, it is observed in this study that, with pressure assistance, full densification can occur using aluminium LPS (see Figure 6.15). Commercial Ti powder showed an increase in density with 5-10 at% Al sintered at 700-900°C under 80 MPa for 30 minutes. A fully dense microstructure is seen when sintering with 10 at% Al at 800 and 900°C (see Figures 7.2 and 6.18). Here, the liquid aluminium is able to surround the titanium particles, whereas for finer ball milled powders, this did not occur.

In previous studies by Liu et al. (2006) and Savitskii and Burtsev (1979), the use of aluminium in LPS caused a reduction in density during free sintering. The diffusion between liquid aluminium and solid titanium caused the formation of pores, known as the Kirkendall effect. However, in this present study it was found that full densification is possible using LPS through pressure assisted sintering for Al

concentrations lower than 10 at%.

It must be noted that at 50 at% Al, full density was not obtained using commercial Ti powder. It is interesting that when sintering commercial Ti with 50 at% aluminium, material density decreases with temperature (see Figure 6.15). This agrees with results observed in a study by Liu et al. (2000). The increased concentration of aluminium caused more Kirkendall pores to form, which are enlarged by the increasing temperature.

7.4.1 Flexural Strength and Microstructure of titanium using Aluminium LPS

The flexural strength of selected specimens sintered using aluminium LPS was tested. Three specimens were compared with 0, 10 and 50 at% Al sintered from commercial titanium at 900°C at 80 MPa for 30 minutes (see Figure 6.21). The results of flexural testing are shown in Table 7.1. The pure titanium specimen was observed to be ductile and, with the addition of 10 at% Al, there is a loss in ductility with a slight increase in flexural yield strength. Figure 7.3 shows the microstructure of these specimens. The microstructure of the specimen, with 10 at% Al, has titanium particles surrounded by a matrix of intermetallic compounds (mainly Ti_3Al, as observed by XRD). These intermetallics have a high strength while exhibiting low ductility (See Table 2.2). The matrix of brittle intermetallics causes brittle failure. At 50 at% Al the increased concentration of aluminium has lead to great porosity caused by the Kirkendall effect. This has greatly reduced the flexural strength. Porosity gives lower strength parts (Wang et al., 2010b) because of the reduced amount of material and increased stress concentrations around voids. While hot press sintering of titanium with liquid aluminium has achieved full density, the microstructure of titanium grains with a brittle intermetallic

matrix has lead to a brittle material.

Table 7.1: Flexural strength and strain at yield and break of specimens from commercial Ti powder sintered at 900°C under 80 MPa for 30 minutes

at% Al	σ_{fY} (MPa)	ϵ_{fB} (mm/mm %)
0	870	11.2
10	1070	1.3
50	210	0.2

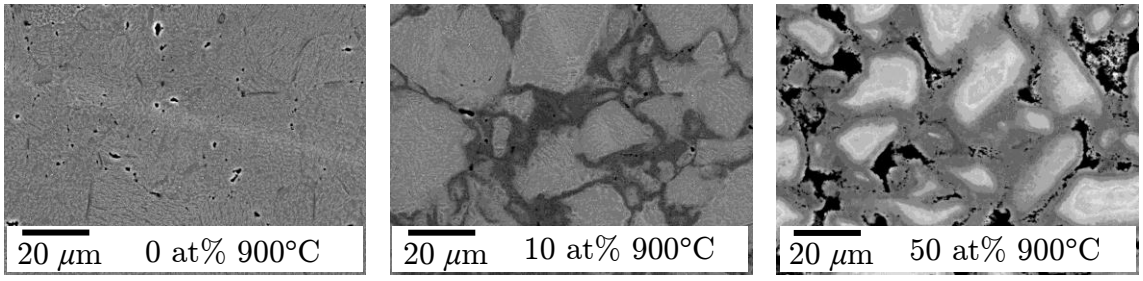

Figure 7.3: SEM mircrographs of commercial Ti powder sintered with 0, 10 and 50 at% Al, at 900°C under 80 MPa for 30 minutes

7.5 Practical Implications of Research Outcomes

This section discusses the possible utilisation of the outcomes of the current research to the improvement of PM efficiency and cost reduction. The ball milling process can significantly reduce energy consumption for powder production compared with conventional REP and GA processes (McCracken et al., 2010). The direct sintering of TiH_2, which was the focus of the current research, eliminates the dehydrogenation process and can further improve the cost of fabrication of titanium components.

In this thesis it was demonstrated that the utilisation of the ball milling technique can significantly facilitate the densification process, so the density of the fabricated part, which is one of the most important indicators of quality, is

comparable with the density obtained through other commercial techniques (Wang et al., 2010a). Therefore, this technique is promising for the fabrication of titanium products intended for high performance applications.

In addition, with the ball milling powder production technique, a significant reduction in particle and crystallite size can be achieved. Finer powder can be dehydrogenated and sintered at lower temperatures (see Section 6.2), which could have a large positive impact on the cost efficiency of titanium component manufacturing.

However, one of the shortcomings of the ball milling technique is the increase of oxygen content, which is likely to be responsible for the increased hardness and brittleness of the fabricated samples (see Section 6.2.4). Thus, the improved sintering efficiency achieved through particle size reduction could be compromised by the introduction of oxygen impurity leading to embrittlement of the fabricated component. Therefore, the methods of oxygen content reduction through all stages of fabrication must be explored and this issue must be addressed in future work, specifically for application which require high fracture toughness.

A significant outcome from this thesis is that titanium sintering efficiency can be improved by the use of aluminium LPS during pressure assisted sintering, which can be completed at low temperatures. This particular outcome can have a large impact on the overall energy consumption needed for titanium products. Unfortunately, a significant drawback of this technique is the formation of a brittle intermetallic matrix during sintering. One potential solution could be homogenisation of the obtained microstructure by using a suitable heat treatment to achieve ductility necessary for certain structural applications. However, in other applications which do not require high ductility of the fabricated part, specifically for high temperature applications, this sintering technique can provide many economic advantages.

7.6 Conclusion

This Chapter has discussed the results of the experimental study presented in Chapters 5 and 6. The dehydrogenation behaviour of ball milled powders was shown to be improved by the size and crystallite reduction and the increase of lattice defect density. Ball milled TiH_2 was seen to improve densification and produce almost full density parts at low temperatures. During direct sintering of ball milled TiH_2, dehydrogenation was seen to be impaired by the compaction pressure inside the graphite mould. The hardness of sintered TiH_2 was seen to be high compared with pure titanium which was shown to caused by increased oxygen content as a result of the size reduction through ball milling.

The results of titanium LPS with aluminium were then discussed. The addition of 5-10 at% Al to commercial titanium powder increases part density from pressure assisted sintering. The resulting microstructure show titanium particles surrounded by intermetallics. The complete loss of ductility of these specimens was caused by the brittle intermetallics. Finer ball milled powders (TiH_2 and HDH) decreased the density because of the accelerated reaction between titanium and liquid aluminium. The resulting microstructure shows intermetalics surrounding an aluminium pore site, and dense, pure titanium elsewhere.

Chapter 8

Conclusions and Future Work

8.1 Conclusions

The cost of current processing techniques of titanium parts is high because of titanium's affinity for atmospheric impurities and the use of traditional energy-expensive fabrication techniques. The application of new methods of advanced powder metallurgy are investigated as a means to reduce the overall cost of titanium by producing net shape parts, whereby ingot production and machining are almost eliminated, and the utilization of energy-effective methods for production of titanium powder and sintering can be exploited. This thesis has investigated two enhanced methods of titanium powder metallurgy: (I) the use of hydrogen as a temporary alloying element in the production of titanium powder, and (II) the application of the Liquid Phase Sintering (LPS) method to enhance the densification.

In this study TiH_2 was synthesised and ball milled. Then the TiH_2 powders were used directly or mixed with aluminium and sintered in an induction hot press. The effect of ball milling duration on the densification and dehydrogenation behaviour during sintering was studied. The effect of aluminium concentration and titanium

particle size on the required sintering temperatures were investigated. The major findings and contributions to the state of current research are:

1. DSC experiments on TiH_2 ball milled for 5-180 minutes in Chapter 5, showed that dehydrogenation occurs faster and at lower temperatures when ball milled for longer durations. The decrease in particle size and high defect density caused by mechanical work, increases the dehydrogenation kinetic. This confirms results from a previous study by Bhosle et al. (2003).

2. The ball milled TiH_2 powder was hot press sintered and characterised for density, phase composition and microstructure in Chapter 6. The reduction of TiH_2 particle sizes by ball milling was shown to improve densification and dehydrogenation significantly. The increase of ball milling duration from 5 to 180 minutes significantly increases the sintered density and dehydrogenation. Ball milling up to 180 minutes enables full densification by hot press sintering at 700°C, under 80 MPa, for 30 minutes. Such an investigation has not been conducted before, on the improvements to sintering through ball milling TiH_2.

3. Dehydrogenation of TiH_2 is impaired during pressure assisted sintering inside a graphite mould. The DSC of cold pressed TiH_2 powder in Chapter 5 showed that dehydrogenation was slower for higher compaction pressure. The incomplete dehydrogenation during sintering occurred for powders which completely dehydrogenated as loose powder. This restriction will require that pressure assisted sintering of TiH_2 be optimised so that complete dehydrogenation occurs. This novel result, in addition to the improvements to sintering TiH_2 from ball milling, shows that sintering parameters can be reduced through optimisation.

4. An increase in ball milling duration of TiH_2 leads to an increase in oxygen concentration. The excessive oxygen content in ball milled powders was seen

to cause high hardness values of sintered specimens in Chapter 6. The reduction of powder size caused by ball milling has increased the powders' specific surface area. The increased oxygen content is then introduced into the sintered specimen by the oxide layer on the surface of the particles. The introduction of oxygen by mechanical milling has been seen in studies by Ivasishin et al. (2002) and Bolzoni et al. (2012a).

5. The reaction between titanium and liquid aluminium during LPS was observed by experimental sintering. Aluminium diffuses into Ti to form $TiAl_3$, causing the occurance of Kirkendall pores, until there is no aluminium remaining. Further diffusion then occurs between Ti and $TiAl_3$ to form phases richer in Ti ($TiAl_2$, TiAl and Ti_3Al). Further diffusion then occurs until homogenisation. These stages of interaction have been studied previously by Sujata et al. (2001).

6. The effect of particle size during aluminium LPS of titanium was studied. The densification of specimens occurred differently between titanium powders of different sizes. Diffusion occurred faster and more locally for smaller ball milled TiH_2 with a mode particle size of 1.0 μm compared to commercial Ti with a mode particle size of 44 μm. For commercial Ti powders, pores formed between titanium particles through the Kirkendall effect. For ball milled powder, the aluminium formed rigid titanium aluminide shells around an aluminium particle site. This new result contributes to the understanding of the dependence on particle size during LPS.

7. Densification of commercial titanium was improved by the addition of 5-10 at% aluminium. Full densification by LPS of titanium was achieved using 10 at% aluminium at 900°C under 80 MPa for 30 minutes. Previously, the use of aluminium LPS of titanium during free sintering caused porosity through the Kirkendall effect (Liu et al., 2000, 2006; Savitskii and Burtsev, 1979). In this

study, a new result is observed: densification is improved during LPS through the use of pressure assisted sintering.

8. The flexural strength of specimens sintered by LPS was shown to increase at 10 at% aluminium, while there was a complete loss of ductility. The brittle intermetallic phases surrounded the titanium particles and was the cause of failure.

8.2 Future Work

The findings from this study show that ball milling of TiH_2 is a promising method for increasing densification during sintering. Fabrication of specimens for mechanical testing must be done to verify the quality of fabricated parts further. Possible oxygen contamination from ball milling may lead to formation of microstructures susceptible to brittle fracture. Therefore, an investigation of ball milling duration on mechanical properties, specifically fracture resistances, must be performed.

It has been shown that through pressure assistance, density is improved with aluminium concentrations between 5 and 10 at%. The use of fine titanium particle sizes promotes rapid diffusion and decreases the density, indicating that the speed of diffusion between liquid aluminium and titanium is influenced by the size of the powders. Thus, to improve the quality of the fabricated parts, a broader study directed at the relative particle sizes of titanium and aluminium is needed.

Finally, to evaluate the improvement in titanium PM techniques presented in this fundamental study, a comparative study must be conducted. The energy and cost savings and achievable mechanical properties of the techniques presented in this thesis must be compared with other and currently used techniques.

It is believed that the research outcomes presented in the thesis have contributed to the understanding of the fabrication techniques, as well as contributed to the

knowledge and improvement of titanium PM techniques. Overall, the use of ball milled TiH_2 powders and aluminium LPS have shown to have the potential to reduce the cost of the fabrication of titanium.

Appendix A

Conference Paper for ICCM19

TITANUM ENHANCED SINTERING THROUGH LIQUID PHASE SINTERING

E. Schumann*, M. Majimel, J-L Bobet, J-F Silvain, A. Kotousov
ICMCB-CNRS, Université Bordeaux 1, Pessac, 33608, France
*schumann@icmcb-bordeaux.cnrs.fr

Keywords: *Titanium, Sintering, Aluminium, Hydride, Composite, Liquid Phase Sintering*

1 General Introduction

Titanium has good specific strength and corrosion resistance at a broad working temperature which makes it attractive for use in many aerospace, automotive, and biomedical applications. However, its high processing cost limits its use greatly. The net shape production of powder-metallurgy reduces material waste and cost from machining. Ti sintering is in current use and shows further potential to reduce cost of parts. The use of 1) blended elemental Aluminium in reactive Liquid Phase Sintering (LPS) of Ti and 2) TiH_2 powders enhance densification at low temperatures. With the reduction of sintering temperatures through enhanced sintering, titanium product costs are hoped to be reduced for broader industrial application. This current investigation aims to achieve fully dense titanium through sintering blended elemental Ti/TiH_2-Al powders at low temperatures, thus reducing processing costs, and achieve industrially applicable mechanical properties.

2 Theory and Experiments

2.1 Liquid Phase Sintering

Liquid Phase Sintering is an enhanced sintering method in which a secondary element becomes liquid during sintering while the primary element remains solid. Densification is enhanced firstly by liquid flow and rearrangement and capillary action, then also through rapid solid-liquid diffusion, and solution reprecipitation. In this investigation, the sintering of titanium is of interest, and aluminium is used as the secondary liquid phase which is a common element in Ti-alloys and melts at a lower temperature than normal Ti sintering temperatures of approximately 1400°C. During sintering atomic diffusion will occur at the Ti-Al solid-liquid interface to form intermetallics, where $TiAl_3$ has been shown to form preferentially in this situation [1]. It is predicted that a Ti particle matrix will be surrounded by Ti-Aluminide reinforcement forming a metallic composite. However, the formation of such a composite depends on the diffusion that is allowed to occur by the sintering parameters designed.

2.2 TiH_2 powders

TiH_2 powders have been shown to dehydrogenate during sintering to form a pure Ti final product and it is proposed that the exposed active Ti surfaces enhance sintering [2]. The hydrogenation of titanium makes it brittle and it can be milled to form a fine Ti hydride powder. In this investigation TiH_2 powders are used to help the formation of a dense Ti part at reduced sintering temperatures. Depending on the size of the powder, during sintering the dehydrogenation process can occur at low temperatures below 600°C [2]. In this investigation it is hoped that TiH_2 powder can be used as a matter of convenience and to enhance sintering at low temperatures below 700°C. The interaction of the simultaneous use of a liquid Al phase will be important, because dehydrogenation is expected to be nearly complete before the melting of the Al phase, and experimentation will be required to see the ability of Al to flow through the Ti powder if the powder has begun to densify.

2.3 Experiments

Ti sponge was hydrogenated at 450-500°C under a pressurised hydrogen atmosphere until hydrogen absorption ceased. The TiH_2 sponge was then planetary ball milled with a 10:1 stainless steel ball:powder mass ratio under a hydrogen or argon atmosphere, and handled in a argon glove box. Various commercial Al powders from mean diameter 12 μm to 86 μm were mixed with Ti or

TiH_2 powders in a 3D mixer for 30 minutes. The powders were then hot-press sintered in a 6mm diameter graphite mould in an induction furnace under a primary vacuum at temperatures from 600-700°C at 80 MPa for 30 minutes. The percentage aluminium was varied at 0, 5, 10, 20 atomic percent.

2.4 Discussion and Results

The relative densities of the sintered specimens using pure Ti powder are compared to those using TiH_2 in Fig. 1. Under the experimental conditions set the Ti-Al specimens densify well at low percentages of aluminium. The specimens which use TiH_2 powders densify at 0 at% Al while poor densification is seen when pure Ti powder is used. XRD results detect no hydride titanium remaining. However, because the mechanical properties of titanium are sensitive to trace amounts of hydrogen the amount of hydrogen should be quantified.

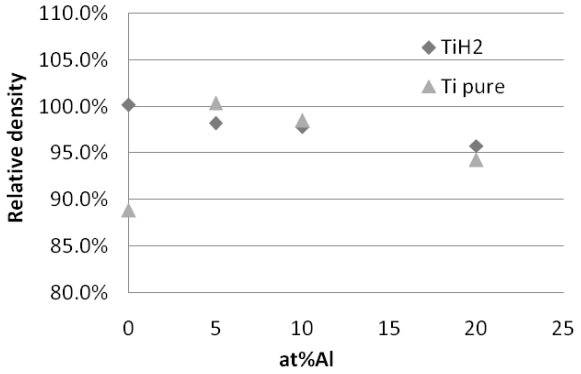

Figure 1. Relative densities of sintered Ti and TiH_2 powders with varied atomic percentages of Al.

The microstructure achieved using TiH_2 powder during the experiments performed show dense Ti areas and porous areas surrounded by Ti-Al intermetallics, shown in Fig. 2, despite enhanced densification.

2.6 Further work

The final form of the composite and the amount and type of intermetallics formed will depend on diffusion, and hence, the sintering parameters used. Sintering has been performed with consistent parameters, and experimental variation of parameters will be studied. The detailed chemical analysis of the specimens will be carried out to evaluate the extent of dehydrogenation during sintering and the quantity of impurities. Final mechanical testing will be performed to determine the mechanical properties of the metallic composite formed.

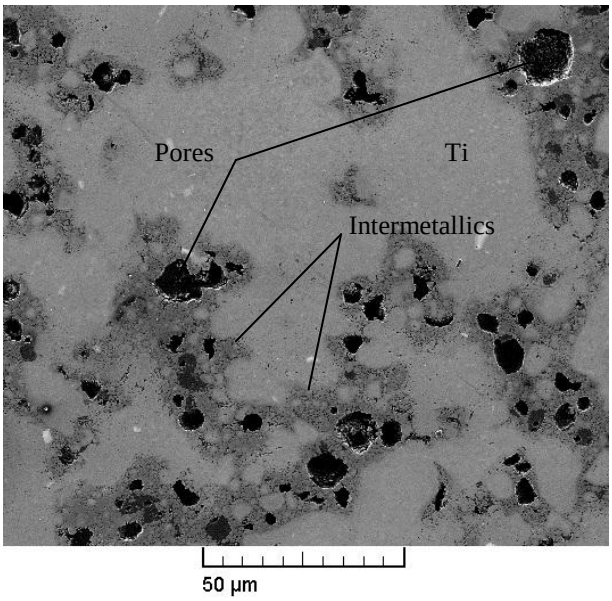

Figure 2. SEM micrograph of a sintered TiH_2-20at%Al specimen.

3 Conclusion

The enhanced sintered methods of LPS and the use of hydride titanium during sintering are investigated to reduce the sintering temperature and thus cost of titanium parts. In this investigation enhanced densification has been seen at low temperature, and further experimentation is required to achieve an optimal titanium specimen.

References

[1] M. Sujata, S. Bhargava, S. Sangal "On the formation of $TiAl_3$ during reaction between solid Ti and liquid Al". *Journal of Materials Science Letters*, Vol. 16 pp 1175-1178, 1997.

[2] H. Wang, M. Lefler, Z. Zak Fang, T. Lei, S. Fang, J. Zhang, and Q. Zhao "Titanium and Titanium Alloy via Sintering of TiH_2". *Key Engineering Materials*, Vol. 436 pp. 157-163, 2010.

Appendix B

XRD of HDH powder

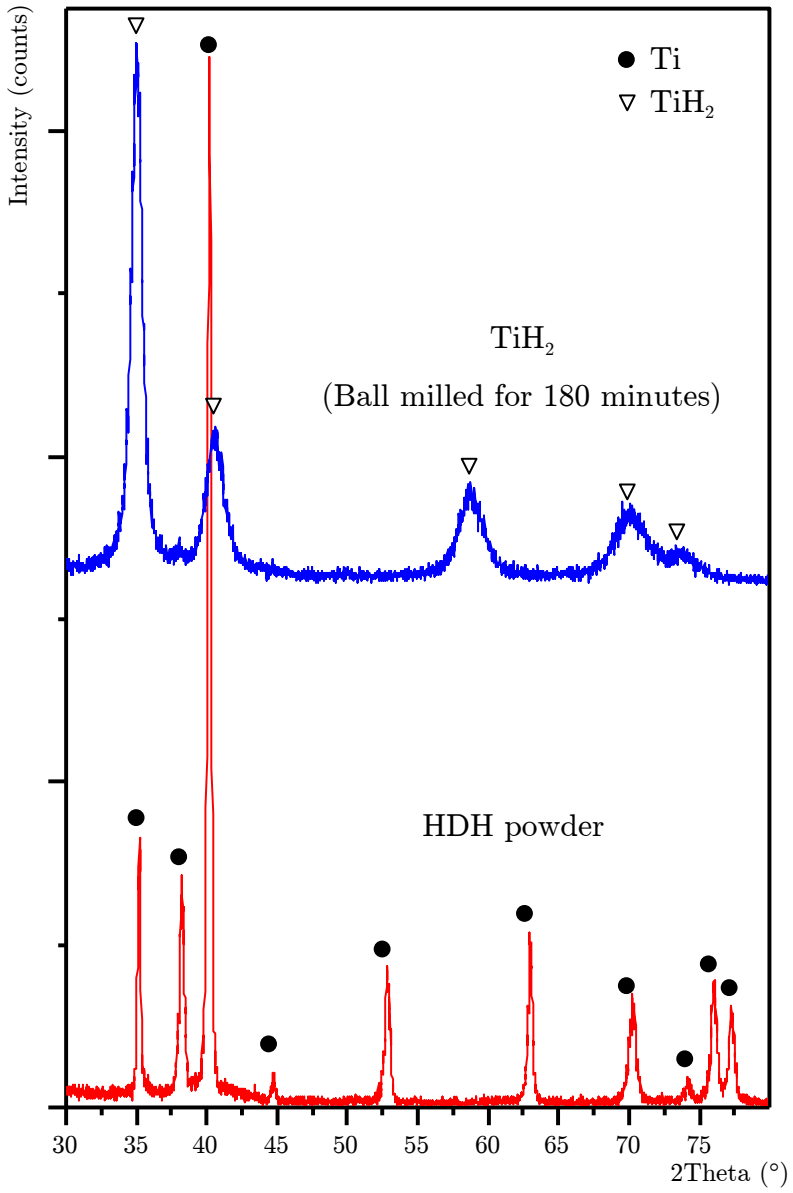

Figure B.1: XRD Patterns of HDH powder, ball milled for 180 minutes and dehydrogenated in a vacuum oven at 500°C for 3 hours, as well as of a TiH_2 powder ball milled for 180 minutes

Appendix C

Powder Mixing Calculations

The calculation of the mass of Ti and Al required to fabricate a specimen with a desired atomic percentage (at%) of Al in Ti is presented here. The designated concentration of aluminium is between 0 and 75 at%, and the desired specimen is a cylinder of diameter 6 mm and of height 5 mm. If TiH_2 is used and dehydrogenated during sintering, the designated mass of Ti is used to calculate the initial mass of TiH_2 required in the mixture.

The mass percent of aluminium, $m\%_{Al}$, in a specimen containing a mass of Ti, m_{Ti}, and Al, m_{Al} is:

$$m\%_{Al} = \frac{m_{Al}}{m_{Ti} + m_{Al}}$$

Where the mass is the number of Mols, n_{Al} or n_{Ti}, times the Molar mass, M_{Al} or M_{Ti}:

$$m\%_{Al} = \frac{n_{Al}M_{Al}}{n_{Ti}M_{Ti} + n_{Al}M_{Al}}$$

If we convert the number of Mols to atomic percent, $at\%$:

$$m\%_{Al} = \frac{n_{Al}M_{Al}/n_T}{n_{Ti}M_{Ti}/n_T + n_{Al}M_{Al}/n_T}$$

$$m\%_{Al} = \frac{at\%_{Al} M_{Al}}{at\%_{Ti} M_{Ti} + at\%_{Al} M_{Al}} \tag{C.1}$$

The mass of required aluminium, m_{Al}, and titanium, m_{Al}, of a desired final total mass, m_T, are then:

$$m_{Al} = m\%_{Al} \times m_T$$

$$m_{Ti} = (1 - m\%_{Al}) \times m_T$$

The theoretical density of a specimen, ρ_T is given by

$$\rho_T = \frac{m_T}{V_T} = \frac{V_{Al}\rho_{Al} + V_{Ti}\rho_{Ti}}{V_T} = V\%_{Al}\rho_{Al} + V\%_{Ti}\rho_{Ti}$$

Where the volume percentage, $V\%_{Al}$, is given by

$$V\%_{Al} = \frac{V_{Al}}{V_{Ti} + V_{Al}} = \frac{\frac{m_{Al}}{\rho_{Al}}}{\frac{m_{Ti}}{\rho_{Ti}} + \frac{m_{Al}}{\rho_{Al}}} = \frac{\frac{n_{Al} M_{Al}}{\rho_{Al}}}{\frac{n_{Ti} M_{Ti}}{\rho_{Ti}} + \frac{n_{Al} M_{Al}}{\rho_{Al}}}$$

Converting again to atomic percentage,

$$V\%_{Al} = \frac{at\%_{Al} \frac{M_{Al}}{\rho_{Al}}}{at\%_{Ti} \frac{M_{Ti}}{\rho_{Ti}} + at\%_{Al} \frac{M_{Al}}{\rho_{Al}}} \tag{C.2}$$

Then for a given atomic percentage of Al, for a given specimen volume, we can calculate the volume percenatage of each element using Equation C.2 and then the specimen density and then its mass. Then the mass percentage of each element can be calculated using Equation C.1. If TiH_2 is used in place of Ti, then the number of Mols of Ti are replaced with the equivalent of TiH_2:

$$n_{TiH_2} = n_{Ti} \Rightarrow \frac{m_{TiH_2}}{M_{TiH_2}} = \frac{m_{Ti}}{M_{Ti}} \Rightarrow m_{Ti} = M_{Ti} \frac{m_{TiH_2}}{M_{TiH_2}}.$$

The calculations for required masses of Al and Ti or TiH_2, are shown in Table

C.1, using the known material values of Al, Ti and TiH_2:

$M_{Al} =$ 26.982 g/Mol

$M_{Ti} =$ 47.9 g/Mol

$M_{TiH_2} =$ 49.9 g/Mol

$\rho_{Al} =$ 2.700 g/cm^3

$\rho_{Ti} =$ 4.506 g/cm^3

Table C.1: Powder mixing calculation table

$\%at._{Al}$	$\%at_{Ti}$	$\%V_{Al}$	$\%V_{Ti}$	ρ_T (g/cm^3)	m_T (g)	$\%m_{Al}$	$\%m_{Ti}$	m_{Al} (g)	m_{Ti} (g)	m_{TiH_2} (g)
0	100	0.000	1.000	4.506	0.382	0.000	1.000	0.000	0.382	0.398
2	98	0.019	0.981	4.472	0.379	0.011	0.989	0.004	0.375	0.391
5	95	0.047	0.953	4.421	0.375	0.029	0.971	0.011	0.364	0.379
10	90	0.095	0.905	4.335	0.368	0.059	0.941	0.022	0.346	0.361
20	80	0.190	0.810	4.162	0.353	0.123	0.877	0.044	0.309	0.322
50	50	0.485	0.515	3.631	0.308	0.360	0.640	0.111	0.197	0.205
66	34	0.646	0.354	3.339	0.283	0.522	0.478	0.148	0.135	0.141
75	25	0.738	0.262	3.173	0.269	0.628	0.372	0.169	0.100	0.104

Bibliography

S. Asavavisithchai, V.H. Lopez, and A.R. Kennedy. Non-Isothermal Decomposition of As-Received and Oxidised TiH2 Powders. *Materials Transactions*, 48:2712–2714, 2007.

ASTM B 348. Standard Specification for Titanium and Titanium Alloy Bars and Billets, American Society for Testing and Materials. 2000.

ASTM D 790. Standard Test Methods for Flexural Properties of Unreinforced and Reinforced Plastics and Electrical Insulating Materials, American Society for Testing and Materials. 2002.

ASTM E 92. Standard Test Method for Vickers Hardness of Metallic Materials, American Society for Testing and Materials. 2003.

C.R.F. Azevedo, D. Rodrigues, and F. Beneduce Neto. Ti-Al-V Powder Metallurgy (PM) via the Hydrogenation-Dehydrogenation (HDH) process. *Journal of Alloys and Compounds*, 353:217–227, 2003.

J.E. Barnes, W. Peter, and C.A. Blue. Evaluation of Low Cost Titanium Alloy Products. *Material Science Forum*, 618-619:165–168, 2009.

V. Bhosle, E.G. Baburaj, M. Miranova, and K. Salama. Dehydrogenation of TiH_2. *Materials and Engineering A*, 356:190–199, 2003.

J.-L. Bobet, C. Even, and J.-M. Quenisset. On The Production of Ultra-Fine Titanium Hydride Powder at Room Temperature. *Journal of Alloys and Compounds*, 348:247–251, 2003.

L. Bolzoni, P.G. Esteban, E.M. Ruiz-Navas, and E. Gordo. Mechanical Behaviour of Pressed and Sintered Titanium Alloys Obtained from Prealloyed and Blended Elemental Powders. *Journal of the Mechanical Behavior of Biomedical Materials*, 14:29–30, 2012a.

L. Bolzoni, E.M. Ruiz-Navas, E. Neubauer, and E. Gordo. Inductive Hot-Pressing of Titanium and Titanium Alloy Powders. *Materials Chemistry and Physics*, 131: 672–679, 2012b.

S.A. Brown and J.E. Lemons. *Medical Applications of Titanium and Its Alloys: The Material and Biological Issues.* American Society for Testing and Materials, 1996.

W. Chen, Y. Yamamoto, W.H. Peter, S.B. Gorti, A.S. Sabau, M.B. Clark, S.D. Nunn, J.O. Kiggans, C.A. Blue, J.C. Williams, B. Fuller, and K. Akhtar. Cold Compaction study of Armstrong Process Ti-6Al-4V powders. *Powder Technology*, 214:194–199, 2011.

G. Crowley. How to Extract Low-Cost Titanium. *Advanced Materials and Processes*, 161:25–27, 2003.

J.R. Davis. *Properties and Selection: Nonferrous Alloys and Special-Purpose Materials.* ASM International, Materials Park, OH, USA, 1990.

C. Doblin, D. Freeman, and M. Richards. The TiRO Process for the Continuous Direct Production of Titanium Powder. *Key Engineering Materials*, 551:37–43, 2013.

M.J. Donachie. *Titanium: A Technical Guide 2nd Edition.* ASM International, Materials Park, OH, USA, 2000.

J. Emsley. *Nature's Building Blocks: An A-Z Guide to the Elements.* Oxford University Press, New York, 2001.

E.A. Evard, I.E. Gabis, and A.P. Voyt. Study of the Kinetics of Hydrogen Sorption and Desorption from Titanium. *Journal of Alloys and Compounds*, 404-406:335–338, 2005.

D. Eylon and S.R. Seagle. *Titanium 99, Science and Technology.* CRISM "Prometey", St. Petersburg, Russia, 2000.

K. Faller and F.H. Froes. The Use of Titanium in Family Automobiles: Current Trends. *JOM*, 53:27–28, 2001.

Z.Z. Fang. Powder Metallurgy Titanium - Challenges and Opportunities. *International Journal of Powder Metallurgy*, 46/5:9–10, 2010.

Z.Z. Fang, P. Sun, and H. Wang. Hydrogen Sintering of Titanium to Produce High Density Fine Grain Titanium Alloys. *Advanced Engineering Materials*, 14:383–387, 2012.

F.H. Froes. Synthesis, Properties and Applications of Titanium Aluminides. *Journal of Materials Science*, 27:5113–5140, 1992.

F.H. Froes. *Handbook of Advanced Materials.* Springer, Berlin, 2001.

F.H. Froes. Titanium Powder Metallurgy: A Review - Part 1. *Advanced Materials and Processes*, 170:16–22, 2012.

S.J. Gerdemann. Titanium Process Technologies. *Avanced Materials adn Processes*, 159:41–43, 2001.

R.M. German. *Liquid Phase Sintering*. Plenum, New York, 1985.

R.M. German. Phase Diagrams in Liquid Phase Sintering Treatments. *Journal of Metals*, 38:26–29, 1986.

R.M. German. *Sintering Theory and Practice*. Wiley, New York, 1996.

R.M. German and R.G. Cornwall. *Sintering Technology*. Marcel Dekker, New York, 1996.

A.D. Hartman, S.J. Gerdemann, and J.S. Hansen. Producing Lower-Cost Titanium for Automotive Applications. *JOM*, 50:16–19, 1998.

Y. He, Y. Jiang, N. Xu, J. Zou, B. Huang, C.T. Liu, and P.K. Liaw. Fabrication of TiAl Micro/Nanometer-Sized Porous Alloys through the Kirkendall Effect. *Advanced Materials*, 19:2102–2106, 2007.

M.A. Hunter. Metallic Titanium. *Journal of the American Chemical Society*, 161: 330–336, 1910.

O.M. Ivasishin, A.N. Demidik, and D.G. Savvakin. Use of Titanium Hydride for the Synthesis of Titanium Alumides from Powder Materials. *Powder Metallurgy and Metal Ceramics*, 38:9–10, 1999.

O.M. Ivasishin, D.G. Savvakin, F. Froes, V.C. Mokson, and K.A. Bondareva. Synthesis of Alloy Ti-6Al-4V With Low Residual Porosity by a Powder Metallurgy Method. *Powder Metallurgy and Metal Ceramics*, 41:382–390, 2002.

O.M. Ivasishin, D.G. Savvakin, and N.M. Gumenyak. Dehydrogenation of a Titanium-Hydride Powder and its Role in the Activation of Sintering . *Metalofiz Noveishie Tekhnol*, 33:899–917, 2011.

A.R. Kennedy. The effect of TiH_2 heat treatment on gas release and foaming in $AlTiH_2$ preforms. *Scripta Materialia*, 47:763–767, 2002.

A.R. Kennedy and V.H. Lopez. The Decomposition Behavior of As-Received and Oxidized TiH_2 Foaming-Agent Powder. *Materials Science and Engineering: A*, 357:258–263, 2003.

Y.W. Kim. Strength and Ductility in TiAl Alloys. *Intermetallics*, 6:623–628, 1998.

W.D. Kingery. Densification during Sintering in the Presence of a Liquid Phase. I. Theory. *Journal of Applied Physics*, 30:301–306, 1959.

L.I. Kivalo, V.V. Skorokhod, and N.F. Grigorenko. Volume Changes Accompanying the Sintering of Compacts from Mixtures of Titanium and Iron Powders. *Poroshkovaya Metallurgiya*, 5:17–21, 1982.

W. Kroll. The Production of Ductile Titanium. *Journal of The Electrochemical Society*, 78:35–47, 1940.

T.K. Lee, J.H. Kim, and S.K. Hwang. Direct Consolidation of γ-TiAl-Mn-Mo from Elemental Powder Mixtures and Control of Porosity through a Basic Study of Powder Reactions. *Metallurgical and Materials Transactions A*, 28A:2723–2729, 1997.

H.A. Lipsitt. *Advanced High Temperature Alloys: Processing and Properties*. ASM International, Materials Park, OH, USA, 1986.

H. Liu, P. He, J.C. Feng, and J. Cao. Kinetic study on nonisothermal dehydrogenation of TiH_2 powders. *International Journal of Hydrogen Energy*, 34:3018–3025, 2009.

Y. Liu, B.-Y. Huang, Y.-H. He, and K.-C. Zhou. Densification abnormality in reactive hot pressing of Ti and Al elemental powders. *Transactions of Nonferrous Metals Society of China*, 10:453–455, 2000.

Y. Liu, L.F. Chen, H.P. Tang, C.T. Liu, B. Liu, and B.Y. Huang. Design of powder metallurgy titanium alloys and composites. *Materials Science and Engineering A*, 418:25–35, 2006.

R.J. Low, I.M. Robertson, and G.B. Schaffer. Excessive Porosity after Liquid-Phase Sintering of Elemental titanium Powder Blends. *Scripta Materialia*, 56:895–898, 2007.

S.D. Luo, Y.F. Yang, G.B. Schaffer, and M. Qian. Novel Fabrication of Titanium by Pure Microwave Radiation of Titanium Hydride Powder. *Scripta Materialia*, 69:69–72, 2013.

G. Lütjering and J.C. Williams. *Titanium Engineering Materials and Processes 2nd Edition*. Springer, Berlin, 2007.

A.R. Machado and J. Wallbank. Machining of Titanium and its Alloysa Review. *Proceedings of the Institution of Mechanical Engineers, Part B: Journal of Engineering Manufacture*, 204:53–60, 1990.

C.G. McCracken, C. Motchenbacher, and D.P. Barbis. Review of Titanium Powder Production Methods. *International Journal of Powder Metallurgy*, 46:19–26, 2010.

J.L. Murray. *The Al-Ti (Aluminum-Titanium) System, Phase Diagrams of Binary Titanium Alloys*. ASM International, Materials Park, OH, USA, 1987.

M. Nakamura and K. Kimura. Elastic constants of $TiAI_3$ and $ZrAI_3$ single crystals. *Journal of Materials Science*, 26:2208–2214, 1991.

H. Numakura and M. Koiwa. Hydride Precipitation in Titanium. *Acta Metallurgica*, 32:1799–1807, 1984.

A.A. Odwani, M. Al-Tabtabaei, and A. Abdel-Nabi. Performance of high chromium stainless steels and titanium alloys in Arabian Gulf seawater. *Desalination*, 120: 73–81, 1998.

H. Okamoto. H-Ti (Hydrogen-Titanium). *Journal of Phase Equilibria and Diffusion*, 32:174–175, 2011.

A.P. Pankevich, A.F. Chertovich, and G.A. Libenson. Production of Titanium Specimens from a Titanium Hydride Powder by Hot Pressing. *Poroshkovaya Metallurgiya*, 2:14–18, 1986.

E. Paransky, E.Y. Gutmanas, I. Gotman, and M. Koczak. Pressure-Assisted Reactive Synthesis of Titanium Aluminides from Dense 50AI-50Ti Elemental Powder Blends. *Metallurgical and Materials Transactions A*, 27A:2130–2139, 1996.

M. Peters and C. Leyens. *Titanium and Titanium Alloys: Fundamentals and Applications*. Wiley, New York, 2003.

M. Peters, J. Kumpfert, C.H. Ward, and C. Leyens. *Titanium and Titanium Alloys: Fundamentals and Applications*. Wiley, New York, 2003.

M. Qian. Cold Compaction and Sintering of Titanium and its Alloys for Near-Net-Shape or Preform Fabrication. *International Journal of Powder Metallurgy*, 46: 29–44, 2010.

J.C. Rawers and W.R. Wrzesinski. Reaction-Sintered Hot-Pressed TiAl. *Journal of Materials Science*, 27:2877–2886, 1992.

I.M. Robertson and G.B. Schaffer. Some Effects of Particle Size on the Sintering of Titanium and a Master Sintering Curve Model. *Metallurgical and Materials Transactions A*, 40:1968–1979, 2009.

T. Saito. The Automotive Application of Discontinuously Reinforced TiB-Ti Composites. *JOM*, 46:30–34, 2004.

A. San-Martin and F.D. Manchester. The H-Ti (Hydrogen-Titanium) System. *Bulletin of Alloy Phase Diagrams*, 8:30–42, 1987.

H.R.Z. Sandim, B.V. Morante, and P.A. Suzuki. Kinetics of Thermal Decomposition of Titanium Hydride Powder Using in situ High-temperature X-ray Diffraction (HTXRD). *Materials Research*, 8:293–297, 2005.

A.P. Savitskii and N.N. Burtsev. Compact Growth in Liquid Phase Sintering. *Powder Metallurgy and Metal Ceramics*, 2:31–38, 1979.

A.P. Savitskii and N.N. Burtsev. Effect of Powder Particle Size on the Growth of Titanium Compacts During Liquid-Phase Sintering with Aluminium. *Powder Metallurgy and Metal Ceramics*, 20:618–621, 1981.

D.H. Savvakin, M.M. Humenyak, M.V. Matviichuk, and O.H. Molyar. Role of Hydrogen in the Process of Sintering of Titanium Powders. *Materials Science*, 47: 651–661, 2012.

P. Scherrer. Bestimmung der Grösse der Inneren Struktur von Kolloidteilchen Mittels Röntgenstrahlen, Nachrichten von der Gesellschaft der Wissenschaften, Göttingen. *Mathematisch-Physikalische Klasse*, 2:98–100, 1918.

O.N. Senkov and F.H. Froes. Thermohydrogen processing of titanium alloys. *International Journal of Hydrogen Energy*, 24:565–576, 1999.

D. Setoyama, J. Matsunaga, H. Muta, M. Uno, and S. Yamanaka. Mechanical Properties of Titanium Hydride. *Journal of Alloys and Compounds*, 381:215–220, 2004.

M. Sujata, S. Bhargava, S. Suwas, and S. Sangal. On Kinetics of $TIAl_3$ Formation During Reaction Synthesis From Solid Ti and Liquid Al. *Journal of Materials Science Letters*, 20:2207–2209, 2001.

K. Taguchi, M. Ayada, K.N. Ishihara, and P.H. Shingu. Near-net shape processing of TiAI intermetallic compounds via pseudo HIP-SHS route. *Intermetallics*, 3: 91–98, 1995.

B. Tsuchiya, S. Nagata, N. Ohtsu, K. Toh, and T. Shikama. Thermal Desorption of Hydrogen at the Titanium Hydride-Oxide Interface. *Materials Transactions*, 46: 196–198, 2005.

Y. Umakoshi, M. Yamaguchi, T. Sakagami, and T. Yamane. Oxidation Resistance of Intermetallic Compounds AI_3Ti and TiAl. *Journal of Materials Science*, 24: 1599–1603, 1989.

G.S. Upadhyaya. *Powder Metallurgy Technology*. Cambridge International Science Publishing, Cambridge, 1997.

H. Wang, Z.Z. Fang, and P. Sun. A Critical Review of Mechanical Properties of Powder Metallurgy Titanium. *International Journal of Powder Metallurgy*, 46: 45–57, 2010a.

H. Wang, M. Lefler, Z.Z. Fang, T. Lei, S. Fang, J. Zhang, and Q. Zhao. Titanium and Titanium Alloy via Sintering of TiH_2. *Key Engineering Materials*, 436:157–163, 2010b.

J.H. Westbrook and R.L. Fleischer. *Intermetallic Compounds.* Wiley, New York, 2000.

J.B. Yang, K.W. Teoh, and W.S. Hwang. Solid-State Hot Pressing of Elemental Aluminum and Titanium Powders to Form TiAl + (γ+α_2) Intermetallic Microstructure. *Journal of Materials Engineering and Performance*, 5:583–588, 1996.

H. Zhang and E.H. Kisi. Formation of Titanium Hydride at Room Temperature by Ball Milling. *Journal of Physics: Condensed Matter*, 9:L185–L190, 1997.

P. Zhang, S.X. Li, and Z.F. Zhang. General Relationship Between Strength and Hardness. *Materials Science and Engineering: A*, 529:62–73, 2011.